



**HAL**  
open science

# Modélisation et optimisation des réseaux optiques à plusieurs niveaux de granularité

Paul Ghobril

► **To cite this version:**

Paul Ghobril. Modélisation et optimisation des réseaux optiques à plusieurs niveaux de granularité. domain\_other. Télécom ParisTech, 2005. English. NNT: . pastel-00001252

**HAL Id: pastel-00001252**

**<https://pastel.hal.science/pastel-00001252>**

Submitted on 3 Jun 2005

**HAL** is a multi-disciplinary open access archive for the deposit and dissemination of scientific research documents, whether they are published or not. The documents may come from teaching and research institutions in France or abroad, or from public or private research centers.

L'archive ouverte pluridisciplinaire **HAL**, est destinée au dépôt et à la diffusion de documents scientifiques de niveau recherche, publiés ou non, émanant des établissements d'enseignement et de recherche français ou étrangers, des laboratoires publics ou privés.

# Thèse

présentée pour obtenir le grade de docteur  
de l'Ecole Nationale Supérieure des Télécommunications

Spécialité : Informatique et Réseaux

## **Paul GHOBRI**

### **Modélisation et optimisation d'un réseau optique à plusieurs niveaux de granularité**

Soutenue le 28 avril 2005 devant le jury composé de :

Gérard HEBUTERNE	Président
Dominique BARTH	Rapporteurs
André GIRARD	
Jean-claude BERMOND	Examineurs
Jean-Michel FOURNEAU	
Maurice GAGNAIRE	
Samir TOHME	Directeur de Thèse



## REMERCIEMENTS

Je remercie Samir Tohmé qui a su comment encadrer ma thèse sans encadrer la liberté nécessaire à tout progrès. Il m'a appris comment viser le but sans se décourager même si la tâche paraît indéfinie et lourde.

Je remercie le président du jury et les examinateurs Gérard Hébuterne, Jean-Claude Bermond, Jean-Michel Fourneau et Maurice Gagnaire qui ont su se montrer disponibles malgré leurs multiples engagements.

Je remercie les deux rapporteurs qui ont donné de leur précieux temps pour lire et rapporter sur ma thèse. Je dois à André Girard les corrections de fond et de forme pour sortir une version de cette thèse aussi irréprochable que possible. Dominique Barth m'a incité à aborder le monde de l'analyse algorithmique que j'approfondis maintenant après la thèse.

Je remercie les directeurs et les personnels de l'ENST.

Je remercie Houda Labiod pour son support et amitié. Je remercie Rola Naja d'avoir confiance en notre amitié. Je remercie Ouahiba Fouial et Mohamad Badra qui, chacun de son côté, m'ont aidé au moment où j'en avais vraiment besoin.

Je n'aurais pas pu finir cette thèse sans les nombreux et parfois longs séjours à Paris. Je remercie Micheline, Jean-Baptiste et tous les Fourest pour leur accueil chaleureux. Je remercie de même Nada, Claudette, Mireille, Rommel, Ziad et Bahia qui m'ont ouvert leur cœur et leur porte.

Je ne dois pas oublier les gens qui m'ont encouragé dans ma vie professionnelle et surtout Sami Tehini à qui je dois mes commencements et P. Fady Fa del qui a bien voulu que je termine ma thèse.



*A mon épouse Dolly et ses parents*

*A mes parents*

*A mes enfants Rita, Thomas et Karine qui ont bien apprécié les figures de ma thèse. J'espère qu'ils ne vont pas être déçus quand ils sauront que le brasseur hiérarchique n'est pas un robot et que son modèle graphique n'est pas la toile de Spiderman...*



# MODELISATION ET OPTIMISATION D'UN RESEAU OPTIQUE A PLUSIEURS NIVEAUX DE GRANULARITE

## RESUME

### ❖ Introduction

La technique du multiplexage de longueurs d'onde ou Wavelength division multiplexing (WDM) s'avère la solution permettant la meilleure exploitation de l'immense bande passante d'une fibre optique. En WDM, cette bande est divisée en plusieurs canaux travaillant chacun sur une longueur d'onde différente et à un débit adapté à la vitesse de traitement des composants électroniques.

La longueur d'onde pourrait être sous utilisée sauf si elle est bien remplie par une bonne agrégation du trafic. Cette agrégation s'effectue, par exemple, à l'aide d'un multiplexage temporel (TDM) ou d'une commutation optique de paquets. D'autre part, le groupage de longueurs d'onde, au niveau des nœuds intermédiaires pour un regroupement en bandes, réduit la complexité de la gestion et du matériel des équipements de commutation.

La coexistence des différents concepts de groupage optique et électronique ainsi que la manipulation de plusieurs niveaux et différentes échelles d'agrégation forment l'idée de base derrière ce qu'on appelle "réseau optique à plusieurs niveaux de granularité".

Cette agrégation hiérarchique est adoptée dans le but de réduire la complexité du matériel tout en permettant une flexibilité opérationnelle. La notion de plusieurs niveaux de granularité ouvre la voie à de nouveaux problèmes de dimensionnement et d'optimisation des réseaux optiques.



Ce qui a été déjà soulevé dans ce domaine reste rudimentaire par rapport à ce qu'on attend de cette approche. Surtout que l'adoption de cette approche s'avère incontournable dans les futurs réseaux optiques avec toute la capacité prévue et la diversité spatiale et temporelle attendue.

Ce résumé souligne nos contributions à ce domaine dans le cadre de cette thèse.

### ❖ **Problématique**

On réduit le coût et on améliore les performances des réseaux optiques en créant des multiples granularités de commutation. La taille et la complexité du brasseur optique peuvent être réduites en traitant en bloc un groupe de longueurs d'onde contiguës. Cette bande d'ondes (waveband) sera éventuellement traitée comme une seule entité. De cette manière, on réduit le nombre de ports d'entrée/sortie par brasseur et par suite la complexité du réseau. La commutation par bloc est uniquement possible si toutes les longueurs d'onde incluses dans la bande sont acheminées ensemble.

Traiter en bloc un nombre de longueurs d'onde encombre l'opération de routage et d'allocation de longueurs d'onde dans le but de convenablement remplir les bandes d'ondes. Afin d'améliorer la flexibilité, quelques ports d'entrée/sortie du brasseur de bandes peuvent éventuellement être connectés à des démultiplexeurs/multiplexeurs pour passer à un brassage par longueurs d'onde. De cette manière, on résout la commutation en bloc et quelques bandes pourront sortir de la continuité des tunnels établis pour passer d'un tunnel à l'autre. Cette notion peut être étendue pour couvrir différentes granularités et différents niveaux de brassage.

En d'autre terme, le groupage optique du trafic en bandes d'ondes et puis en bandes à granularité supérieure réduit la taille et la complexité des brasseurs optiques. Ce groupage réduit le nombre de ports d'entrée/sortie. Par contre, la gestion du remplissage des bandes d'ondes et de l'utilisation des ressources telles que les multiplexeurs/démultiplexeurs de bandes constitue un problème de base. Le groupage en bandes d'onde est efficace là où on peut réduire le besoin de commuter individuellement les longueurs d'ondes. Ceci est vrai dans les réseaux cœur où le trafic de transit est estimé de 60% à 80% du trafic total.

### ➤ **Contrôle des brasseurs hiérarchiques**

Les brasseurs hiérarchiques disposent de plusieurs niveaux et granularités de brassage. Au routage et à l'allocation des longueurs d'onde s'ajoute le contrôle des brasseurs hiérarchique qui consiste à prendre les décisions suivantes :

- a. Dans le contexte du trafic statique, on doit décider au niveau de chaque nœud quels sont les porteurs du trafic devant partager le même traitement en bloc et sous quelle granularité
- b. Dans le contexte du trafic dynamique, pour établir une connexion on doit décider, au niveau de chaque nœud, jusqu'à quel niveau on doit démultiplexer. D'une autre part, on doit décider si on doit ouvrir de nouvelles ressources ou bien partager les ressources déjà utilisées.

Choisir la meilleure solution pour établir une connexion donnée ne se limite pas à trouver le meilleur candidat en terme d'intervalle de temps, de longueur d'onde, fibre, ... et l'ensemble des nœuds intermédiaires mais aussi la meilleure granularité de commutation au niveau de chaque nœud intermédiaire. Notons que dans le contexte du trafic dynamique, le choix de la granularité de commutation n'affecte pas nécessairement la connexion en cours d'établissement mais a un grand effet sur l'établissement des futures demandes.

#### ➤ **Ingénierie du trafic**

Les démultiplexeurs/multiplexeurs permettant de passer d'un niveau de brassage à un autre doivent représenter les rares ressources pour l'ingénierie du trafic. La clé de la solution est de trouver jusqu'à quel niveau doit-on démultiplexer et comment établir les tunnels et distribuer le trafic sur ces tunnels.

Dans le contexte du trafic dynamique, l'ordre suivant lequel les demandes arrivent est important pour les performances du réseau et surtout quand on doit prendre la décision de commuter en bloc (par exemple: commutation par bande d'ondes). Cette commutation en bloc résulte en un brusque changement du nombre de plans d'interconnexion possibles. Ces changements continus de la topologie logique doivent être contrôlés dans le but de réduire la probabilité de blocage des futures demandes. Donc en plus du routage et de l'allocation des longueurs d'onde, on doit mener à bien le contrôle des brasseurs hiérarchiques.

Si, au niveau d'un nœud donné, on passe à travers les différentes granularités et arrivant à une granularité particulière (par exemple: une bande d'onde), on doit, quand on en a le choix, décider de:

- démultiplexer et passer à une plus fine granularité (par exemple: une longueur d'onde) et améliorer la flexibilité d'acheminement des canaux cohabitant ce porteur du trafic (les autres longueurs d'onde de la même bande).
- contourner les commutations à des granularités plus fines pour économiser les ressources rares (démultiplexeurs/multiplexeurs). Ceci revient à passer la flexibilité aux autres porteurs du trafic.

Le problème de base est de savoir quand est-ce qu'il faut s'arrêter de démultiplexer en passant d'une granularité à une autre granularité plus fine au niveau de chaque nœud et pour chaque demande.

### ➤ **Base d'informations pour l'ingénierie du trafic**

Pour mener à bien l'ingénierie du trafic et pour optimiser l'opération de groupage, on a besoin d'une base d'informations permettant de suivre les progrès du réseau à plusieurs niveaux de granularité.

La plupart des algorithmes de groupage se basent sur un modèle graphique multicouche. Pour ces algorithmes, le modèle du coût détermine la stratégie proposée. On se sert de l'algorithme du plus court chemin ou tout autre algorithme d'optimisation des graphes pour établir une connexion.

Dans ces modèles graphiques, le modèle du nœud est une extension du nœud physique pour inclure les caractéristiques de ce nœud par une combinaison de sommets et d'arcs. Pour un modèle multicouche, on définit pour chaque granularité, une couche contenant l'image des nœuds physiques. Au fur et à mesure qu'on utilise les porteurs de trafic à une granularité de commutation donnée (en contournant les plus fines granularités) on supprime les arcs utilisés de la couche correspondante. L'information portant sur ces arcs doit être sauvée quelque part. Pour un groupage à deux niveaux, ceci ne pose pas un grand problème mais pour plusieurs niveaux de granularité on a besoin d'une base d'informations capable de gérer l'évolution du réseau.

On tire de cette base d'informations la topologie logique qui est le support de toute décision à prendre et de tout objectif à viser par l'ingénierie du trafic.

## ❖ Contributions

Nous présentons dans cette section nos contributions dans cette thèse.

### ➤ **Le modèle graphique du réseau optique à plusieurs niveaux de granularité MGGM (Multi-Granularity Graph Model).**

Ce modèle fournit une base d'informations complète au service de l'ingénierie du trafic. Avec ce modèle, la décision cruciale de contourner ou d'aborder la commutation à fines granularités au niveau des nœuds intermédiaires fait partie de l'optimisation du graphe. Ce qui permet la mise en œuvre de différentes politiques de groupage et de contrôle des brasseurs hiérarchiques dans le contexte du réseau optique à plusieurs niveaux de granularité.

On définit la granularité d'un canal comme étant le rapport de la capacité du canal à la plus petite capacité qu'on peut individuellement commuter dans l'ensemble des brasseurs du réseau. On définit l'élément de base du réseau ou Basic Network Element (BNE) comme étant toute interconnexion possible dans le réseau entre n'importe quel pair de ports d'entrée/sortie.

Chaque port (d'entrée ou de sortie) est représenté par un nombre de couples arc/nœud égal à sa granularité. L'arc représente le canal à commuter et le nœud représente le point d'accès. Dans un même BNE les ports sont appliqués l'un à l'autre à travers des nœuds propres à ce BNE. Les arcs sont regroupés selon la granularité de commutation possible. Chaque port du BNE (entrée ou sortie) peut avoir une différente granularité de commutation ce qui rend le modèle compatible aux architectures du réseau à plusieurs niveaux de granularité.

Les arcs du BNE représentent les porteurs du trafic. Les nœuds de base (Main Vertices) définissent l'appartenance de ces porteurs à un BNE donné et séparent le port d'entrée du port de sortie en laissant à chacun sa propre granularité de commutation.

Les groupes représentent toute sorte d'agrégation (optique ou électronique). Cette notion de groupes permet l'abstraction des agrégateurs/déagrégateurs et définit par suite la granularité de commutation de chaque côté du BNE. L'opération de commutation est représentée par une simple opération de réunion des groupes. Aucun porteur de trafic ne peut être utilisé avant de prendre la décision d'acheminement en bloc ; ce qui revient à définir les groupes à réunir. Les nœuds de groupe (Group Vertices) permettent l'interconnexion des différents BNEs.

Un groupe est un objet portant les données suivantes :

- a. L'identificateur du groupe.

- b. La granularité ou nombre d'arcs.
- c. Les pointeurs aux nœuds de base.
- d. Les pointeurs aux nœuds de groupe.
- e. Le nombre d'arcs libres ou unités de trafic non utilisées. Comparé à la granularité, ce nombre est utilisé pour déterminer quand est-ce qu'il faut séparer les groupes réunis et permettre par suite une nouvelle commutation en bloc.
- f. L'identificateur du groupe réuni. Ce champ est mis à «Nul» quand tous les porteurs de trafic du groupe sont libres.
- g. Un indicateur pour déterminer si les nœuds du groupe représentent des sources ou bien des destinations pour les arcs correspondants. En d'autre terme, c'est pour trouver à quel côté du BNE le groupe appartient.
- h. Le type ou profil du coût. Le type définit la couche (intervalle de temps, longueur d'onde, bande ...) dans le contexte du réseau multicouche. C'est aussi pour définir la politique de groupage. Par exemple, on peut définir le coût des arcs avant et après la commutation en bloc.

On définit alors deux types de nœuds:

- **Les nœuds de base (Main Vertices):** Un nœud de base appartient à un et un seul BNE. Ces nœuds relient le port d'entrée du BNE à son port de sortie. Les arcs sont toujours connectés à ces nœuds quelle que soit l'opération appliquée au groupe. Les nœuds de base de deux groupes adjacents seront directement connectés ensemble après l'opération de réunion (MERGE operation). Plusieurs BNEs ne peuvent pas partager les nœuds de base (à l'exception des nœuds ADD et DROP).
- **Les nœuds de groupe (Group Vertices):** Ce sont les nœuds source et destination du BNE. Ils représentent les points d'interconnexion des différents BNEs. Les arcs sont connectés ou détachés de ces nœuds selon l'opération appliquée au groupe correspondant. Plusieurs BNEs et plusieurs groupes peuvent partager ces nœuds.

L'objet représentant un arc du graphe porte les données suivantes :

- a. Le coût.
- b. L'identificateur du groupe.
- c. Le nœud destinataire.

On définit les quatre opérations suivantes :

- Réunion de deux groupes ou MERGE (grpID1, grpID2)
- Séparation de deux groupes ou UNMERGE (grpID1)
- Exclusion d'un arc ou EXCLUDE (Edge)
- Inclusion d'un arc ou REINCLUDE (Edge).

A l'aide de ces quatre opérations toute action de commutation, de routage ou d'allocation de longueurs d'onde, de bande, d'intervalles de temps, etc. peut être suivie et même optimisée dans le réseau à plusieurs niveaux de granularité.

➤ **Le modèle analytique du brasseur optique hiérarchique.**

Plusieurs paramètres affectent la probabilité de blocage dans le réseau optique. Les connexions peuvent être bloquées suite à un manque d'émetteurs/récepteurs disponibles, un manque de liaisons disponibles, la contrainte de continuité de la longueur d'onde, etc....

La topologie du réseau affecte aussi la probabilité de blocage. Dans certains cas, on pourrait toujours établir des connexions entre n'importe quel pair de source/destination en excluant quelques liaisons et quelques nœuds mais ceci est aux dépens de réduire la connectivité et par suite augmenter la probabilité de blocage. La connectivité constitue alors une mesure de la flexibilité du réseau.

Quand on a recours aux brasseurs hiérarchiques, la commutation en bloc imposé sur un nombre de ports d'entrée/sortie réduit le nombre de plans d'interconnexion supportés par le brasseur. Les plans d'interconnexion non supportés ne pourront plus utiliser ce brasseur ce qui résulte en une réduction de la connectivité.

La performance de blocage d'un brasseur hiérarchique est représentée par le rapport du nombre de plans d'interconnexion bloqués quand ce brasseur vient remplacer un brasseur non hiérarchique sur le nombre total de plans d'interconnexion.

Le modèle analytique des brasseurs hiérarchiques proposé dans cette thèse donne une évaluation de la complexité du matériel d'une part et de la complexité d'opération du réseau à plusieurs niveaux de granularité d'une autre part.

➤ **Le réarrangement des longueurs d'onde dans le contexte du trafic statique.**

On considère le problème du réarrangement de longueurs d'onde pour optimiser l'utilisation des brasseurs hiérarchiques dans le but de réduire la complexité des brasseurs optiques. Ces brasseurs hiérarchiques permettent un brassage par bande de longueurs d'onde comme ils permettent de commuter à une granularité plus fine.

Après le routage et l'allocation des longueurs d'onde, on propose le réarrangement des longueurs d'onde qui consiste à changer l'ordre des canaux de longueurs d'onde sans changer le plan de distribution des longueurs d'onde résultant du routage et de l'allocation des longueurs d'onde. Ce réarrangement est dans le but de réduire la taille et la complexité des brasseurs hiérarchiques sans se servir de traducteurs de longueurs d'onde. Ce but est atteint en travaillant la contiguïté des longueurs d'ondes pour former des bandes prêtes à un brassage par bloc.

Pour une opération en ligne, le réarrangement n'est pas pratiquement permis comme il cause l'interruption du trafic. Pourtant dans certain cas, on peut tolérer des interruptions de courte durée et appliquer donc le réarrangement de longueurs d'onde dans le but d'optimiser le regroupement en bande et par suite diminuer la probabilité de blocage des futures demandes. La méthode ainsi décrite réduit les informations à communiquer et les changements à faire (et par suite la durée d'interruption) pour compléter le réarrangement.

On présente d'abord un programme linéaire à variables entières pour formuler le problème et ensuite on propose une méthode heuristique pour trouver une solution applicable aux grands réseaux.

Comme méthode heuristique, on propose de remplir les bandes d'ondes l'une après l'autre. Pour chaque position (ou canal) libre dans la bande d'ondes, on choisit la longueur d'onde logique non placée (candidat) qui contribue le mieux à former des bandes à commuter en bloc.

Le nombre de bandes à commuter en bloc est estimé sur l'ensemble des nœuds. Dans une bande donnée et au niveau de chaque nœud, trois cas sont possibles :

1. Le candidat contribue à former une bande pouvant être commutée en bloc.
2. Le candidat détruit la possibilité de brasser en bloc.
3. Le candidat est neutre puisque déjà la bande ne peut pas être commutée en bloc.

Notons qu'après avoir trouvé la solution, chaque nœud est considéré à part. Si le nombre total de ports du brasseur hiérarchique est inférieur à celui du brasseur simple, on adopte le brasseur hiérarchique. Sinon le brasseur simple sera adopté.

### ➤ **L'ingénierie du trafic et le trafic dynamique.**

L'optimisation du contrôle des brasseurs optiques hiérarchiques dans le contexte du trafic dynamique fait l'objet d'une solution d'ingénierie du trafic proposée dans cette thèse. On commence par la construction de la topologie logique multicouche à partir du modèle graphique proposé. Cette topologie constitue la base d'information pour l'ingénierie du trafic. On applique l'algorithme du flot maximal pour trouver les liaisons de sortie sollicitées par le plus grand nombre de liaisons d'entrée afin de leur donner la priorité à utiliser les démultiplexeurs/multiplexeurs permettant le passage d'un niveau de granularité à un autre.

Le problème de base c'est de bien partager les multiplexeurs/démultiplexeurs menant d'une granularité à l'autre (d'une couche à l'autre). Pour un chemin à établir et au niveau de chaque nœud intermédiaire, on doit poser la question suivante : jusqu'à quelle granularité faut-il démultiplexer?

Dans les travaux documentés, le problème se limite à trouver la granularité au niveau de la source et la destination sans considérer ce choix pour les nœuds intermédiaires, sauf pour les ressources utilisées en partie.

Les multiplexeurs et les démultiplexeurs permettent le passage d'une granularité de commutation à l'autre. Le nombre de ces éléments doit être limité afin de réduire la complexité. Ce sont considérés comme étant les rares ressources.

La décision de multiplexer ou de démultiplexer crée un plan de distribution de tunnels emboîtés. On doit optimiser l'établissement de ces tunnels pour bien exploiter l'utilisation des



multiplexeurs et des démultiplexeurs tout en réduisant la probabilité de blocage des futures demandes.

La structure des tunnels emboîtés, donnée par la topologie logique multicouche, nous permet d'évaluer combien, à chaque granularité, une liaison de sortie (d'entrée) donnée est sollicitée par différentes liaisons d'entrée (de sortie) en tenant compte du trafic potentiel sur ces différentes liaisons. Cette information est très utile pour décider si on doit privilégier l'attribution d'un multiplexeur (démultiplexeur) à une liaison ou bien favoriser de contourner les commutations à fines granularités.

Pour estimer le trafic potentiel, tout en ayant la structure des tunnels emboîtés, on propose d'utiliser l'algorithme du flux maximal (Ford-Fulkerson) qui donne une distribution possible du trafic qui maximise le remplissage des supports de trafic. En privilégiant l'utilisation des multiplexeurs et des démultiplexeurs selon ce trafic potentiel, on favorise la convergence vers une distribution du trafic qui optimise l'utilisation des ressources et maximise le remplissage des supports de trafic.

#### ❖ Conclusion

Cette conclusion récapitule les contributions de cette thèse et ouvre la voie à de nouveaux thèmes de recherche.

Par suite du groupement par bandes d'onde, la complexité du matériel des brasseurs optiques peut être réduite en utilisant des brasseurs hiérarchiques ou à plusieurs niveaux de granularité où on a le choix de contourner ou non un brassage individuel par longueur d'onde. Par suite du multiplexage temporel, le groupage électronique du trafic est largement utilisé pour exploiter l'immense bande spectrale d'une longueur d'onde comparée à la vitesse des composants électroniques. L'idée de base derrière les réseaux optiques à plusieurs niveaux de granularité c'est de regrouper ces deux concepts de groupage optique et électronique ainsi qu'avec de différents niveaux d'agrégation.

On propose un modèle graphique pour décrire l'évolution d'un réseau optique à plusieurs niveaux de granularité. L'importance de ce modèle revient à fournir une base d'informations complète pour servir à l'ingénierie du trafic. Comparé aux modèles existants, celui-ci est caractérisé par:

- Supporter les niveaux multiples de groupage.

- La capacité de poursuivre le progrès du réseau optique à plusieurs niveaux de granularité.
- Le fait que, à l'établissement d'une connexion, la décision cruciale de contourner ou passer aux plus fines granularités au niveau des nœuds intermédiaires fait partie de l'optimisation du graphe.
- La possibilité de donner un modèle à tous les composants d'un réseau optique à plusieurs niveaux de granularité.

On étudie la réduction de la complexité du matériel et l'augmentation de la complexité opérationnelle quand on remplace un brasseur optique simple par un brasseur optique hiérarchique. Le modèle analytique conçu permet de décrire comment la connectivité est réduite si on considère le brasseur hiérarchique à la place d'un brasseur simple. C'est important dans la phase de planification et de dimensionnement du réseau à plusieurs niveaux de granularité où on doit comparer différentes réalisations utilisant les mêmes ressources avec des différentes granularités, différents nombres de longueurs d'onde dans une fibre en réglant le nombre de fibres dans un réseau multifibre, etc. ... Par exemple, la même réduction de la complexité du matériel peut être obtenue pour différentes granularités de bandes d'ondes avec un nombre différent de fibres par liaison ; pourtant la probabilité de blocage n'est pas la même. Le modèle analytique proposé trouve la réalisation permettant d'améliorer la connectivité du réseau.

On propose le réarrangement des longueurs d'onde comme solution pour optimiser l'utilisation des brasseurs optiques hiérarchiques dans le contexte des réseaux optiques à plusieurs niveaux de granularité. Ceci est réalisé sans changer la distribution du trafic résultant du routage et de l'attribution des longueurs d'onde. En utilisant un algorithme heuristique, on montre comment, dans plusieurs cas, le réarrangement est efficace. Ceci ne concerne pas uniquement le trafic statique. En effet, le réarrangement proposé dans cette thèse ouvre de nouvelles perspectives pour améliorer l'état du réseau optique à plusieurs niveaux de granularité avec un minimum de changement pour réduire le nombre de connexions interrompues durant le réarrangement dans le contexte du trafic dynamique.

On propose de construire, en utilisant le modèle graphique, une topologie logique multicouche dans le but d'avoir une base d'informations adaptée à la proposition d'ingénierie

de trafic. Dans cette solution d'ingénierie du trafic, on se base sur l'algorithme du flot maximal, en particulier celui de Ford-Fulkerson. Cette approche de flot est utilisée pour estimer la meilleure utilisation éventuelle des ressources du réseau. Cette meilleure utilisation est considérée comme référence pour fournir la meilleure distribution possible des futures demandes. La solution de l'ingénierie du trafic consiste à renforcer cette distribution en accordant les multiplexeurs/démultiplexeurs (ressources rares) aux liaisons critiques. Les résultats des simulations montrent la réduction de la probabilité de blocage quand cette solution d'ingénierie du trafic est adoptée par rapport au cas où, au niveau des nœuds intermédiaires, on choisirait de contourner ou de toujours passer à travers le brassage à de fines granularités. Ceci montre l'importance de la décision cruciale de choisir jusqu'à quel niveau doit-on démultiplexer au niveau des nœuds intermédiaires et l'importance d'inclure cette décision dans l'optimisation du graphe.

Quelques domaines à aborder en perspective :

- La protection et le rétablissement dans le contexte des réseaux à plusieurs niveaux de granularité et comment bénéficier du réarrangement dans ce cas.
- Le plan de contrôle comme par exemple GMPLS et la signalisation nécessaire au réarrangement proposé pour réduire la probabilité de blocage avec le minimum de trafic à interrompre durant ce réarrangement.
- Conception de méthodes de simplification du graphe proposé pour réduire le nombre de sommets et arcs et appliquer les algorithmes d'optimisation aux larges réseaux. La construction de la topologie logique multicouche peut constituer un point de départ.
- L'adaptation des outils et solutions d'ingénierie du trafic au réseau du monde réel.

# MULTI-GRANULAR WDM OPTICAL NETWORK MODELING AND OPTIMIZATION

## ABSTRACT

Wavelength-routed optical networks use optical cross-connects (OXC) to route data flows on the basis of the assigned wavelength and the input fiber. These all-optical networks reduce the optical-to-electronic and electronic-to-optical (O/E/O) conversion that represents the dominant cost factor.

The migration from ring to arbitrary mesh topologies and from static to dynamic traffic in optical networks gives rise to increased complexity. Larger OXCs are needed (increased hardware complexity) to handle this time and space diversity and hence ensure individual forwarding and operational flexibility. On the other hand, scalability and tractability problems arise and large OXCs are difficult to realize, much more expensive than small optical switches and also much more complex in term of management controls.

To reduce the size and complexity of OXCs, the optical granularity or optical grooming is introduced. This describes the ability to treat a number of wavelengths in the same way without any distinction as if the component is unaware of their individual identity. Contiguous wavelengths treated as a single entity form a waveband that uses a single pair of input/output ports to cross a node. This is compared to electronic granularity achieved by means of time-division multiplexing.

This grooming concept is extended to create hierarchical levels of grooming in the optical as well as in the electronic domain. This way we can create what is called multi-granular optical network characterized by different scales of differentiation in the switching operations.

This multi-granular optical network creates a compromise between hardware and operational complexity. New optimization and network dimensioning problems arise to

control and design the multi-granular or hierarchical optical cross-connects (MG-OXC or HXC).

In this thesis, we model first the multi-granular network using a novel Multi-Granularity Graph Model (MGGM) to keep track of the state evolution of MG-OXCs with connection setting up and exclusion. We can weight the edges in the MGGM to apply graph optimization algorithms. We can also use it to update the logical topology and have an information base to apply traffic engineering solutions.

In the MGGM, we define the basic network element (BNE) as a sub-graph having a set of edges and vertices representing input and output ports. The BNE is used as a basic object to model any network element in the multi-granular context, such as fibers, wavelength converters, tuned and fixed transmitters/receivers, MG-OXCs, etc...

The key of this model is the group concept that defines the belonging of BNE's edges to entities (or ports) having a given granularity and also the switching state of these entities. Input and output ports of the same BNE can have different granularities but an output port of a BNE is applied to an input port of another BNE at the same granularity. This makes the model well adapted to multi-granular optical networks. We define a set of four operations applied on groups and edges to consider any operation on the network and hence update the MGGM.

We then propose an MG-OXC (or HXC) analytical model to analyze the intrinsic operational complexity of an MG-OXC before studying its behavior in an optical network. This is done by defining a model to count the number of possible connection patterns to serve a given number of connections and then comparing this number to that obtained when a non-hierarchical WXC is used. Numerical applications are given to compare different MG-OXC hardware implementations.

We then propose a wavelength rearrangement to optimize, when it is possible, the state of a multi-granular optical network with a minimum of information to broadcast all along the network. In fact, this is placed in the static traffic context where we have a given traffic demand pattern. After applying routing and wavelength assignment algorithms (RWA) independently of the multi-granular nature of OXCs (note that this could be the natural result of dynamic traffic planning when rearrangement is to be done), wavelength rearrangement can change the order of wavelengths to satisfy, as far as possible, the contiguity of wavelengths making useful wavebands ready to be cross-connected as a single entity. This is done without disturbing the

RWA operation, i.e., without changing the distribution plan resulting from RWA. In the case of optimizing the state of the network, the mapping of wavelength channels to be assigned to logical wavelengths (characterizing lightpaths that must have the same wavelength channel as specified by RWA) is to be exchanged in order to rearrange wavelengths while minimizing interrupted traffic and signaling information. This produces new cross-connect schemes in the network and freeing some interlayer multiplexers/demultiplexers representing the expensive resources in MG-OXCs. Interlayer multiplexers/demultiplexers provide access to pass from a switching granularity to another.

To achieve rearrangement, we propose an integer linear programming (ILP) formulation and a heuristic method to find a valid design solution for large-scale networks. Upper bounds on the hardware complexity reduction are also found.

Finally, we consider the dynamic traffic context in multi-granular optical networks where demands arrive at the finest granularity and should be connected without any information on future demands. This must be done in a way to minimize the blocking probability of subsequent demands.

The main problem is to know when to proceed with demultiplexing/multiplexing to use finer and finer granularities at each node for a given demand. First we define the layered logical topology and how we could build it using the MGGM. Then we discuss the different possible cases before proposing a traffic engineering solution.

The proposed traffic engineering solution is based on applying the Ford-Fulkerson maxflow algorithm on the layered logical topology. This algorithm gives a possible realization of the flow distribution to reach the upper bound on the traffic flow between a potential source and destination. This possible flow distribution is assumed to be a target to optimize the network. We mean by target a possible traffic distribution that maximizes the use of available resources. Based on targets collected for all potential source/destination pairs, we deduce in each node and at each switching layer (i.e. switching granularity) the set of input ports and output ports that are potentially the best to be interconnected. We promote then these input/output ports to be applied to interlayer multiplexers/demultiplexers.

# TABLE OF CONTENTS

TABLE OF CONTENTS.....	I
LIST OF FIGURES.....	IV
I. INTRODUCTION.....	1
I.1. Introduction to Multi-Granular Optical Networks.....	2
I.1.1 Granularity.....	2
I.1.2 Wavebanding or Optical Grooming.....	2
I.1.3 Multi-Granularity and Multi-Layer.....	3
I.1.4 Single and Multi-Layer Optical Cross-Connect.....	4
I.1.5 Uniform and Non-Uniform Wavebands.....	5
I.1.6 Control Plane.....	6
I.2. Motivation and Contributions of this Thesis.....	7
I.3. Related Works.....	9
I.3.1 Graph Model.....	9
I.3.2 Analytical Model.....	10
I.3.3 Static Traffic.....	10
I.3.4 Dynamic Traffic.....	11
I.3.4.1. Traffic Grooming.....	11
I.3.4.2. Multi-Granular Optical Network.....	12
I.4. Organization of the Document.....	14
II. MULTI-GRANULARITY GRAPH MODEL (MGGM).....	16
II.1. Introduction.....	16
II.2. The Basic Network Element.....	19
II.3. Group Concept.....	21
II.4. Shared Vertices, Sharing Condition and the Waveband Cross-Connect Model.....	22
II.5. Operations.....	23
II.5.1 Shared Vertices and Grooming Capable WXC with Wavelength Converters.....	25
II.6. Dead Edges.....	26
II.7. Hierarchical Cross-Connect Model and the Need for Dead Edges.....	28
II.8. The Generalized MGGM.....	31
II.8.1 Intra-Shared Group Vertex.....	31
II.8.2 Add and Drop Vertices: The Only Two Shared Main Vertices.....	32
II.9. Differentiated Cost and Extra Dead Edges.....	33
II.10. Setting Up or Tearing Down a Connection.....	35
II.11. Useful Examples.....	36
II.11.1 Tuned Receivers/Transmitters.....	36
II.11.2 Limited Number of Wavelengths Converters.....	37
II.12. Conclusion.....	38

### III. ANALYTICAL MODEL FOR HIERARCHICAL OPTICAL CROSS-CONNECT

39

III.1.	Introduction.....	39
III.2.	The Hardware Complexity Reduction Ratio .....	40
III.3.	The Operational Complexity Increase Ratio .....	45
III.4.	The Wavelength Cross-Connect Model .....	46
III.5.	The Hierarchical Cross-Connect Model.....	48
III.5.1	Internal Flexibility and Evaluation of $\mathbf{x}_{\mathbf{v}^{in}, \mathbf{v}^{out}}^{N, M, W}(y)$ .....	52
III.5.2	Evaluation of $r_w^{n, m}(y)$ .....	54
III.6.	Numerical Results.....	57
III.7.	Conclusion .....	59
IV.	STATIC TRAFFIC AND WAVELENGTH REARRANGEMENT.....	60
IV.1.	Introduction.....	60
IV.1.1	Wavelength Banding and Hierarchical Cross-Connect.....	60
IV.1.2	Related Works.....	61
IV.2.	Wavelength Rearrangement.....	61
IV.2.1	The Purpose of Wavelength Rearrangement .....	61
IV.2.2	The Number of Possible Solutions .....	62
IV.3.	Problem Formulation.....	63
IV.3.1	Constants and Variables .....	63
IV.3.2	The Integer Linear Programming.....	66
IV.3.3	Bounds on the Complexity Reduction .....	68
IV.3.4	The Proposed Heuristic Method.....	72
IV.4.	Numerical Results.....	75
IV.4.1	Uniform Traffic .....	75
IV.4.2	Non Uniform Traffic .....	75
IV.5.	Conclusion .....	77
V.	DYNAMIC TRAFFIC AND TRAFFIC ENGINEERING.....	78
V.1.	Introduction.....	78
V.1.1	Switching Granularity .....	78
V.1.2	Cross-Connect Control.....	78
V.2.	Multi-Layer Switching.....	79
V.3.	Multi-Layer Tunneling and the Layered Logical Topology .....	80
V.4.	Layered Logical Topology Construction Using MGGM .....	88
V.5.	Traffic Engineering Solution.....	91
V.5.1	Problem Description.....	91
V.5.2	Proposed Solution.....	93
V.6.	Numerical Results.....	96
V.7.	Conclusion .....	100
VI.	CONCLUSION OF THE THESIS .....	102



A.	WAVELENGTH ASSIGNMENT AND TRAFFIC GROOMING IN RING NETWORK TOPOLOGIES.....	105
A.1.	Introduction.....	105
A.2.	Representing Lightpaths.....	106
A.3.	Problem Description.....	107
A.4.	Wavelength Assignment.....	109
A.4.1	The Purpose of Wavelength Assignment.....	109
A.4.2	Allocating Uniform Traffic.....	110
A.4.3	Allocating Non-Uniform Traffic.....	112
A.5.	Traffic Grooming.....	115
A.6.	Problem Formulation.....	121
A.6.1	Matrix Representation.....	121
A.6.2	The ILP Formulation.....	124
A.7.	Conclusion.....	125
B.	A BRIEF ON THE FORD-FULKERSON MAXFLOW ALGORITHM.....	126
C.	THE PRINCIPLE OF INCLUSION AND EXCLUSION.....	127
D.	THE REARRANGEMENT ILP IN GLPK.....	129
D.1.	Coding Model Rearr.mod.....	129
D.2.	Data Model Rearr.dat.....	130
	LIST OF PUBLICATIONS.....	131
	MAIN REFERENCES.....	132
	INDEX.....	135

## LIST OF FIGURES

<i>Number</i>	<i>Page</i>
Figure 1: Three-layer multi-granular optical cross-connect.....	4
Figure 2: Single-layer multi-granular optical cross-connect.....	5
Figure 3: Multi-granular OXC taxonomy.....	6
Figure 4: Establishing connections through different grooming and granularity layers.....	7
Figure 5: Layered graph model.....	17
Figure 6: Alternate routes given in [40].....	18
Figure 7: Two possible switching granularities, at intermediate node 0, for the same route on the layered graph. ....	19
Figure 8: A Basic Network Element (BNE) modeling a fiber.....	20
Figure 9: Waveband Cross-Connect Graph Model. ....	23
Figure 10: MERGE operation.....	24
Figure 11: A wavelength cross-connect with and without wavelength conversion capability. .	25
Figure 12: First problem arising when applying the shortest path.....	26
Figure 13: Second problem arising when applying the shortest path.....	26
Figure 14: Merging groups connected through dead edges.....	27
Figure 15: HXC graph model where we must allow negative costs.....	28
Figure 16: HXC graph model with dead edges to avoid negative costs.....	29
Figure 17: Example showing the passing through the $\lambda$ XC in the MGGM. ....	30
Figure 18: Example showing the wavelength switching operation in the MGGM.....	31
Figure 19: ADD/DROP vertices and the generalized MGGM. ....	32
Figure 20: For a given wavelength, we have the same preference (between bypassing and passing through) for all input/output pairs.....	34
Figure 21: Differentiated preference (between bypassing and passing through) depending on the input/output pair.....	35
Figure 22: Tuned receivers.....	36
Figure 23: limited number of wavelength converters.....	37
Figure 24: Two-layer Hierarchical Cross-Connect (HXC).....	40
Figure 25: Blocking probability and HCCR for different values of $\mathbf{f}$ and $\mathbf{q}$ when $\rho=600$ .....	44

Figure 26: The WXC array model. ....	47
Figure 27: The HXC model. ....	49
Figure 28: The $\lambda$ XC model for a given waveband (e.g. O2). ....	50
Figure 29: Another representation of the array of figure 27 for a given waveband (e.g. O2)...	50
Figure 30: Internal flexibility: three ways to implement the same connection pattern. ....	53
Figure 31: An example where a bypassed waveband cannot be substituted to a crossed waveband. ....	53
Figure 32: The set of W sub-boards for a given waveband where for the $i$ th position we exclude all other entries in the same row and column. ....	55
Figure 33: We have the same number of connection patterns for all positions so we consider the first one. ....	55
Figure 34: Considering that for a given waveband we have the property 1 and the property 2.56	
Figure 35: OCIR( $y$ ) for different waveband granularities and different HCRRs. ....	57
Figure 36: The number of possible connection patterns for $N=M=6$ and $\Lambda=8$ . ....	58
Figure 37: $N=M=8$ and $\Lambda=8$ . ....	58
Figure 38: $N=M=6$ and $\Lambda=12$ . ....	59
Figure 39: An example showing a network where $T=10$ to clarify the definition of $\sigma_{pq}$ . ....	64
Figure 40: example to clarify the definition of $\eta_{ip}$ , $\Psi_{ipq}$ and $\chi_{ipq}$ . ....	65
Figure 41: The number of input ports in a WXC. ....	69
Figure 42: Best case for an HXC. ....	70
Figure 43: The upper bound on HCRR for uniform traffic. ....	71
Figure 44: A candidate contributing in forming a packed waveband. ....	72
Figure 45: A candidate breaking a packed waveband. ....	73
Figure 46: Already broken waveband. ....	73
Figure 47: Complexity reduction for uniform traffic. ....	75
Figure 48: Complexity reduction for a non-uniform traffic pattern ( $\mu=7$ ) with a waveband granularity $W=4$ . The results of the described heuristic algorithm and upper bounds are shown for each node. ....	76
Figure 49: The number of nodes in the network where HXC is cost-effective. ....	76
Figure 50: Mapping tunnels and interlayer multiplexers for a multi-layer MG-OXC. ....	81
Figure 51: Example five-node network physical topology. ....	82

Figure 52: Example of establishing three connections through different grooming and granularity layers.....	83
Figure 53: Initial layered logical topology.....	84
Figure 54: First connection path and multi-layer tunnels.....	85
Figure 55: Logical topology after setting up the first connection. ....	86
Figure 56: Second connection path and new multi-layer tunnels. ....	87
Figure 57: Logical topology after setting up the second connection.....	88
Figure 58: Third connection path and new multi-layer tunnels. ....	89
Figure 59: Logical topology after setting up the third connection. ....	90
Figure 60: Tunnel indexing in layer i.....	93
Figure 61: Passing from layer j to layer i and interlayer multiplexers/demultiplexers.....	94
Figure 62: Passing from layer j to layer k through an i-layer switching. ....	95
Figure 63: Test network for dynamic traffic.....	97
Figure 64: Results when we have <b>five</b> interlayer multiplexers/demultiplexers per waveband. HCRR is shown for each node in the network. ....	97
Figure 65: Results when we have <b>four</b> interlayer multiplexers/demultiplexers per waveband. HCRR is shown for each node in the network. ....	99
Figure 66: Blocking probability for hybrid network where the number of interlayer multiplexers/demultiplexers is chosen in order to have a HCRR=33.33% for all transit nodes.....	100
Figure 67: Representing lightpaths. ....	106
Figure 68: Example on circle representation.....	107
Figure 69: example showing that packing demands into circles and then grouping circles can lead to 20% more ADMs than considering the two steps jointly. ....	109
Figure 70: Wavelength assignment example minimizing the number of wavelengths.....	109
Figure 71: Wavelength assignment with more wavelengths but less ADMs. ....	110
Figure 72: Four and three-connection circles.....	111
Figure 73: Gaps in a circle construction.....	113
Figure 74: A. Full circles generated by CATS. B. Another type of full circles.....	114
Figure 75: A. Trying CATS' full circles with all possible rotations. B. Trying CATS' full circles with no rotation.....	115
Figure 76: Saved ADMs when applying full circles rotation. ....	115
Figure 77: Example of traffic to groom.....	117

Figure 78: Comparing AlgI and AlgII ( $\mu=2$ ).....	118
Figure 79: Saving in ADMs number using AlgII versus AlgI ( $\mu=2.5$ ).....	118
Figure 80: AlgI and AlgII applied on different randomly generated traffic demand matrix...	119
Figure 81: AlgI versus AlgII for $\mu=2$ .....	120
Figure 82: Saving ADMs (AlgII versus AlgI).....	120
Figure 83: AlgIII versus AlgIV for $\mu=2.5$ .....	121
Figure 84: Example of circles to groom.....	122
Figure 85: Test network used to generate the data model.....	129

## I. INTRODUCTION

Next-generation optical networks or Automatic Switched Optical Networks (ASON) are characterized by enabling dynamic setup and tear down of lightpath connections through optical switching equipments such as optical cross-connects (OXC). Using OXC, we can route data flows on the basis of the assigned wavelength and the input fiber. These all-optical networks reduce the optical-to-electronic and electronic-to-optical (O/E/O) conversion that represents the dominant cost factor.

Wavelength division multiplexing (WDM) is the most promising solution to exploit the huge bandwidth of a fiber. In WDM, the fiber bandwidth is divided into multiple channels, each operating at a given wavelength, and specific data rate tailored to the speed of electronic devices.

The wavelength could be underutilized unless it is filled up by an efficiently aggregated traffic through, for instance, time division multiplexing (TDM) or burst or packet switching. From another point of view, grooming wavelengths at intermediate nodes through wavebanding improves scalability and reduces the hardware complexity of switching equipments.

Combining different concepts of optical and electronic grooming toward a scalable, controllable and cost-effective optical network is the main idea behind multi-granular optical networks. This is done by handling different dynamic scales and different levels of aggregation when this aggregation could be done in space (WDM and wavebanding) and time (TDM or burst switching) domain.

Different scales of differentiation in the switching operation characterize the multi-granular optical network by combining electronic and optical grooming and defining multiple level of aggregation.

There is a compromise between hardware and operational complexity in multi-granular optical networks. New optimization and network dimensioning problems arise to design and control these networks.

What is already done in this field is still rudimentary compared to what is expected from this approach. In fact, we cannot imagine an all-optical network with all the foreseen capacity (increased number of wavelengths per fiber) and time and space diversity (this depends on how far we are going to implement optical burst and packet switching and where) without exploiting multiple levels of aggregation.

In this document, we expose our contributions in this field by providing some tools, models and network engineering solutions. Our work highlights new proposed ideas and open the way to further researches toward a generalized implementation of this approach.

## **I.1. Introduction to Multi-Granular Optical Networks**

This section introduces multi-granular optical networks and presents some basic concepts and main architectures.

### **I.1.1 Granularity**

The term granularity is used in different fields (astronomy, fractal models, physics, information technology,...) and its meaning depends on the context in which it is being used. It can be the unit of observation or the scale of detail that characterizes an object.

In this document, the granularity of a channel is the ratio of the channel capacity to the base bandwidth rate. Switching granularity describes the number of traffic units or channels treated in the same way as a single entity without any distinction as if the component is unaware of their individual identity.

### **I.1.2 Wavebanding or Optical Grooming**

We can reduce the cost and improve the optical network performance and scalability by creating multiple switching granularities. The size and complexity of an optical cross-connect (OXC) can be reduced by treating a bundle of contiguous wavelengths within a waveband as a single entity. By this way, a pair of input/output ports is used instead of  $W$  pairs, where  $W$  is the waveband granularity, i.e. the number of wavelengths within a waveband channel. This is

only feasible if all included wavelengths are routed in the same way. Treating a number of wavelengths in bulk adds burden to the routing and wavelength assignment (RWA) in order to conveniently fill the waveband and enhance the optical throughput.

To add some flexibility, some input and output ports of the waveband cross-connect are connected through demultiplexers/multiplexers to a wavelength cross-connect. By this way, we can resolve the bulk switching of some wavebands and break the tunneling continuity and hence pass from a given waveband tunnel to one or more other tunnels or pass through an optical-electrical-optical (O/E/O) fabric to provide optical 3R (regeneration, reshaping, retiming), electronic grooming or maybe wavelength conversion.

In other words, traffic grooming at the optical layer by grouping wavelengths into wavebands and wavebands into coarser wavebands or into fibers reduces the size and complexity of optical cross-connects. Coarse granularities minimize the number of ports however to manage the utilization of wavebands or what we call optical throughput we must switch to finer granularities.

Wavebanding is cost-effective when we can reduce the need to switch the individual wavelengths by demultiplexing a waveband. Therefore, wavebanding is attractive in the backbone where the bypass traffic accounts for 60% to 80% of the total traffic [1].

### **I.1.3 Multi-Granularity and Multi-Layer**

Multi-granularity and multi-layer are often confused or sometimes intentionally used interchangeably as in [40] where multi-granularity is considered as a more general concept than what is usually referred as multi-layer. In this document, we mean by multi-granularity the ability to interconnect elements experiencing different switching granularities. Multi-layer is when a connection can pass through different levels of aggregation inside the same node. We can have a single layer multi-granular optical cross-connect where inside the same node we find different switching granularities but where a connection can pass through only one optical aggregation, i.e. there is no possible passage inside the node from a switching granularity to the other. In [16], the multi-granularity optical network is classified as homogeneous where all nodes are hierarchical nodes or heterogeneous where some nodes are not. In this document, the word multi-granularity goes beyond this classification since it covers the case where two different nodes have different hierarchical structures. For instance, in a given node, we can



define a waveband granularity of 4 wavelengths, in a second node, a waveband granularity of 6 wavelengths and in a third one, only individual wavelengths can be switched.

#### I.1.4 Single and Multi-Layer Optical Cross-Connect

Two main architectures of multi-granular optical cross-connects (MG-OXC) are found in literature: the multi-layer MG-OXC and the single-layer MG-OXC. In both architectures, we have a hierarchy of cross-connects each at a different switching granularity.

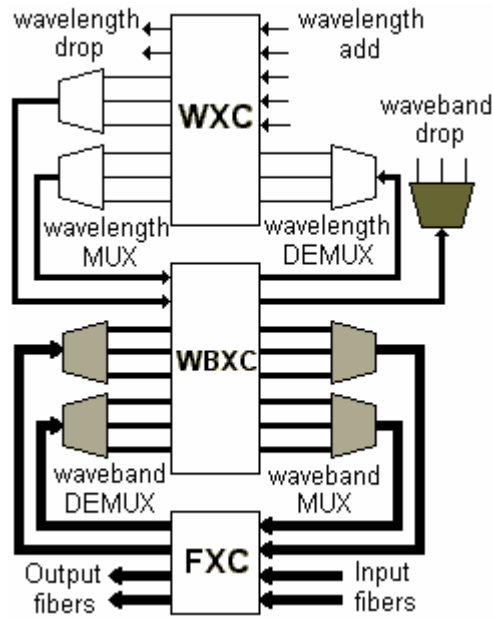


Figure 1: Three-layer multi-granular optical cross-connect.

In the multi-layer MG-OXC, a lightpath is first demultiplexed to the coarsest granularity to pass through the coarsest granularity switch. Then it either bypasses all finer granularities or it is switched to a demultiplexer (interlayer demultiplexer) providing channels at a finer granularity. These channels can bypass or pass through a finer granularity switch and so on. Note that to go back to the output fiber the lightpath must cross all coarser layers again (through interlayer multiplexers). Figure 1 shows a three-layer MG-OXC, at the finest granularity we have the wavelength cross-connect (WXC), then the waveband cross-connect (WBXC) and at the coarsest granularity we have the fiber cross-connect (FXC).

In the single-layer MG-OXC, designated fibers pass through the FXC; others are demultiplexed to a finer granularity such as wavebands. Designated wavebands pass through

the WBXC and others are demultiplexed to pass through the WXC as shown in figure 2. There are no interlayer multiplexers/demultiplexers which results in a better reduced complexity. As mentioned in [1] the signal quality is better than that of a multi-layer MG-OXC since all lightpaths go through only one switching fabric.

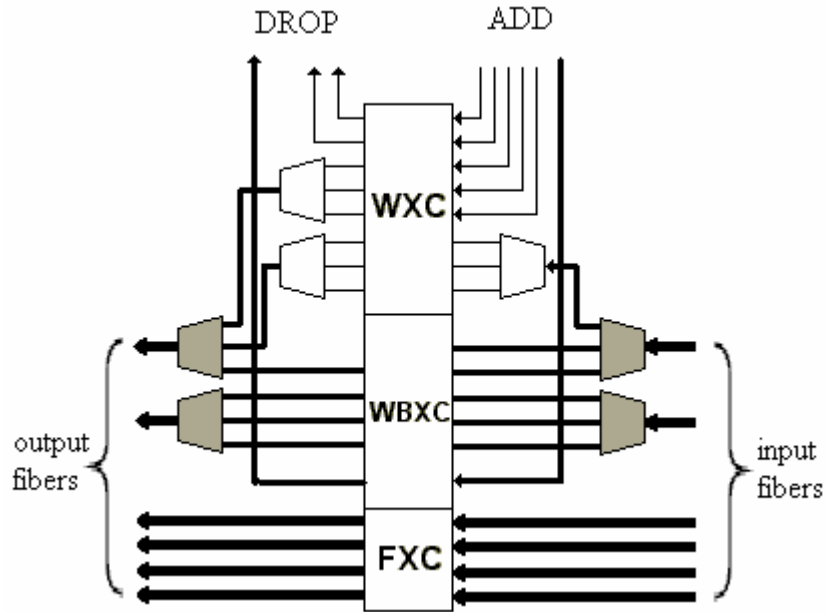


Figure 2: Single-layer multi-granular optical cross-connect.

The multi-layer and single-layer architectures are compared in [1]. The comparison indicates that the single-layer is more suitable for the off-line case (static traffic) since it uses 15% fewer ports than the three-layer; while for the on-line case (dynamic incremental traffic), the three-layer is better since it achieves a lower blocking probability.

The graph model proposed in the next chapter can cover the two architectures but in this document we focus on the multi-layer MG-OXC since it is more flexible and more adapted to dynamic network operations.

### I.1.5 Uniform and Non-Uniform Wavebands

Distributing demands on wavebands having different granularities can match the granularity to the size of the demand. This improves the optical throughput. Hybrid hierarchical optical networks with non-uniform wavebands are studied in [17] and [16]. The all-optical non-uniform solution can replace in many cases the O/E/O solution. In fact, passing

through a finer granularity switch (e.g. an O/E/O wavelength switch) could be replaced by passing through a finer granularity waveband.

In other words, the non-uniform waveband solution can be seen as a general case of the single-layer multi-granular optical cross-connect. We propose then the multi-granular optical cross-connect taxonomy shown in figure 3. Note the intersection between the non-uniform waveband case and the multi-layer case since in the latter case, each layer can have a non-uniform deaggregator/aggregator and a single-layer-like structure.

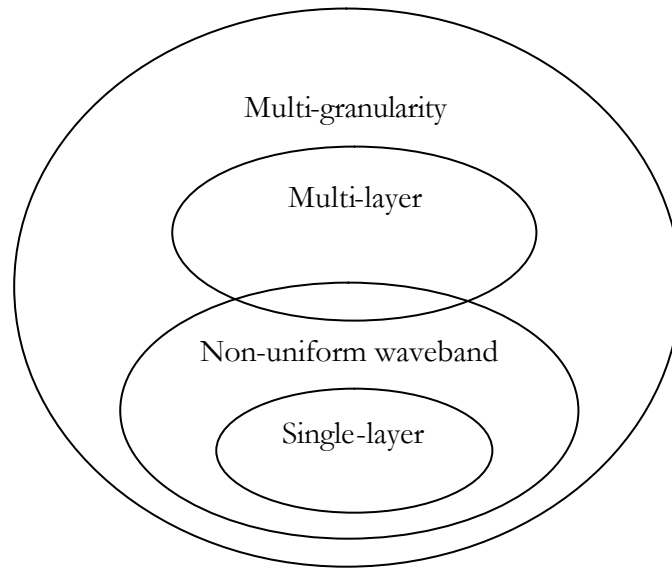


Figure 3: Multi-granular OXC taxonomy.

The graph model described in the next chapter can support among others hybrid optical networks with non-uniform wavebands.

### I.1.6 Control Plane

A Generalized Multi-Protocol Label Switching (GMPLS) control protocol is assumed so that all information on the network status is updated at each node. This protocol is an extension of MPLS where labels can represent wavelengths, wavebands (set of contiguous wavelengths), fibers, etc ... and multi-granular optical flows are supported by a hierarchical structure.

## I.2. Motivation and Contributions of this Thesis

As mentioned before, new optimization and network dimensioning problems arise to design and control multi-granular optical networks. Multi-granular grooming and multi-layer switching result in a multi-layer tunneling scheme. It is crucial to map the established tunnels at their proper layer in order to control the network cross-connects. Controlling a cross-connect means to decide at which granularity the switching must be done. That is answering the following question: how far we must proceed with demultiplexing/multiplexing channels for a given path at each node? The answer depends on the current traffic allocation, the logical topology and the objective to reach in network optimization.

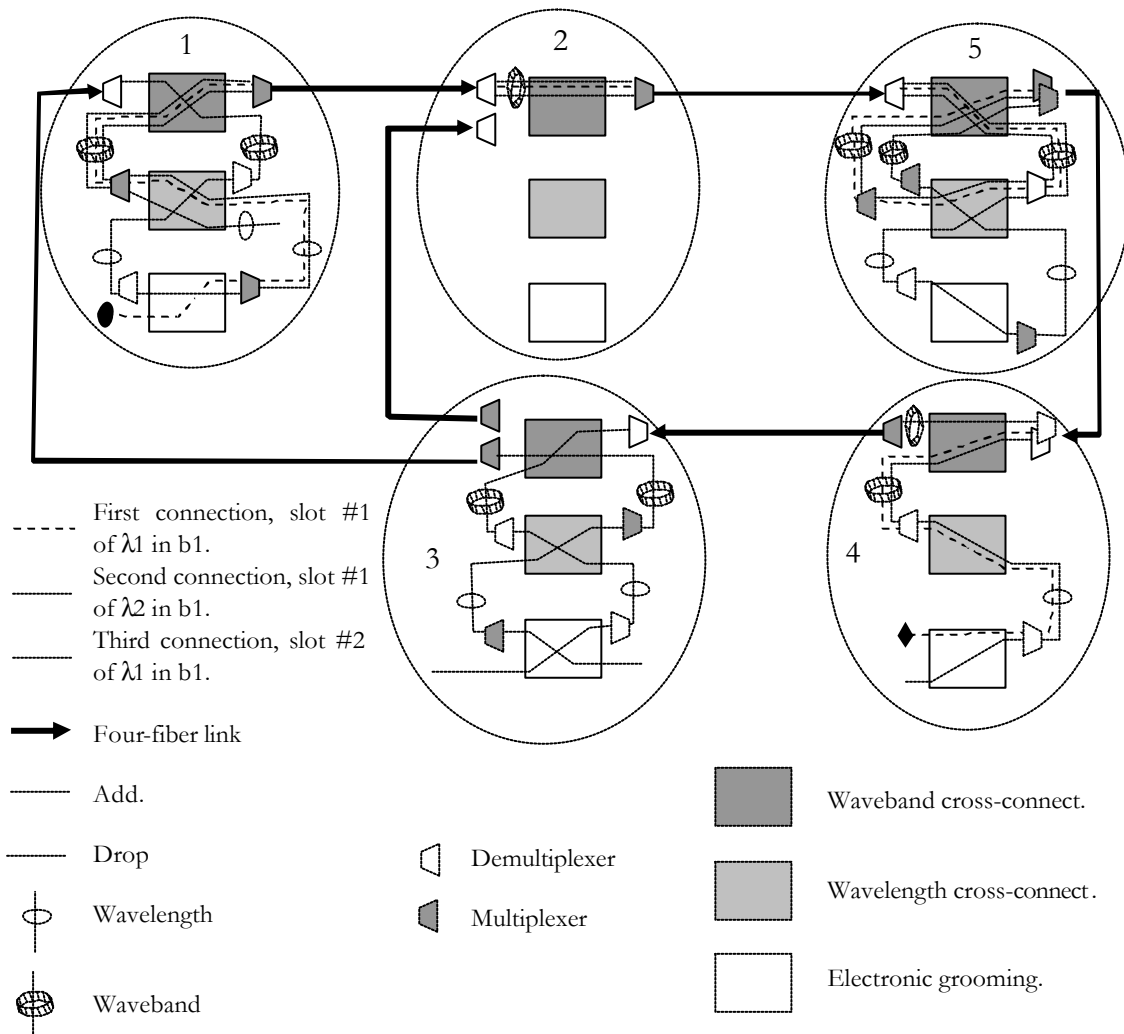


Figure 4: Establishing connections through different grooming and granularity layers.

Figure 4 illustrates how a connection can pass through different levels of aggregation at intermediate nodes between source and destination (note that we will emphasize this example later in chapter 5). To reduce the hardware complexity, we reduce the number of interlayer aggregators/deaggregators and the problem of managing the use of these interlayer elements, representing the expensive resources, arises. This is what we call in this thesis "the cross-connect control" (where the OXC is a MG-OXC) that we must add to RWA. Moreover, the choice of the route should not only depend on RWA optimization but also on optimizing this control.

The contributions of this thesis are the following:

- The Multi-Granularity Graph Model or MGGM (chapter 2) providing a complete base of information to be used by traffic engineering solutions. With this model, the crucial decision of bypassing or passing through lower layers at intermediate nodes is part of the graph optimization and different grooming and cross-connect control policies can be implemented.
- An evaluation of the hardware and operational complexities and their impact on the multi-granular network design (chapter 3).
- The concept of wavelength rearrangement to benefit from hierarchical cross-connects, its formulation and a heuristic solution (chapter 4).
- The optimization of the cross-connect control in the dynamic traffic context (chapter 5). The construction of a layered logical topology using the MGGM is described. The traffic engineering solution consists in applying the maximum flow algorithm to the layered logical topology in order to find out how much an output link is solicited from different input links in order to decide how to share interlayer multiplexers/demultiplexers. This is done by updating the cost of the MGGM edges.

### **I.3. Related Work**

Recently, attention has focused on multi-granularity in optical networks to maintain the scalability and to overcome the complexity, while increasing the optical network capacity. In this section, we go over different sectors of our contributions in this field in the framework of this thesis. We discuss the state of the art and our contributions.

#### **I.3.1 Graph Model**

Despite the diversity of implementations, an optical wavelength division multiplexed (WDM) network is modeled by an auxiliary graph expanding a node to a set of edges and vertices in order to include wavelength assignment and traffic grooming requirements. For example, the graph model given in [5] and then in [25] creates for each wavelength entering the node an input vertex and an output vertex for each wavelength leaving the node. In a given node, input and output vertices are interconnected if they represent the same wavelength or if wavelength conversion between their wavelengths is possible. Interconnecting edges are weighted to the wavelength conversion cost.

Traffic grooming, where the wavelength capacity is shared by different connections, gives rise to more complicated details concerning sub-wavelength connections. Different versions of layered graph model are then proposed in literature as in [19] and [36]. In the layered graph model, unused wavelengths are represented by edges connecting vertices in the wavelength layer (in this layer connections replicate the fiber physical links). When a demand is connected using a fraction of the wavelength capacity, the remaining capacity switches to the lightpath layer as a direct connection between the dedicated vertices in the input and output nodes of the lightpath (lightpath tunnel).

The graph is modified after each successfully routed connection. In these models, all information on used connections, lightpaths route (traversed nodes, wavelengths ...) and used slots in the lightpath must be retained in a way that is not inherently defined by the graph model. And since the graph model is much larger than the graph representing the network topology, it is not simple to keep track of the network state. Moreover, if we add a waveband layer tracking this will get worse. The layered model is used, without covering wavebanding, in [39] for traffic grooming with different granularities in term of bandwidth requirement or grooming factor.

We propose in this thesis to model the multi-granular network using a novel Multi-Granularity Graph Model (MGGM) in order to keep track of the state evolution of multi-granular optical cross-connects (MG-OXC) with connection setting up and exclusion. We can weight the edges in the MGGM to apply graph optimization algorithms. We can also use it to update the logical topology and have an information base to apply traffic engineering solutions.

The graph model we propose is adapted to multi-granular networks with multi-layer or single-layer node structure but can also cover any grooming problem. In this model, we can inherently keep track of the network evolution and state and simplify the updating when tearing down a connection. This is done by means of objects (groups) defining the belonging, the state and the significance of an edge representing any resource in the network. Instead of passing from a layer to another one in the graph, we define only four operations executed on groups of consecutive edges all along the lightpath of any granularity. By using what we call Basic Network Element, or simply BNE, we can interconnect different granularities and model the multiplexing, demultiplexing, switching, wavelength conversion, etc...

### **I.3.2 Analytical Model**

In [3], an analytical model for a wavelength cross-connect (WXC) is proposed to determine if a given connection pattern can be supported by the WXC and to evaluate the number of possible connection patterns to study the blocking performance of a WXC. In this thesis, we propose an MG-OXC (or HXC) analytical model to analyze the intrinsic operational complexity of an MG-OXC and how far it is less flexible than a simple WXC before studying its behavior in an optical network.

### **I.3.3 Static Traffic**

Connecting a given traffic demand matrix in a single and multi-level multi-granular optical network is optimized in different works. Different integer linear programming formulations and heuristic algorithms are proposed in [23], [33], [13], [28] and [2].

In [15], the design of MG-OXCs is optimized in order to expand the network according to traffic growth.

In this thesis, we propose a wavelength rearrangement to optimize, whenever possible, the state of a multi-granular optical network with a minimum of information to broadcast all along

the network. In fact, this is placed in the static traffic context where we have a given traffic demand pattern. After applying routing and wavelength assignment algorithms (RWA) independently of the multi-granular nature of OXCs (note that this could be the natural result of dynamic traffic planning when rearrangement is to be done), wavelength rearrangement comes to change the order of wavelengths to satisfy, as far as possible, the contiguity of wavelengths making useful wavebands ready to be cross-connected as a single entity. This is done without disturbing the RWA operation, i.e. without changing the distribution plan resulting from RWA. In the case of optimizing the state of the network, the mapping of wavelength channels to be assigned to logical wavelengths (characterizing lightpaths that must have the same wavelength channel as specified by RWA) is to be exchanged in order to rearrange wavelengths while minimizing interrupted traffic and signaling information. This produces new cross-connect schemes in the network and freeing some interlayer multiplexers/demultiplexers representing the expensive resources in MG-OXCs. Interlayer multiplexers/demultiplexers provide access to pass from a switching granularity to another.

To achieve rearrangement, we propose an integer linear programming (ILP) formulation and a heuristic method to find a valid design solution for large-scale networks. Upper bounds on the hardware complexity reduction are also found.

### **I.3.4 Dynamic Traffic**

In the case of dynamic traffic, demands arrive at the finest granularity and should be connected without any information on future demands. The blocking probability of subsequent demands is to be minimized. In this case, a stochastic process characterizes the traffic and traffic-engineering solutions are used to deal with the randomness and dynamics of the traffic. Note that in [22], a dynamic but deterministic traffic model is introduced and called Scheduled Lightpath Demands (SLDs). Based on the periodicity of real-world traffic, the SLDs model captures space and time distribution of traffic demands in a given network. Routing and grooming of SLDs in a multi-granular network are investigated in [21].

#### **I.3.4.1 Traffic Grooming**

Dynamic traffic grooming, without covering wavebanding, is studied in recent work. In [39], [40] and [37], the dynamic traffic grooming problem is solved using the layered graph model. By changing the cost model, different grooming policies can be achieved.



When the best path is found, it is usually a set of already used lightpaths and lightpaths to be set up. Lightpaths to be set up can cross a number of nodes. The layered graph generally and these algorithms particularly do not consider any demultiplexing/multiplexing at these intermediate nodes. In the dynamic context, the optical-to-electronic and electronic-to-optical (O/E/O) conversion should be optimized rather than minimized. Setting up a lightpath (especially a long one) affects a lot the logical network topology and the routing flexibility.

We must then decide where and when to demultiplex/multiplex. It is similar to the problem of distributing wavelength converters to be shared in a node or also to find the optimal place of regenerators but in a dynamic context.

We focus, in our traffic engineering proposal, on this decision since it will affect the logical topology evolution and its adaptability to the dynamic traffic demand.

On the other hand, in the dynamic context and since rearrangement or reconfiguration is not usually possible, the lightpath shared by different connections remain set up until all concerned connections are torn down. Since already established lightpaths are usually promoted by dynamic traffic grooming algorithms (in our solution this not the case) the life time of these lightpaths increases and this will delay the network adaptability.

#### **I.3.4.2. Multi-Granular Optical Network**

Hierarchical levels of grooming in the optical as well as in the electronic domain or what is called multi-granular optical network is studied in recent work in the dynamic traffic context.

A comparison between multi and single-layer MG-OXC is made in [1], first in the static traffic or off-line context and then for the on-line case. We are more interested in this thesis in the multi-layer architecture since it is more adequate to dynamic traffic. However, in [1] and in the on-line case, the incremental traffic is considered, i.e., additional lightpaths are set up and established connections are never torn down. For this traffic, the maximum overlap (maximizing the filling of already established waveband paths) algorithm is applied. This algorithm consists in choosing the path maximizing  $L/H$  where  $L$  is the sum of overlap length or the number of links in common with existing lightpaths and  $H$  is the number of hops. But still there is some ambiguity on the layers (or switching granularities) to bypass and those to pass through (as mentioned above in the traffic grooming section).

A modified version of multi-layer architecture, where the number of bypassing channels at a given granularity is fixed, is given in [14]. This needs more input/output ports than the multi-layer architecture described in this thesis. The problem is to optimize tunnel establishment. In this work, the priority is given to the higher granularity. Two algorithms are proposed; in the first one, the dynamic tunnel allocation is based on using existing tunnels first while giving priority to the higher granularity and in the second one, tunnels are allocated at the planning stage (off-line) by analyzing the physical topology to deduct the largest potential nodes to be ingress or egress of a tunnel.

In [20], a special version of MG-OXC is used to reduce the passage through the optical-to-electronic and electronic-to-optical (O/E/O) switch and hence reduce the use of wavelength converters. The proposed algorithm based on dynamic programming formulation can be used off-line and on-line. It minimizes the number of wavelength conversions for one request at a time. First the network is redefined using an enlarged state space where a node represents a physical node, a physical link and a wavelength by a triple  $[m, k, j]$  that represents a lightpath from node  $m$  to node  $j$  using wavelength  $k$ . Then six steps (one for initialization and five steps repeated for each request) are followed to define costs and find the path minimizing the number of O/E/O conversions. Despite the complexity of the problem, it gives the optimal solution. The used MG-OXC is different from those evoked in this thesis for different reasons:

- Deaggregators/aggregators of wavebands from and to fibers and multiplexers/demultiplexers connecting wavebands to the O/E/O switch allow adding wavelengths to a waveband bypassing the O/E/O switch. So if a waveband path starts at node  $a$  and terminates at node  $b$ , a new request can be added on a free included wavelength at any node on this waveband path (not necessarily  $a$ ) but should terminate at node  $b$ .
- When a waveband is applied to the O/E/O switch, only the wavelengths used in that waveband are assumed to require O/E/O ports since unused wavelengths do not consume any wavelength conversion resources. So, only active wavelengths are counted to value the complexity reduction, which is not the case if a waveband demultiplexer is simply applied to an O/E/O switch.

When it comes to the dynamic traffic, the main problem highlighted in this thesis is to know when to proceed with demultiplexing/multiplexing to use finer and finer granularities at each node for a given demand.

We define first the layered logical topology for a multi-granular network and we describe how we could build it using the MGGM. Then we discuss the different possible cases before proposing a traffic engineering solution.

The proposed traffic engineering solution is based on applying the Ford-Fulkerson maxflow algorithm on the layered logical topology. This algorithm gives a possible realization of the flow distribution to reach the upper bound on the traffic flow between a potential source and destination. This possible flow distribution is assumed to be a target to optimize the network. Based on targets collected for all potential source/destination pairs we deduce in each node and at each switching layer (i.e. switching granularity) the set of input ports and output ports that are potentially the best to be interconnected. We promote then these input/output ports to be applied to interlayer multiplexers/demultiplexers.

#### **I.4. Organization of the Document**

This document is organized as follows:

In chapter 2, we propose and define the Multi-Granularity Graph Model (MGGM). In this chapter, we present a graph model to keep track of the evolution of the multi-granular network state. This model can be used to apply routing and wavelength assignment and to control the MG-OXCs. We can also use it to optimize the network operation by traffic engineering solutions.

In Chapter 3, the intrinsic operational complexity of an MG-OXC is evaluated using an analytical model to count the number of possible connection patterns when a number of connections are to cross the MG-OXC. This is compared to the case of a non-hierarchical wavelength cross-connect (WXC).

The wavelength rearrangement to benefit from hierarchical cross-connects is proposed in chapter 4. Rearrangement consists in changing the order of wavelengths to satisfy, as far as possible, the contiguity of wavelengths making useful wavebands ready to be cross-connected

as a single entity. This is done without disturbing the routing and wavelength assignment (RWA) operation, i.e. without changing the distribution plan resulting from RWA.

In chapter 5, we consider the dynamic traffic context in multi-granular optical networks where demands arrive at the finest granularity and should be connected without any information on future demands. This must be done in a way to minimize the blocking probability of subsequent demands. The main problem is to know when to proceed with demultiplexing/multiplexing to use finer and finer granularities at each node for a given demand. First we define the layered logical topology and how we can build it using the MGGM. Then we discuss the different possible cases before proposing a traffic engineering solution.

We conclude this thesis in chapter 6.

In appendix A, we summarize the first part of our work in this thesis concerning wavelength assignment and traffic grooming to reduce the cost of ring based optical network. Due to the migration from ring to mesh topologies and from static to dynamic traffic in optical networks, we moved to work on multi-granular optical networks.

A brief on the maximum flow algorithm used in chapter 5 is given in appendix B.

Appendix C reviews the principle of inclusion and exclusion used in chapter 3.

Appendix D presents the coding in GLPK of the ILP given in chapter 4.

## II. MULTI-GRANULARITY GRAPH MODEL (MGGM)

### II.1. Introduction

Despite the tunneling nature of a lightpath setup where the one step cost is not always significant, most of the grooming algorithms work on a layered graph as in [36]. In these algorithms, the cost model determines the proposed strategy. The shortest path or any other graph optimization algorithm is used to connect traffic demands.

Regardless the graph structure and its layered or simple flavor, the node model is an extension of the physical node to include some of its characteristics by a combination of edges and vertices. For example, the graph model given in [5] and then in [25] to study wavelength conversion creates for each wavelength entering the node an input vertex and each wavelength leaving the node an output vertex. In a given node, input and output vertices are interconnected if they represent the same wavelength or if wavelength conversion between their wavelengths is possible. Interconnecting edges are weighted to the wavelength conversion cost.

In the layered graph model given in [36] and then in [40], unused wavelengths are represented by edges connecting vertices in the wavelength layer (in this layer, connections replicate the fiber physical links). If wavelength conversion is not allowed, we need a wavelength layer for each wavelength channel. When a demand is connected using a fraction of the wavelength capacity, the remaining capacity switches to the lightpath layer as a direct connection between the dedicated vertices in the input and output nodes of the lightpath (lightpath tunnel). In [40], the lightpath layer is divided into muxtplexing layer and grooming layer to differentiate between the cases where a wavelength is multiplexed without or with low-speed traffic streams switching (electronic switch fabric).

Figure 5 shows an example. The state of the network is shown with the corresponding layered graph for a simple three-node network. Nodes 1 and 2 are single-hop grooming OXCs

with only wavelength ports and where switching is always at wavelength granularity. Node 0 is a multi-hop partial-grooming OXC with two switch fabrics (all-optical and electronic).

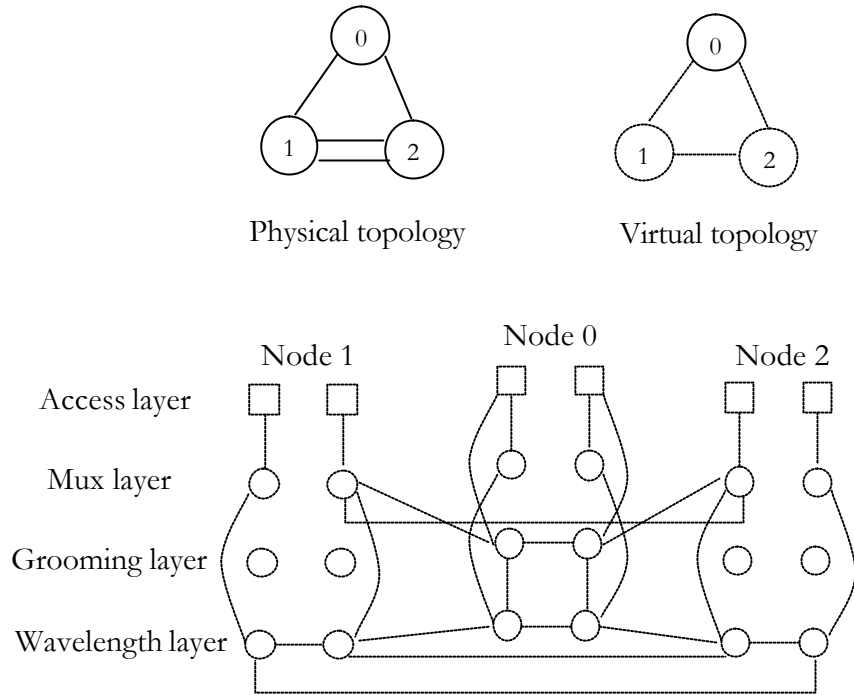


Figure 5: Layered graph model.

In the given example, we still can arrange traffic units in the already established lightpaths from node 1 to node 0, node 0 to node 2 and node 1 to node 2 (as shown in the virtual topology). The first point to mention is that no information on the origin of these lightpaths is present in the graph. For instance, we cannot tell from the graph if the lightpath from node 1 to node 2 pass through node 0 or uses the direct fiber connection between node 1 and node 2. We cannot also find out the wavelength channel (or channels when wavelength conversion is allowed) of this lightpath. Furthermore, we cannot tell which connections are groomed together in the same lightpath. All this information must be held separately. Not to mention that already filled lightpaths are not shown in the graph model. Therefore, when it comes to updating the graph, tearing down a connection is a heavy operation and is not supported by the graph model itself. When we add a waveband layer, this becomes too complicated and we are faced with the updating problem at different levels.

Let us show another and important reason to conceive a new model to handle dynamic traffic grooming in multi-granular networks. We present in figure 6 the alternate routes given in [40] to connect node 1 to node 2 in the given example. The cost assigned to the set of edges determines the route to choose by applying a graph optimization algorithm such as the shortest path.

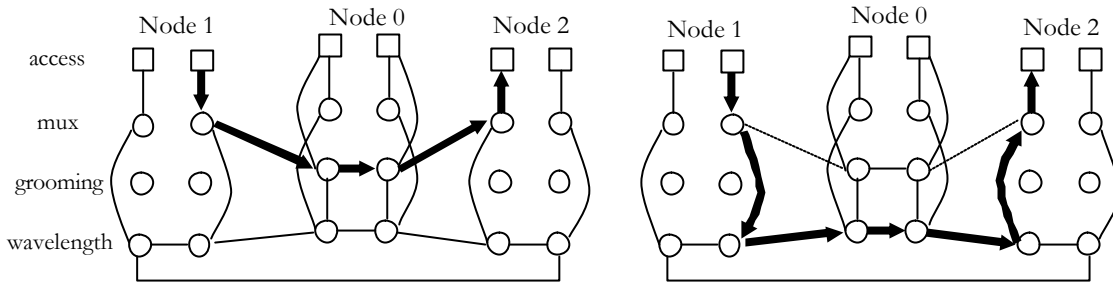


Figure 6: Alternate routes given in [40].

We are interested in the route going through the wavelength layer. This route means that a new wavelength is to be used in order to set up the connection. This can be done by using one lighthpath from node 1 to node 2, as in figure 5, or by using two lighthpaths as the already established ones (from node 1 to node 0 and then from node 0 to node 2). This choice depends on how interesting it is to bypass or pass through the grooming layer in order to reduce the blocking probability of future demands. In the layered graph model, this distinction can only be done when lighthpaths passing through intermediate nodes are already established (already used wavelengths). This may be done also after choosing the path and hence does not affect the route selection. Bypassing or passing through a given layer at a given node is a critical problem in multi-granular networks and depends on available resources. Figure 7 shows two variants when using a new wavelength with one intermediate node. In this figure, we assume that one wavelength only is still available on that path. This explains why two edges in the wavelength layer disappear.

We are unable to include, for unused wavelengths, the layer exploitation in the edges' cost. When we have multiple choices, through multiple routes and when a multi-granular switching is carried out, the graph optimization algorithm applied on the layered graph model is not effective in exploiting layer. We need to conceive a graph model where the cost of the edge can also cover the importance of bypassing or passing through the offered layers.

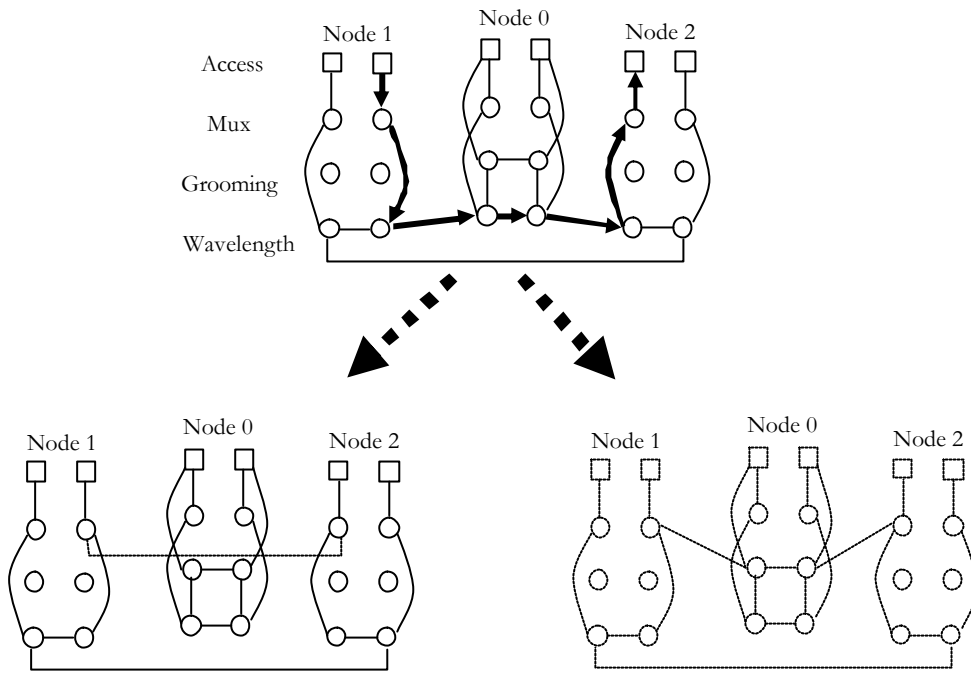


Figure 7: Two possible switching granularities, at intermediate node 0, for the same route on the layered graph.

The graph model we propose in this chapter is adapted to multi-granularity networks with multi-layer or single-layer node structure but can also cover any grooming problem. In this model, we can keep track of the network evolution and state and simplify the updating when tearing down a connection. This is done by means of objects (groups) defining the belonging, the state and the significance of an edge representing any resource in the network. Instead of passing from a layer to another one in the graph, we define only four operations executed on groups of consecutive edges all along the lightpath at a given granularity. By using what we call Basic Network Element, or simply BNE, we can interconnect different granularities and model the multiplexing, demultiplexing, switching, wavelength conversion, etc...

## II.2. The Basic Network Element

We define the granularity of a channel to be the ratio of the channel capacity to the base bandwidth rate. The base bandwidth rate is the smallest capacity that we can individually switch in the network. We define the Basic Network Element (BNE) to be any possible interconnection in the network between any input and output ports. For instance, a BNE can be a fiber, a pair of input/output ports of a wavelength cross-connect, a pair of input/output



ports of a wavelength converter each at a different wavelength, etc... Each port (input or output) of the BNE is modeled by  $g_e$  edges in the graph model.  $g_e$  is the granularity of the BNE channel. For instance, if the BNE is a fiber supporting 32 wavelengths and each wavelength has an OC-192 channel capacity and if, in the whole network, we can multiplex/demultiplex down to OC-12 streams then the fiber granularity is  $g_e=32*16=512$  (16 is the number of OC-12 streams in an OC-192 wavelength). For each port (input or output), the  $g_e$  edges are gathered in groups of  $g_s$  elements.  $g_s$  is the switching granularity that is the bundle of multiplexed or demultiplexed channels at the given port. Input and output ports can have different switching granularities and this makes the model well adapted to multi-granularity architectures.

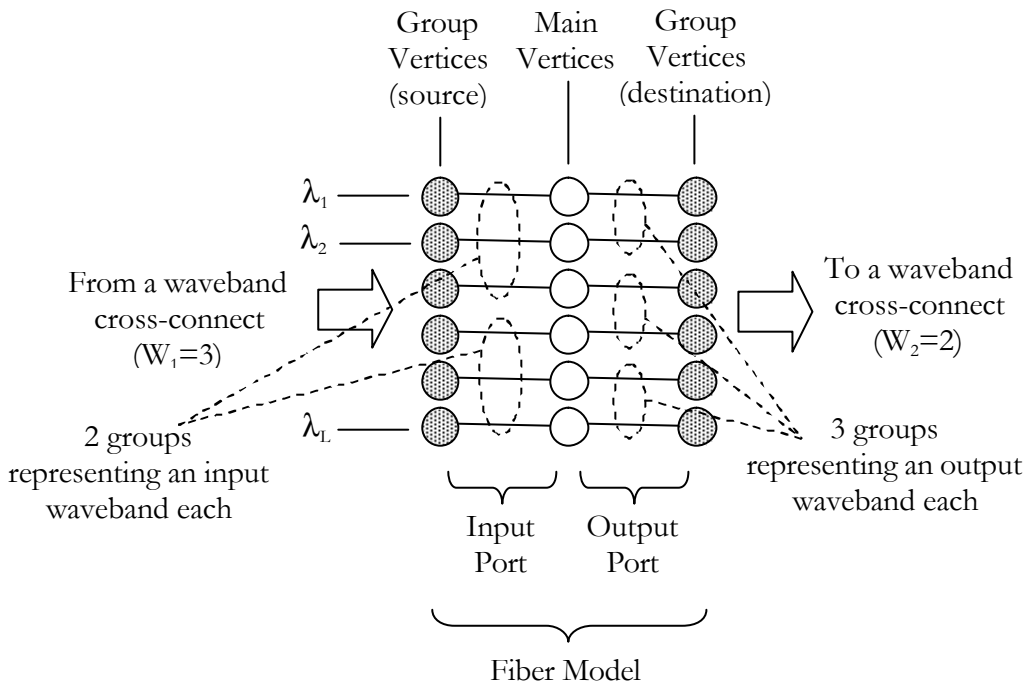


Figure 8: A Basic Network Element (BNE) modeling a fiber.

Let us consider an example to illustrate how a fiber can be modeled by a BNE. In this example, the lowest granularity is a full wavelength so the base bandwidth rate is simply the wavelength capacity (no electronic grooming is to be modeled here). The fiber, having  $L$  wavelengths, is coming out of a waveband cross-connect having  $W_1$  as a waveband granularity ( $W_1$  wavelengths to be switched in bulk) and going to a waveband cross-connect having  $W_2$  as

a waveband granularity. It is modeled by  $2L$  edges and  $3L$  vertices.  $L$  vertices form end points to the  $L$  input channels of the BNE.  $L$  other vertices form end points to the  $L$  output channels of the BNE. Note that these vertices may be shared with other BNEs as we shall see later in the cross-connect model. We show in figure 8 a BNE modeling a fiber supporting 6 wavelengths with  $W_1=3$  and  $W_2=2$ .

### II.3. Group Concept

Edges in a BNE represent the traffic carriers. Main vertices define the belonging of these carriers to a given BNE and separate the input port from the output port to allow different granularities at the two sides of the BNE. Groups represent any kind of aggregation (optical or electronic) and are used to abstract the aggregators/de-aggregators and hence define the switching granularity at each side of a BNE. Groups can be combined by a merging operation, as we shall see later, to model the switching operation. No traffic carrier can be used before deciding the forwarding scheme of its bundle, which means defining the group of neighboring BNE to be merged with its group. Group vertices are end points to interconnect different BNEs.

A group is an object retaining the following data:

- i. Group ID.
- j. Granularity or number of edges.
- k. Pointers to Main vertices.
- l. Pointers to Group vertices.
- m. Number of unused edges or traffic units. Compared to the granularity, this is used to determine when to unmerge connected groups and hence allow a new forwarding scheme for included traffic carriers.
- n. ID of the merged group. This is set to NULL when the group is not merged, i.e. no include traffic carrier is used and hence no forwarding scheme is determined.

- o. Flag to determine if the Group vertices are source or destination vertices. In other words, this is to find out on which side of the BNE the group is defined.
- p. Type or cost profile. The type defines the layer (slot, wavelength, waveband...) in the multi-layer context. This is also used to define the grooming and wavebanding policy i.e. the cost of an edge when the group is unmerged and its cost when the group is merged or the algorithm used (traffic engineering) to determine the cost.

As already mentioned, we define two types of vertices:

- **Main vertices:** a main vertex belongs to one and only one BNE. These vertices connect the input port to the output port of the BNE. Edges are always connected to these vertices no matter what operation is applied on the group. Main vertices neighboring two given groups will be directly connected together after merging these groups. Main vertices cannot be shared by different BNEs (we will see that add and drop main vertices are shared vertices and make the only exception).
- **Group Vertices:** these are the source and destination vertices of a BNE. These are end points to interconnect different BNEs. Edges are disconnected or reconnected to these vertices depending on the operation applied to the corresponding group. Group vertices can be shared by different groups and different BNEs.

#### II.4. Shared Vertices, Sharing Condition and the Waveband Cross-Connect Model

Group vertices may be shared by different groups having the same type and same granularity (sharing condition). For instance, a cross-connect is simply modeled by shared group vertices.

As an example, figure 9 shows a waveband cross-connect model. In this example, the waveband cross-connect has 2 input links  $I_1$  and  $I_2$  and 2 output links  $O_1$  and  $O_2$ . The waveband granularity is 2 wavelengths, and we have 4 wavelengths per link.

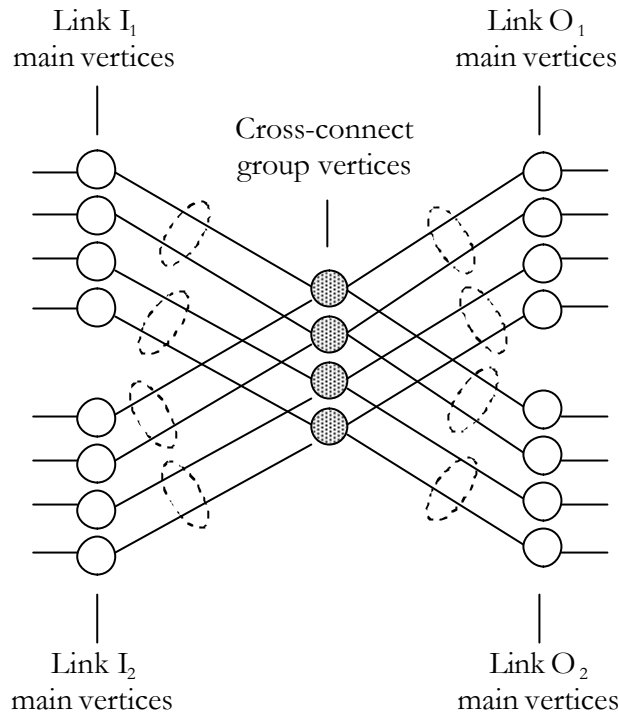


Figure 9: Waveband Cross-Connect Graph Model.

## II.5. Operations

Under the dynamic traffic context, the first wavelength used in a given waveband defines the forwarding of all other wavelengths in this waveband, and this forwarding is kept until all wavelengths in the waveband are torn down even if this first wavelength is torn down.

A waveband switching shall be considered as a bulk forwarding of all included wavelengths (used one and those to be used). This waveband cross-connection is represented on the graph model by a MERGE operation. In a MERGE operation, the group vertices connecting the edges of the input/output wavebands to be interconnected are simply bypassed and these edges are merged to directly connect the concerned Main vertices. These groups are then marked as merged groups (this status is deduced from the number of unused edges). Used wavelengths must no more contribute in the routing until their connections are torn down. So we must exclude the corresponding edges from the graph model (EXCLUDE operation). These edges are mapped in the connection schedule and are marked by their merged group so

that they can be later reintegrated in the graph model after tearing down the connection (REINCLUDE operation). Therefore the Edge object must include:

- d. the cost.
- e. the group ID.
- f. the destination vertex since the source vertex is inherently known by the index of the edge in the edge list. We did not mention also the pointer to the next edge going out of the same vertex.

When all edges of a merged group are re-included (all wavelength are no more used), the corresponding waveband becomes free to be switched again to any other waveband. Here edges must regain the Groups vertices (UNMERGE operation) and their initial groups (to be marked unmerged).

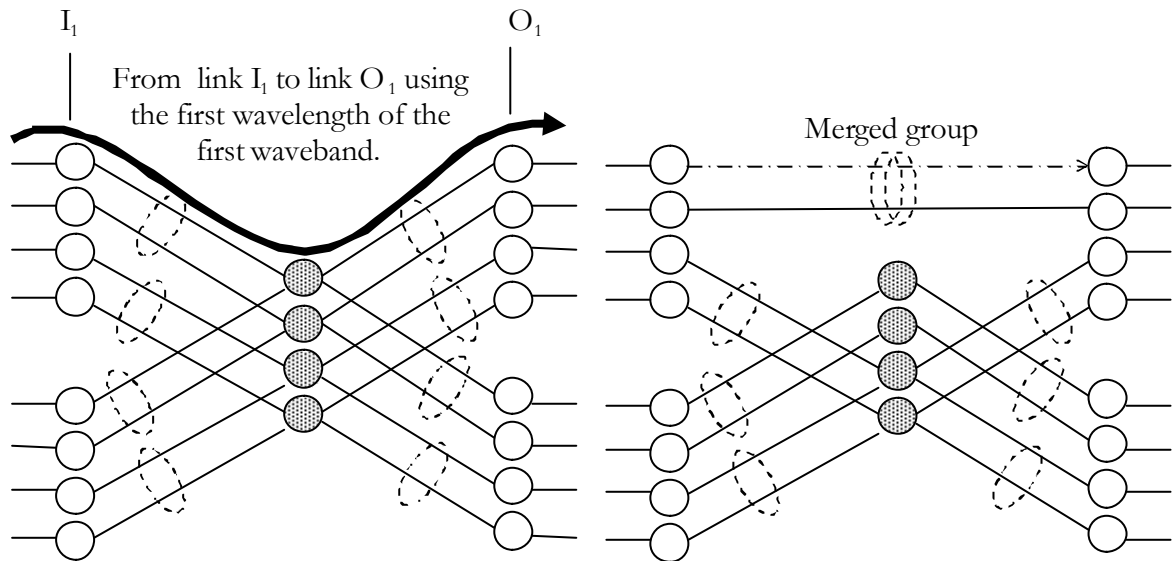


Figure 10: MERGE operation

Figure 10 shows an example to illustrate the MERGE operation. In this example, we have two wavebands per link and two wavelengths per waveband. Consider a connection to be set up using the first wavelength of the first waveband and going from the input link  $I_1$  to the output link  $O_1$ . Due to the waveband switching, this connection forces the second wavelength of the first waveband to reach  $O_1$  coming from  $I_1$ . This is clearly modeled by the MERGE

operation. Note that this operation is directly followed by an EXCLUDE operation applied on the edge representing the channel that initiates this merging.

The defined four operations are then: MERGE (grpID1, grpID2), UNMERGE (grpID1), EXCLUDE (Edge) and REINCLUDE (Edge).

### II.5.1 Shared Vertices and Grooming Capable WXC with Wavelength Converters

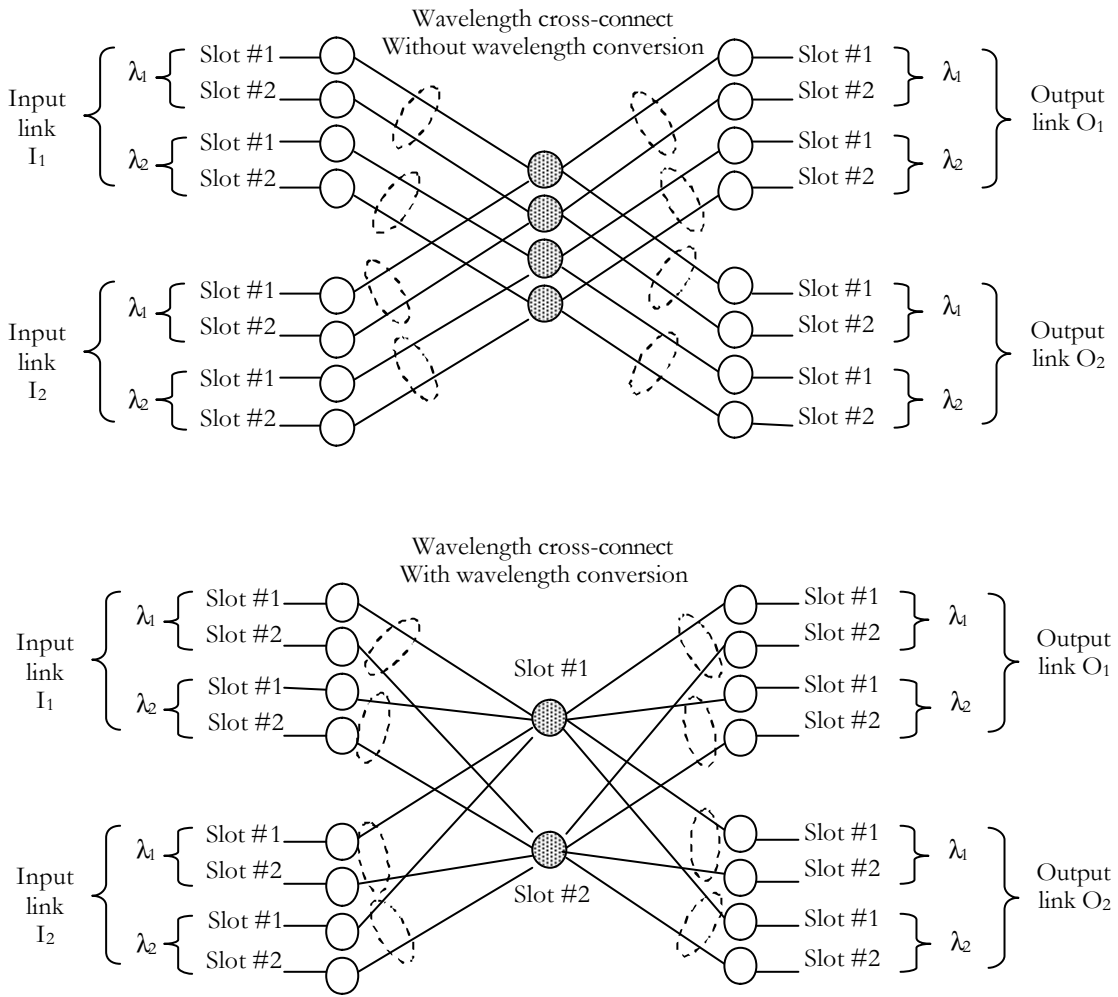


Figure 11: A wavelength cross-connect with and without wavelength conversion capability.

Consider a wavelength cross-connect (WXC) where each wavelength supports  $g$  time slots. The wavelength conversion capability is modeled by sharing group vertices having the same time slot ID. Figure 11 shows this model where we have two input links  $I_1$  and  $I_2$  and two

output links  $O_1$  and  $O_2$ . In this model, we have two slots per wavelength and two wavelengths ( $\lambda_1$  and  $\lambda_2$ ) per link.

## II.6. Dead Edges

When using the shortest path algorithm to route connections on the MGGM, two problems arise as shown in figures 12 and 13.

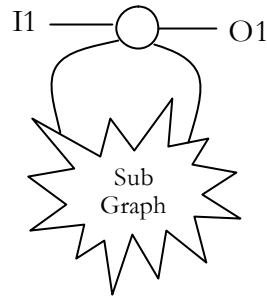


Figure 12: First problem arising when applying the shortest path.

In Figure 12, assume we want to route a connection from input I1 to output O1 and that all link costs are positive. We never pass through the given sub-graph since the cost of the direct path from I1 to O1 is always going to be smaller than the cost through the sub-graph. If we want to be able to route connections through the sub-graph, we need to assign negative costs to some edges inside or reaching this sub-graph. An elaborate shortest path algorithm is needed to support negative costs.

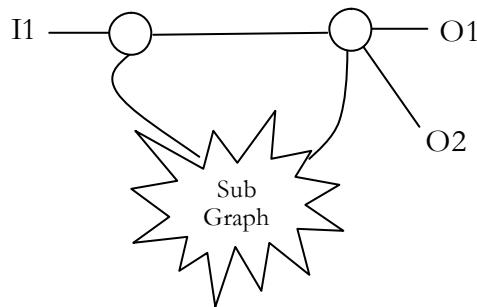


Figure 13: Second problem arising when applying the shortest path.

In figure 13, starting from I1 we cannot, for instance, prefer to pass through the given sub-graph when reaching O1 and bypassing it when reaching O2. The cost difference between passing-through and bypassing the sub-graph does not depend on the route.

To make the network modeling more flexible and especially to avoid negative costs and allow differentiated cost models, we add the possibility to split a group vertex. Splitting a group vertex consists in replacing it by a pair of vertices connected by a fixed edge that we call a dead edge since it is not affected by any operation and it is always connecting the two sub group vertices. We call group edges those connecting main and group vertices. The MERGE operation still connects main vertices by merging group edges. In figure 14, we show the merge operation when we have dead edges.

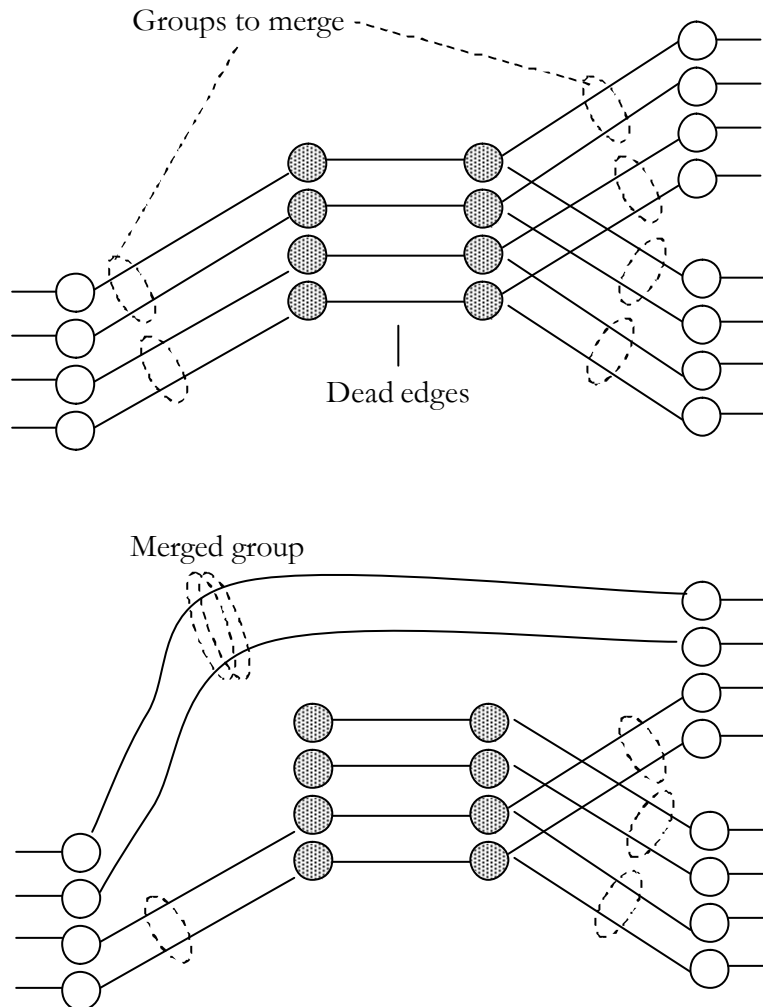


Figure 14: Merging groups connected through dead edges



## II.7. Hierarchical Cross-Connect Model and the Need for Dead Edges

In an HXC, we can either switch a waveband in bulk from an input to an output link (bypassing the  $\lambda$ XC) or demultiplex the waveband to allow a finer granularity switching (passing through the  $\lambda$ XC) before multiplexing again. Passing through the  $\lambda$ XC allows a finer selection of wavelengths coming from different links (or different fibers of the same link) in the same waveband channel to be applied to the same output link. Here we must add a BNE with input and output groups having different granularities. To simplify the representation, we will show the model of a HXC having one input and one output waveband (at the same waveband channel) that can bypass or pass through the  $\lambda$ XC.

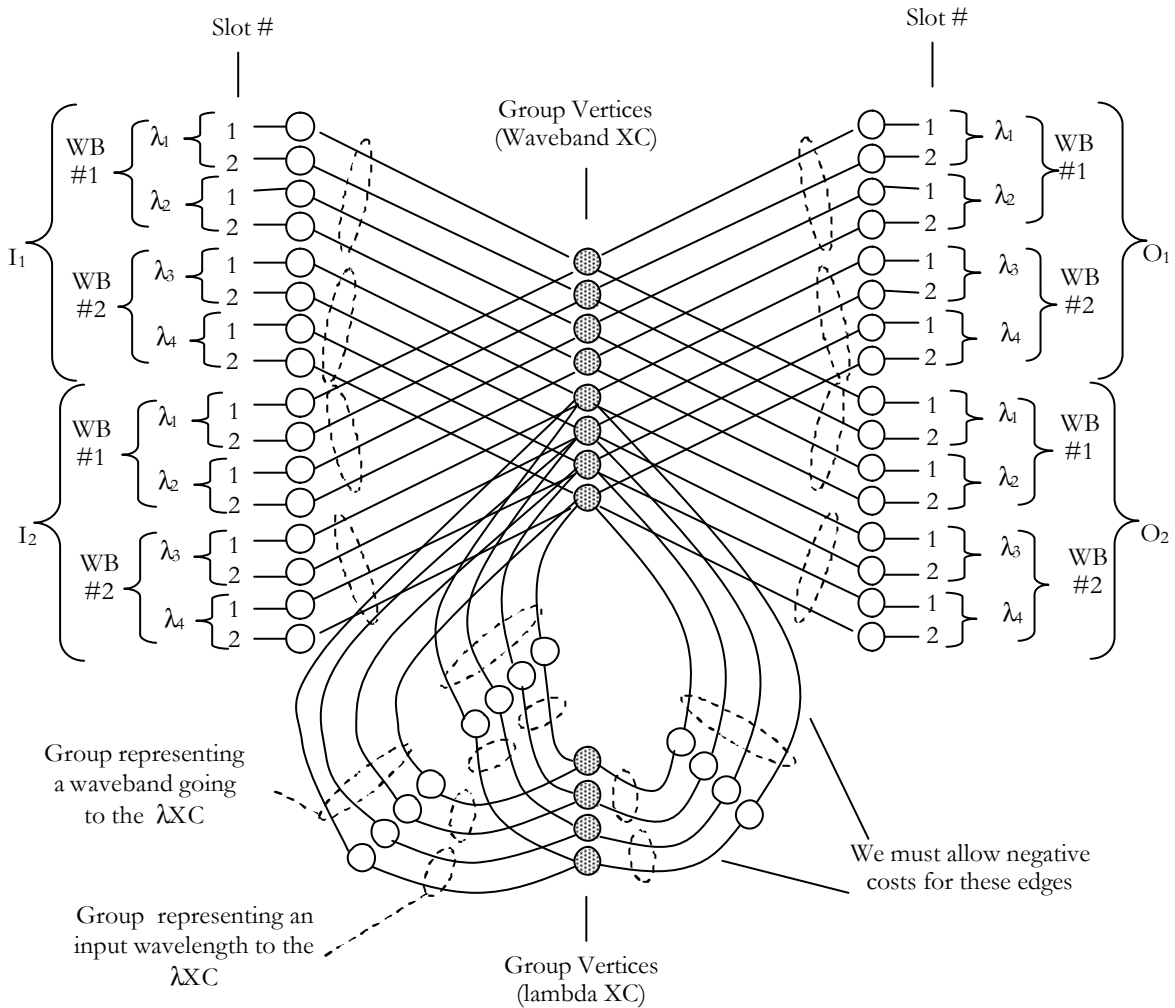


Figure 15: HXC graph model where we must allow negative costs.

At a given waveband channel, a HXC usually has  $n$  input and  $m$  output wavebands, where at most  $x$  input wavebands may be demultiplexed and applied to the  $\lambda$ XC and where the outputs of the  $\lambda$ XC are multiplexed into at most  $y$  output wavebands ( $x < n$  and  $y < m$ ).

An example on HXC is first illustrated in figure 15. We discuss the waveband number 2 where we have  $n=2$  input wavebands,  $m=2$  output wavebands,  $x=2$  wavebands can pass to the  $\lambda$ XC and  $y = 1$  waveband can go out the  $\lambda$ XC to reach the output waveband. We consider two input links  $I_1$  and  $I_2$  and two output links  $O_1$  and  $O_2$ . We have four wavelengths ( $\lambda_1, \lambda_2, \lambda_3$  and  $\lambda_4$ ) per link. Each pair of contiguous wavelengths forms a waveband. Two slots are multiplexed in each wavelength. In this model, we must allow negative costs to be assigned to edges going to and coming from the  $\lambda$ XC, otherwise the shortest path algorithm would always choose to bypass the waveband.

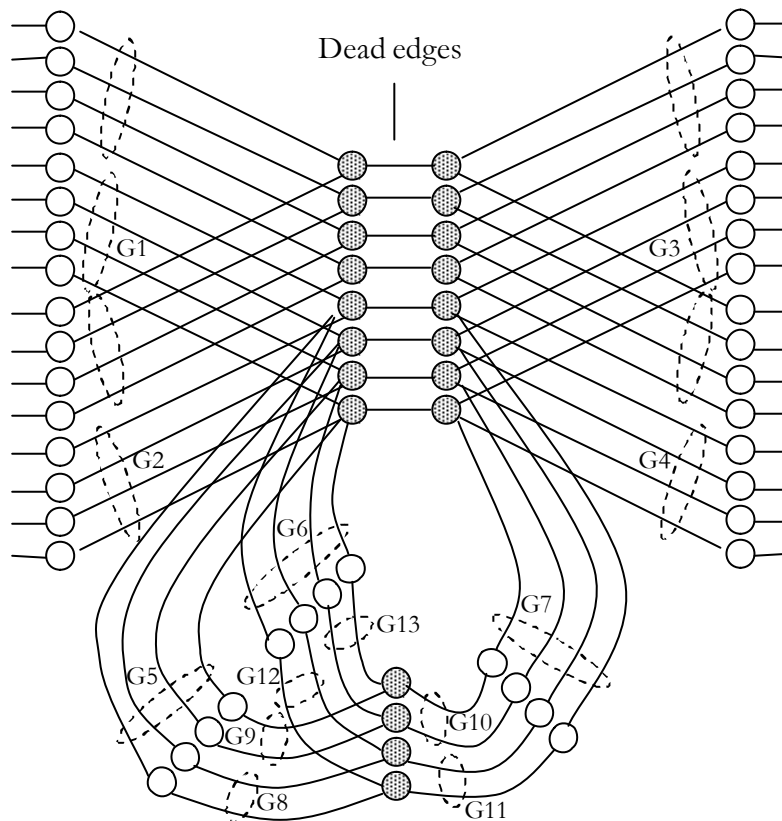


Figure 16: HXC graph model with dead edges to avoid negative costs.

We show therefore the need to split group vertices in order to avoid negative costs. Note here that costs are assigned dynamically as a result of the traffic engineering policy.

Figure 16 shows how we can avoid negative costs by adding dead edges. The cost assigned to dead edges plays the main role in the choice between bypassing and passing through the  $\lambda$ XC for a given pair of input/output waveband depending on the network state. Note the group labels concerning the waveband number 2.

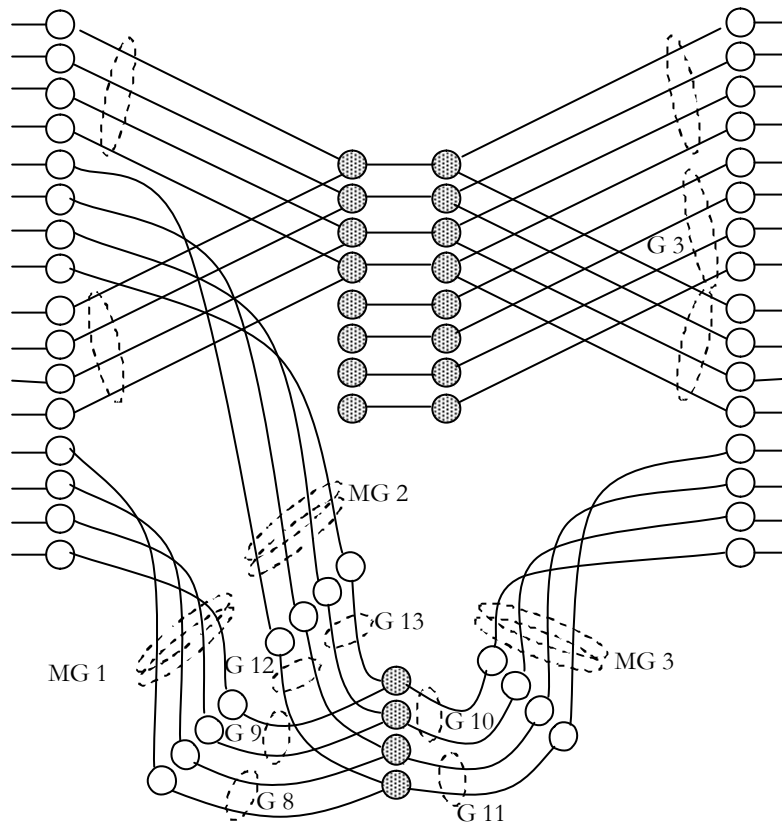


Figure 17: Example showing the passing through the  $\lambda$ XC in the MGGM.

Figures 17 and 18 sketch the hierarchical cross-connect operations and how these operations are modeled on the MGGM. Figure 17 shows, in the second waveband channel, two wavebands going to the  $\lambda$ XC that is merging groups G2 and G5 to give the merged groups  $MG1=MERGE(G2,G5)$  and G1 and G6 to give  $MG2=MERGE(G1,G6)$ . It shows also one waveband going out of the  $\lambda$ XC by merging G7 and G4 to give  $MG3=MERGE(G7,G4)$ . Figure 18 shows the wavelength switching in the HXC where the

two different input wavebands can reach the same output waveband. We show two merged groups:  $MG4=MERGE(G8,G11)$  representing the wavelength  $\lambda_3$  from link  $I_2$  to link  $O_2$  with its two slots and  $MG5=MERGE(G13,G10)$  representing the wavelength  $\lambda_4$  from link  $I_1$  to link  $O_2$  with its two slots. Note how we have to merge groups at different granularities in the HXC (multi-layer).

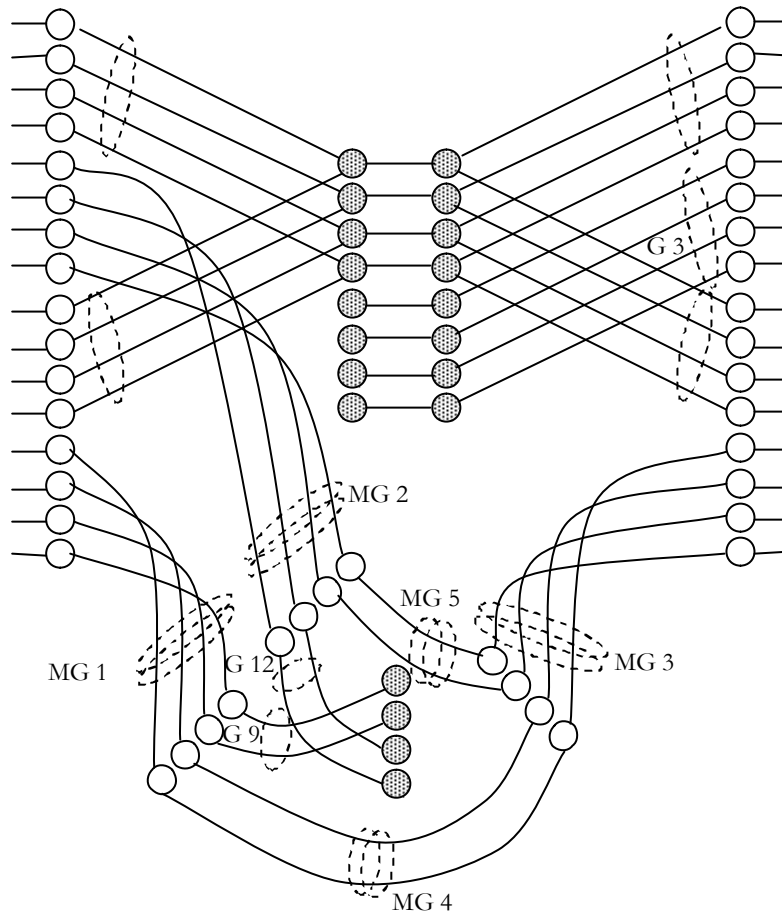


Figure 18: Example showing the wavelength switching operation in the MGGM.

## II.8. The Generalized MGGM

### II.8.1 Intra-Shared Group Vertex

The electronic multiplexing/demultiplexing is the most flexible grooming since a time slot can be easily reassigned to any other slot in any groomed wavelength electronically added and dropped. Time slots are easily interchanged at the electronic processing level and this is, at the

time slot granularity, equivalent to the wavelength conversion possibility at the wavelength granularity. A shared group vertex by all time slot edges models this (figure 19).

### II.8.2 Add and Drop Vertices: The Only Two Shared Main Vertices

From another point of view, we must add and drop wavelengths; sometimes we add or drop a whole waveband. At a finer granularity, we must add and drop time slots. At a given node, we have only one entry for all added traffic and another entry for all dropped traffic. This is modeled by a shared input main vertex (add vertex or simply ADD) and a shared output main vertex (drop vertex or DROP). Figure 19 illustrates an example on the generalized MGGM and how the model can support multi-layer or hierarchical architectures.

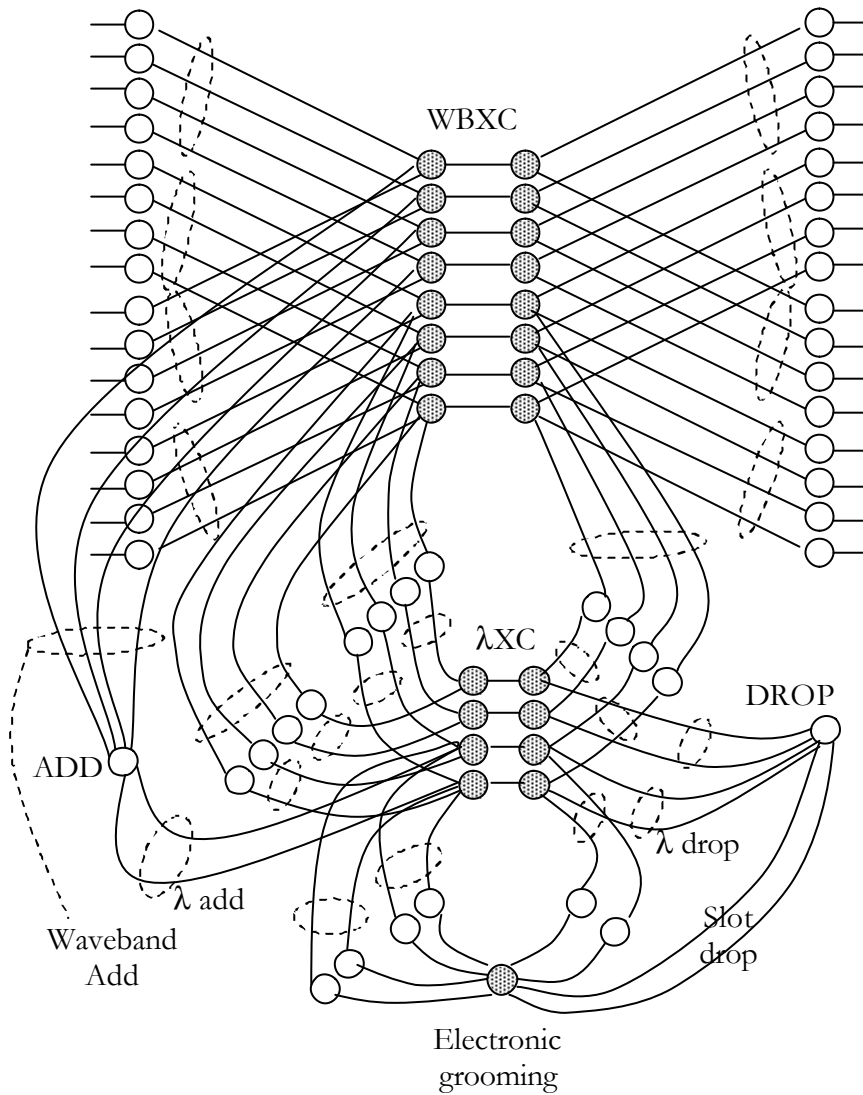


Figure 19: ADD/DROP vertices and the generalized MGGM.

## II.9. Differentiated Cost and Extra Dead Edges

Depending on the traffic engineering policy, we may need to differentiate the cost of a group edge depending on the choice of other edges in the path. Dead edges and their cost are useful to solve this problem. For instance, passing through the  $\lambda$ XC is a critical problem. We show in the following why we do need differentiated cost and how to solve the problem using dead edges.

Let  $n$  be the number of input links at a given waveband channel and  $m$  the number of output links. Let  $x$  be the maximum number of wavebands that can be demultiplexed and  $\lambda$  cross-connected at this waveband channel and  $y$  the maximum number of multiplexed wavebands at the output of the  $\lambda$  cross-connect. To make the HXC cost effective,  $x$  and  $y$  are chosen to be low enough to have an acceptable hardware complexity reduction and high enough to have an acceptable blocking probability. But always  $x$  and  $y$  are less than  $n$  and  $m$  respectively. So we must choose the wavebands to be  $\lambda$  cross-connected and those to bypass the  $\lambda$ XC. In the case of dynamic traffic, the choice is made upon the request arrival without knowing a priori all the traffic demand. Also, it is not possible to rearrange the traffic and change the switching state of a waveband until all included connections are torn down. Bypassing the  $\lambda$ XC reduces the number of possible forwarding patterns to all included wavelengths and passing through the  $\lambda$ XC decreases the number of wavebands that can later on pass through the  $\lambda$ XC. In the model shown in figure 16, the cost difference between passing through the  $\lambda$ XC and bypassing it does not depend on the input/output links involved. We have then the same preference between bypassing and passing through for all input/output pairs.

As an example to illustrate this problem, figure 20 shows a HXC graph model when the cost of some edges is shown nearby. In this example, the HXC has two input links I1 and I2 ( $n=2$ ), two output links O1 and O2 ( $m=2$ ), two wavebands that can be demultiplexed ( $x=2$ ) and  $\lambda$  cross-connected. For the sake of simplicity we limit the number of input links to two; even though we should have  $x < n$  and one waveband goes out of the  $\lambda$ XC ( $y=1$ ). Each waveband gathers two wavelengths and each wavelength contains two slots. For the first slot in the first wavelength, the cost difference between bypassing and passing through the  $\lambda$ XC is  $C'2-C'4-C'5-C'6-C'7$  (this difference can be positive or negative depending on the preference)

to go from any input link to any output link. But, as we shall see in chapter 7, dealing with a limited number of wavebands that can be switched at fine granularities must take into consideration the current logical topology in order to promote the critical link pairs to be interconnected at fine granularities. In other words, some link pairs must have the priority to pass through the  $\lambda$ XC than other pairs.

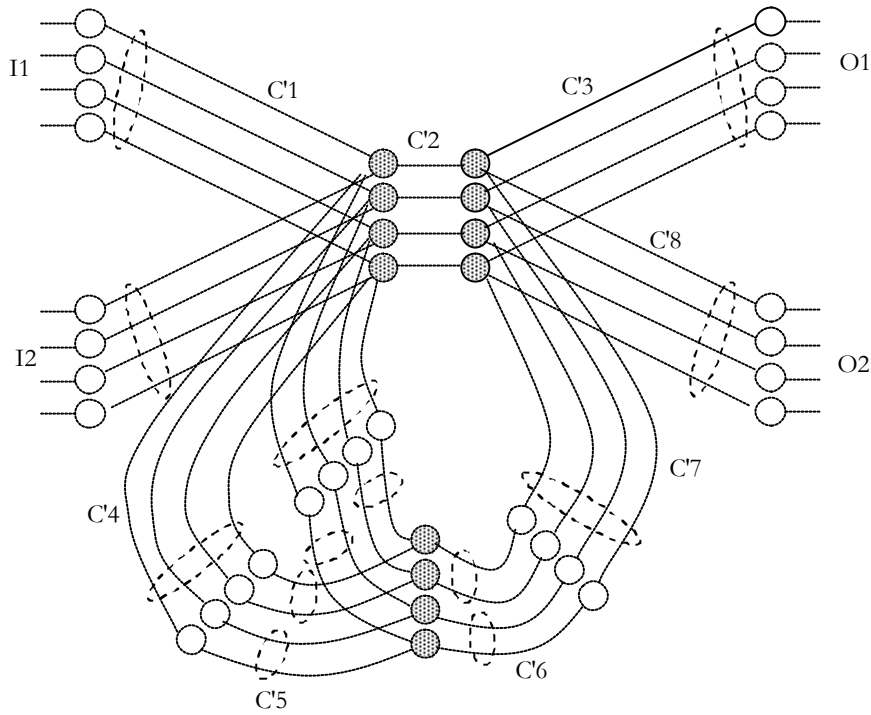


Figure 20: For a given wavelength, we have the same preference (between bypassing and passing through) for all input/output pairs.

Adding dead edges having suitable cost solves the problem when differentiated costs are needed to apply the traffic engineering policy. Figure 21 shows, for the same example, the HXC model with differentiated preference. For the first slot in the first wavelength, the cost difference between bypassing and passing through the  $\lambda$ XC is C2-C4-C5-C6-C7-C8-C9 to go from input link I1 to output link O1 and C10-C4-C5-C6-C7-C8-C11 to go from input link I1 to output link O2. By adding dead links, the MGGM can add more parameters (costs) in order to reach the goal of a traffic engineering policy.

Note how this change increases the number of vertices and edges in the MGGM. However, all dead edges do not contribute in any group operation. That is why we called them dead edges.

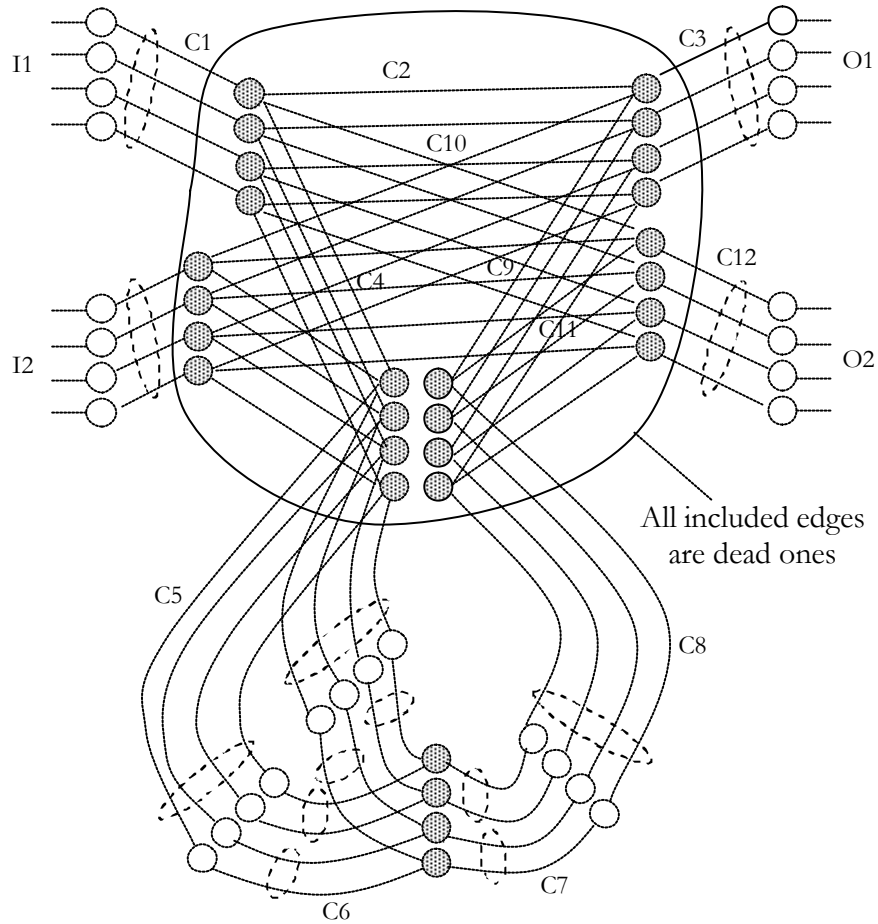


Figure 21: Differentiated preference (between bypassing and passing through) depending on the input/output pair.

## II.10. Setting Up or Tearing Down a Connection

Setting up a connection in the MGGM, after finding the optimal path, starts by merging (MERGE operation) all unmerged consecutive groups along the path. Group to be merged must have the same type and granularity (merging condition). After this step, all edges along the path belong to merged groups. Starting from the add vertex of the source node, the EXCLUDE operation is applied to these edges one by one while updating the cost according to the cost profile if required. Tearing down a connection consists of applying the



REINCLUDE operation and the UNMERGE operation when all edges of a group are re-included. The edges' cost may also in this case need to be updated.

### II.11. Useful Examples

Based on the four defined operations (MERGE, UNMERGE, EXCLUDE and REINCLUDE) and using the two types of vertices (main and group vertices) and the two types of edges (group and dead edges), we can model all elements of a multi-granularity network. In this section, we show two useful examples.

#### II.11.1 Tuned Receivers/Transmitters

Instead of directly connecting the  $\lambda_{XC}$  output group vertices to the drop vertex, we can add dead edges to connect all  $\lambda_{XC}$  output group vertices (full range tuned receiver) or some of the  $\lambda_{XC}$  output group vertices (limited range tuned receiver) to one group vertex and then connect it to the drop one with  $t$  group edges where  $t$  is the number of tuned receivers.

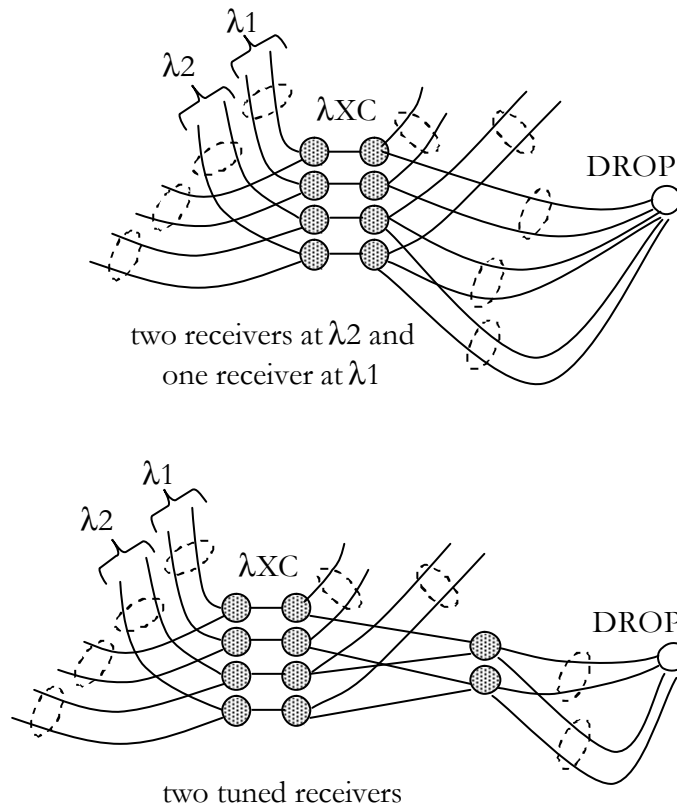


Figure 22: Tuned receivers.

The same solution is used to model a tuned transmitter. Figure 22 shows how we can model two full range tuned receivers where a group vertex is needed for each time slot.

### II.11.2 Limited Number of Wavelength Converters

We can model a wavelength converter by a BNE having:

- The source group vertices connected by dead edges to all (full range conversion) or some of the  $\lambda$ XC input group vertices representing the same slot number.
- The destination group vertices connected by dead links to all (full range conversion) or some of the  $\lambda$ XC output group vertices representing the same slot number.

An example is shown in figure 23. To model  $p$  wavelength converters, we must add  $p$  such BNEs.

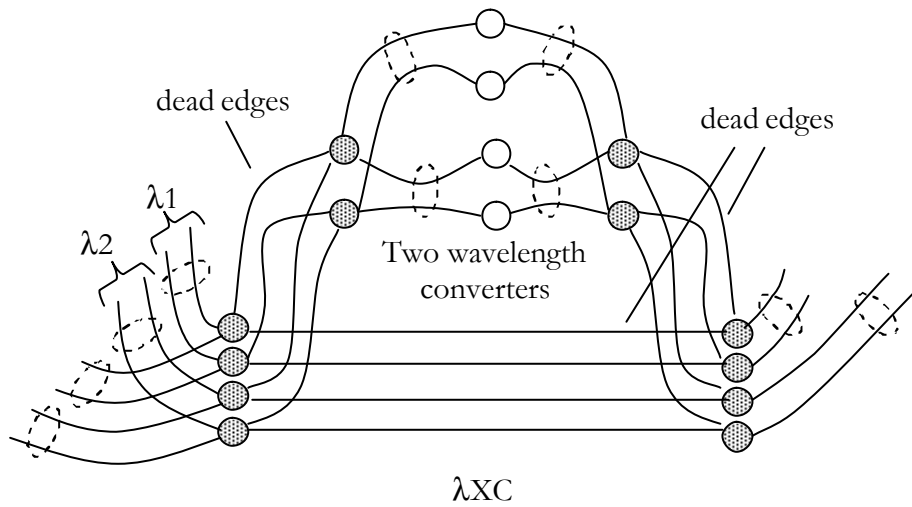


Figure 23: limited number of wavelength converters.

## II.12. Conclusion

In the spirit of a label in GMPLS which may represent a timeslot, a wavelength, a waveband or any other traffic carriers, we came up with a generalized multi-granularity graph model where a group object can represent any kind of aggregation.

The proposed Multi-Granularity Graph Model can inherently keep track of the multi-granular network evolution and state and simplify the updating when setting up or tearing down a connection in the presence of dynamic traffic. We showed in this chapter the need to conceive a new graph model in order to support multiple levels of grooming. In fact, the layered graph model is known to be a suitable model to support traffic grooming in optical networks. However, while trying to expand it to support multi-granular optical networks, we have faced many problems. On the one hand, when new layers are to be added, the manipulation of tearing down and setting up connections becomes too complicated and a lot of information need to be retained in addition to the state of the graph. On the other hand, when setting up a connection between a pair of nodes, the crucial decision of bypassing or passing through lower layers at intermediate nodes cannot be part of the graph optimization unless concerned bunch of traffic carriers are already deaggregated. We need to implement the MGGM when dealing with dynamic traffic in multi-granular optical networks as in chapter 5.

We also showed in this chapter the universality of this model and how the Basic Network Element and the group concept together allow modeling any component in the multi-granular context.

### III. ANALYTICAL MODEL FOR HIERARCHICAL OPTICAL CROSS-CONNECT

#### III.1. Introduction

To reduce the size and complexity of OXCs, the optical granularity is used where channels are optically grouped therefore OXCs can route them as a single waveband. A waveband is a group of  $W$  contiguous wavelengths where  $W$  is the granularity of the waveband.

Large optical switches are difficult to build and are much more expensive than small optical switches [24]. Large OXCs are also much more complex in term of management controls. To reduce the size and complexity of OXCs, the optical granularity is introduced [7] where channels are optically grouped so OXCs can switch them as a single signal. This is compared to the electronic granularity achieved by means of time-division multiplexing such as traffic grooming in SONET add-drop multiplexers. This optical granularity is referred to as the wavelength banding [29]. Since a wavelength can optically bypass a node if it carries no traffic to or from that node, a waveband can optically bypass a node if no included wavelength is dropped or added at that node and if all included wavelengths cross the node toward the same waveband. In such a case, the waveband is called a packed waveband. We also call packed waveband a waveband where all included wavelengths are dropped or added at the corresponding node since these wavelengths do not enter the wavelength cross-connect (WXC) this is the case of a waveband drop or add.

Hierarchical cross-connects (HXC) or multi-granular optical cross-connects (MG-OXC) implement optical bypass at coarse granularity using the wavelength banding technique with waveband cross-connects (WBXC) and at fine granularity using wavelength cross-connects (WXC). This approach is adopted in order to reduce the optical cross-connect (OXC) hardware complexity. However, the reduction in the hardware complexity comes with an increase in the operational complexity since routing and wavelength assignment are then constrained to the cross-connection in bulk. We define in this chapter a model for hierarchical

optical cross-connects to count the number of possible connection patterns to serve a given number of connections and hence compare the HXC and the wavelength-only cross-connect performances.

### III.2. The Hardware Complexity Reduction Ratio

We can benefit from the wavelength banding by using a hierarchical OXC where we have an efficient multi-layer multiplexing methodology. We consider the two-layer HXC presented in Fig. 24 as in [9] and [23] where WBXC is a waveband cross-connect that implements optical bypass at the waveband granularity.

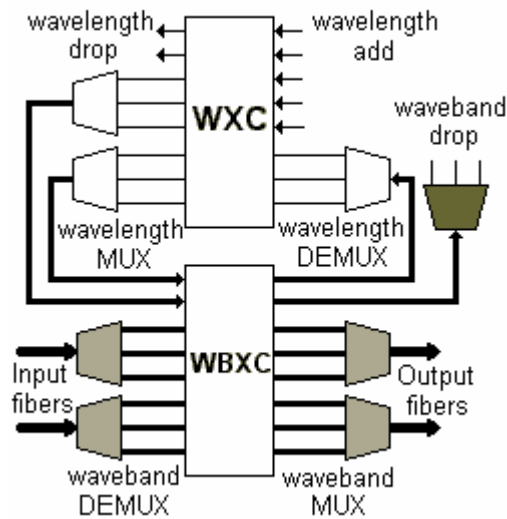


Figure 24: Two-layer Hierarchical Cross-Connect (HXC).

The benefit is then the hardware complexity reduction. This complexity is represented by the size of the optical switch matrix related to the total number of inputs to the OXC. When the WXC is considered alone (single-layer multiplexing), the number of inputs is determined by the number of wavelength channels in service. When a two-layer HXC is considered, up to  $W$  wavelength channels can form only one input port to the WBXC. Note that the reduction in the hardware complexity comes with an increase in the routing and wavelength assignment (RWA) complexity especially for dynamic traffic. This results in a higher blocking probability. To describe the problem, and since the node design consists in distributing the cross-

connecting between the two sub cross-connects WXC and WBXC of the HXC, we illustrate the two extremes:

1. When we decrease the number of wavebands that can pass through the WXC, we tend toward a waveband switching. This reduces the hardware complexity to the detriment of reducing the flexibility since the switching of a given wavelength may be subject to the decision already taken for its waveband at intermediate nodes.
2. When we increase the number of wavebands that can pass through the WXC, we have a better operating flexibility at the cost of an increased hardware complexity. Poor results can be observed since a connection passing through a node must always reach the WXC through the WBXC and in this case a single-layer wavelength cross-connecting would be more cost-effective.

We consider the multi-fiber N-node L-Link network. Each link  $l$  ( $l=1, \dots, L$ ) holds  $F(l)$  fibers. Wavelengths are arranged in  $B$  packets of  $W$  contiguous wavelengths each, depending on the potential capability to cross-connect the  $W$  wavelengths together. The total number of wavelengths in service is  $\Lambda=B \cdot W$ . A wavelength  $\lambda$  ( $\lambda=1, \dots, \Lambda$ ) is then identified by the wavelength  $w$  of the packet  $b$  ( $w=1, \dots, W$  and  $b=1, \dots, B$ ).

We redefine  $HCRR_n = \frac{I_n^W - I_n^H}{I_n^W}$  to characterize the hardware complexity reduction at a

given node  $n$  where  $I_n^W$  is the number of inputs when only a wavelength switching WXC is assumed while  $I_n^H$  is the total number of input when HXC is implemented (i.e. the sum of inputs to both WBXC and WXC).

The network topology gives for each node  $n$ ,  $L_n^{in}$  and  $L_n^{out}$  the number of links entering and outgoing this node.

The traffic estimation gives  $D_n$  and  $A_n$ , the number of wavelengths that can be dropped and added at node  $n$ .

The network design must then give:

$B_n^{drop}$ : the number of potential waveband drops at node n and therefore  $I_n^{drop}$  the number of wavelengths that can be individually dropped (since  $D_n = I_n^{drop} + B_n^{drop} W$ ). Note that for the sake of simplicity, we do not consider here any waveband add.

$I_n^{WXC}$ : the number of inputs to the WXC (of the HXC) at node n.

If we fix the number of fibers per link to F, the waveband granularity to W and since the number of inputs to a switch equals the number of outputs (due to the symmetry of the OXC) we have:

$$I_n^W = L_n^{in} F\Lambda + A_n = L_n^{out} F\Lambda + D_n$$

$$I_n^H = I_n^{WXC} + \frac{L_n^{in} F\Lambda}{W} + \frac{I_n^{WXC} - D_n}{W} + B_n^{drop} = I_n^{WXC} + \frac{L_n^{out} F\Lambda}{W} + \frac{I_n^{WXC} - A_n}{W} + B_n^{drop}$$

$$HCRR_n = \frac{L_n^{in} F\Lambda - L_n^{out} FB + A_n \left(1 + \frac{1}{W}\right) - \left[ I_n^{WXC} \left(1 + \frac{1}{W}\right) + B_n^{drop} \right]}{L_n^{in} F\Lambda + A_n}$$

Since it doesn't make sense to drop an added wavelength at the same node, we have:

$$I_n^{WXC} \geq A_n + I_n^{drop}.$$

If we write HCRR as a function of  $\mathfrak{w}^{in}$ , the number of wavebands going from the WBXC to be lambda switched at the WXC, and  $\mathfrak{w}^{out}$ , the number of wavebands coming from the WXC to enter the WBXC; we get:

$$HCRR_n = \frac{L_n^{in} F\Lambda - L_n^{in} FB - \mathfrak{v}_n^{out} - W\mathfrak{v}_n^{in}}{L_n^{in} F\Lambda + A_n}$$

Since all added wavelengths must have the possibility to get out of the WXC and the maximum number of outgoing wavebands is fixed by the outgoing fibers capacity we have:

$$\frac{A_n}{W} \leq \mathfrak{v}_n^{out} \leq L_n^{out} FB.$$

This can be written as:

$$\mathbf{v}_n^{out} = \left\lceil \frac{A_n}{W} + \mathbf{f}_n \left( L_n^{out} FB - \frac{A_n}{W} \right) \right\rceil \quad 0 \leq \mathbf{f}_n \leq 1.$$

$$\mathfrak{w}^{in} \text{ is related to } \mathfrak{w}^{out} \text{ by: } \mathbf{v}_n^{in} = L_n^{in} FB + \mathbf{v}_n^{out} - B_n^{drop} - L_n^{out} FB.$$

The total number of wavelengths that can be dropped limits  $B^{drop}$ , the number of potential wavebands dropped in bulk:  $0 \leq B_n^{drop} \leq \frac{D_n}{W}$  so we can write:

$$B_n^{drop} = \left\lceil \mathbf{q}_n \frac{D_n}{W} \right\rceil \quad 0 \leq \mathbf{q}_n \leq 1.$$

Then:

$$HCRR_n(\mathbf{f}_n, \mathbf{q}_n) = \frac{L_n^{out} F\Lambda - L_n^{in} FB + W \left\lceil \mathbf{q}_n \frac{D_n}{W} \right\rceil - (1+W) \left\lceil \frac{A_n}{W} + \mathbf{f}_n \left( L_n^{out} FB - \frac{A_n}{W} \right) \right\rceil}{L_n^{in} F\Lambda + A_n}$$

The two parameters  $\mathbf{f}$  and  $\mathbf{q}$  define the hierarchical cross-connect architecture.

Increasing  $\mathbf{f}$  increases the lambda switching possibility and so decreases the blocking probability at the expense of decreasing the complexity reduction ratio.

When we increase  $\mathbf{q}$ , the number of wavelengths to be dropped without entering the WXC is higher and the complexity reduction is improved. However, the wavelength assignment in this case is constrained to the bulk drop when this drop is chosen for a wavelength in a given waveband of a fiber.

When we don't allow wavelength conversion,  $\mathfrak{w}^{in}$ ,  $\mathfrak{w}^{out}$  and  $B^{drop}$  must be a multiple of  $B$  and this is to uniformly distribute switching types between the  $\Lambda$  wavelengths. This assumption is well matched to the multi-fiber hypothesis.



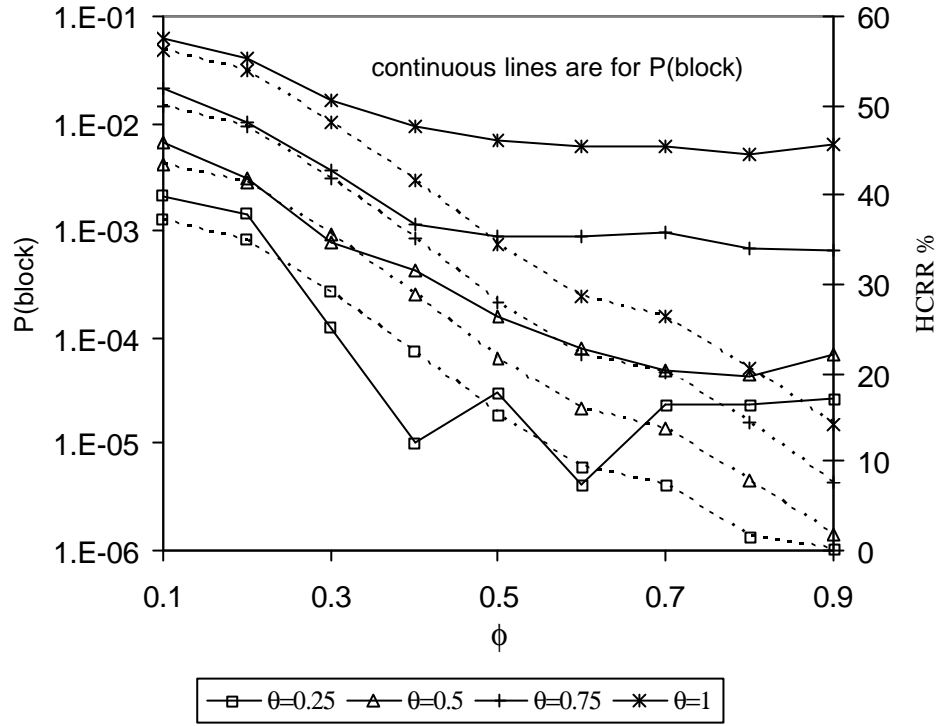


Figure 25: Blocking probability and HCCR for different values of  $\mathbf{f}$  and  $\mathbf{q}$  when  $\rho=600$ .

To show that the HCCR alone is not sufficient as a performance parameter, we consider the following simulation test. We consider the NSFNET 14-node 21-link network as a test network with  $F=4$ ,  $B=4$  and  $W=8$  ( $\Lambda=32$ ). Call requests are assumed to arrive according to an independent Poisson process with an exponentially distributed call holding.  $\rho$  is the mean network load, i.e. the mean load per source-destination node pair is  $\rho/N(N-1)$ . As a cross-connect control strategy, we consider that already used wavebands have the highest priority and keep the same switching until all included connections are torn down. Later in this document when we will discuss the dynamic traffic, we shall see that giving the highest priority to already used wavebands is not the perfect choice.

Figure 25 shows the simulation results with the mean value of the HCCR over the  $N$  nodes. As shown in this figure, there is a compromise between decreasing  $\mathbf{f}$  and increasing  $\mathbf{q}$ . Both increase the gain, however if for example we consider ( $\mathbf{q}=0.25$ ,  $\mathbf{f}=0.5$ ) and ( $\mathbf{q}=0.5$ ,  $\mathbf{f}=0.6$ ) we have almost the same HCCR ( $\approx 15.5\%$ ) but the first is better in term of blocking probability ( $3.E-5$  instead of  $8.E-5$ ).

Finally, in figure 25, note that for the same  $q$  with different values of  $f$  we might have almost the same blocking probability. This is due to the blocking resulting essentially from the limited number of add/drop ports rather than the switching constraint. The impact of the number of add/drop ports is studied in [30].

### III.3. The Operational Complexity Increase Ratio

Many parameters affect the blocking probability in an optical network. Connections may be blocked due to the limited number of add/drop ports, the limited link capacity, the wavelength continuity constraint, etc...

The network topology affects also the blocking probability. In some cases, we still can establish connections between any pair of nodes even if some links or some nodes are excluded. However, this will make the task of routing and wavelength assignment much more complex in order to reduce the blocking probability of future coming connections. Therefore, connectivity provides a measure of the network flexibility.

When HXCs are used, the bulk switching imposed on a number of ports (since the number of wavelengths to pass through the WXC is limited) reduces the number of connection patterns supported by a given HXC. Unsupported connection pattern cannot use this HXC which reduces the network connectivity.

In [18], the blocking behaviors of crosstalk-free optical banyan networks are studied. The blocking probability of a routing strategy is estimated by the ratio of number of blocked connection patterns for the strategy to the total number of connection patterns.

In [3], the blocking performance of non-hierarchical WXC with limited conversion capability is studied. A performance parameter is defined by the ratio of number of blocked connection patterns with limited conversion capability to the total number of connection patterns with full conversion capability.

We define, for  $y$  connections to be set up through an optical cross-connect (OXC), the operational complexity increase ratio  $OCIR(y)$  as a performance parameter to characterize the operational increased hardness of setting up the  $y$  connections when we consider a hierarchical cross-connect (HXC) instead of a wavelength cross-connect (WXC), where:

$$OCIR(y) = \frac{CP_{WXC}(y) - CP_{HXC}(y)}{CP_{WXC}(y)}$$

$CP_{WXC}(y)$  and  $CP_{HXC}(y)$  are the number of possible connection patterns to serve  $y$  connections through the WXC and through the HXC respectively. In both cases, we do not allow wavelength conversion.

The hardware complexity reduction ratio HCRR is another performance parameter to characterize the hardware complexity reduction when replacing a WXC by a HXC. This reduction comes with an increase in the operational complexity. The values of these ratios are not to be compared since the first consider the reduction in the number of inputs and the other considers the reduction in the number of possible ways to serve  $y$  connections.

The  $OCIR(y)$  and the HCRR are important at the design phase since the  $OCIR(y)$  describes how harder the routing and wavelength assignment (RWA) problem will be if we consider the HXC instead of the WXC and the design is done by compromising between a high HCRR and a low  $OCIR(y)$ . However  $OCIR(y)$  affect but does not necessarily reflect the blocking probability since the latter depends on the chosen RWA algorithm especially when the dynamic traffic is considered.

#### III.4. The Wavelength Cross-Connect Model

To find  $CP_{WXC}(y)$ , we consider the array model of a WXC given in [3] where the  $N$ -input and  $M$ -output WXC is modeled using an  $N \cdot \Lambda$  rows by  $M \cdot \Lambda$  columns array.  $\Lambda$  is the number of supported wavelengths per link. Placing an object at the  $n^{\text{th}}$  row  $m^{\text{th}}$  column represents connecting the input  $n$  to the output  $m$ .

Since we can connect a given input to only one output and reciprocally we cannot place more than one object in the same row or in the same column. This array is represented in figure 26. Since no wavelength conversion is allowed, serving  $y$  connections consists in placing  $y$  objects in the shaded area, that is placing  $j_1$  objects in the  $N$  by  $M$  dotted board of  $\lambda_1$ ,  $j_2$  objects in the  $N$  by  $M$  dotted board of  $\lambda_2, \dots$ ,  $j_\Lambda$  objects in the  $N$  by  $M$  dotted board of  $\lambda_\Lambda$  so that  $j_1 + j_2 + \dots + j_\Lambda = y$ .

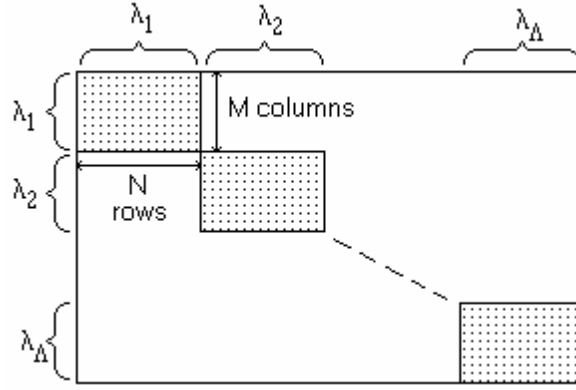


Figure 26: The WXC array model.

Placing  $p$  objects in the  $N$  by  $M$  board is the same as placing  $p$  non taking rooks on an  $N$  by  $M$  chessboard. The number of possible ways is then:

$$TT_p^{N,M} = \binom{N}{p} \binom{M}{p} p!$$

That is choosing  $p$  rows ( $\binom{N}{p}$  ways),  $p$  columns ( $\binom{M}{p}$  ways) and choosing which chosen row to be taken with which chosen column  $p!$  ways.

Since all cells of the  $\Lambda$  shaded sub-boards do not have any row or column in common with any cell in another shaded sub-board  $CP_{WXC}(y)$  is given by:

$$CP_{WXC}(y) = \sum_{\substack{j_1 + j_2 + \dots + j_\Lambda = y \\ l \leq j_n \leq L \quad \forall n}} TT_{j_1}^{N,M} \cdot TT_{j_2}^{N,M} \cdot \dots \cdot TT_{j_\Lambda}^{N,M} = r_\Lambda^{N,M}(y)$$

In each sub-board, we can place at most  $\min(N,M)$  objects since in each row or column we can place at most one object. The number  $n$  of objects to place in a given sub-board must be set such that what is left ( $y-n$ ) still can fit in the  $\Lambda-1$  other sub-board:  $y-n \leq \min(N,M) \cdot (\Lambda-1)$  that is  $n \geq \max(0, y - \min(N,M) \cdot (\Lambda-1))$ . In each sub-board, the number of objects to place must be less than or equal to  $y$  since this is the total number of objects to place:  $L = \min(N,M,y)$ .

If we spread this sum for all possible values of  $j_\Lambda$  we can write:

$$\begin{aligned}
r_{\gamma}^{N,M}(y) &= \sum_{j_1+\dots+j_{\gamma-1}=y-l} TT_{j_1}^{N,M} \dots TT_{j_{\gamma-1}}^{N,M} \cdot TT_l^{N,M} \\
&+ \sum_{j_1+\dots+j_{\gamma-1}=y-l-1} TT_{j_1}^{N,M} \dots TT_{j_{\gamma-1}}^{N,M} \cdot TT_{l-1}^{N,M} + \dots \\
&+ \sum_{j_1+\dots+j_{\gamma-1}=y-L} TT_{j_1}^{N,M} \dots TT_{j_{\gamma-1}}^{N,M} \cdot TT_L^{N,M}
\end{aligned}$$

To obtain the following recursive form as given in [3]:

$$r_{\Lambda}^{N,M}(y) = \sum_{i=l}^L r_{\Lambda-1}^{N,M}(y-i) \cdot TT_i^{N,M} \quad , \quad r_{\Lambda}^{N,M}(0) = 1 \quad , \quad r_1^{N,M}(y) = TT_y^{N,M} .$$

### III.5. The Hierarchical Cross-Connect Model

To find  $CP_{\text{HXC}}(y)$ , we first propose to model the HXC by the array shown in figure 27 where we define three kinds of objects:

- The *box* object that represents the waveband bypassed cross-connection. This object is a  $W$  by  $W$  grid ( $W$  is the waveband granularity,  $B$  is the number of wavebands:  $\Lambda=B.W$ ).
- The *strip* object that represents the waveband cross-connection reaching the  $\lambda\text{XC}$  to allow a wavelength cross-connection. This object is an  $N.W$  by  $W$  or a  $W$  by  $M.W$  grid depending if it represents a waveband cross-connection going to or coming from the  $\lambda\text{XC}$ .
- The *dot* object that represents the wavelength cross-connection. This object is to be placed in the box or in the strip object as we shall see.

Concerning the cross-connecting scheme of the WBXC, a bypassed waveband connecting input  $I_i$  to Output  $O_m$  is represented by placing a box at row  $I_i$  and column  $O_m$ . These row and column must be exclusively used by this object as in the non taking rooks' problem. A waveband cross-connecting the WBXC to the  $\lambda\text{XC}$  and then allowing a wavelength cross-connecting granularity is represented by a strip. Connecting an input waveband to the  $\lambda\text{XC}$  is

represented by a horizontal strip and an output waveband by a vertical strip. The set of areas formed by all intersections of horizontal and vertical strips forms the input/output connection pattern of the  $\lambda$ XC.

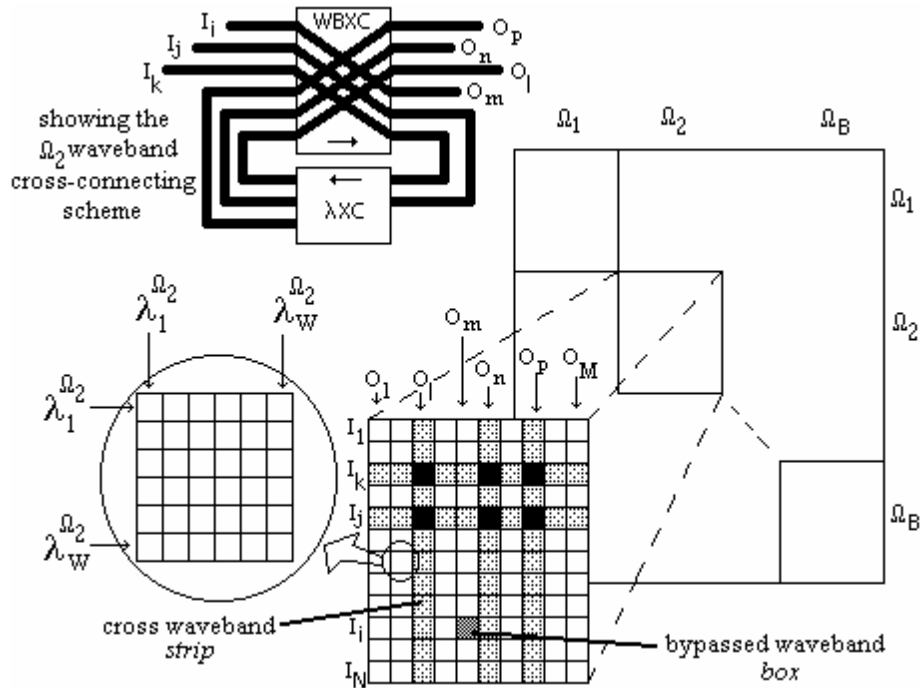


Figure 27: The HXC model.

A dot can be placed either in the box, at the diagonal only since inside a waveband that is switched in bulk no wavelength conversion is possible, or in the mentioned connection pattern of the  $\lambda$ XC, only at the diagonal of each intersection since we do not allow wavelength conversion.

For a given waveband (a given sub-board), for instance  $O_2$ , we can also represent the  $\lambda$ XC connection pattern by the model array given in figure 28. This is done using an easy transformation by rearranging rows and columns considering only the strip intersections (considering no wavelength conversion).

To complete the model, we represent, for a given waveband, in figure 29 the transformed array of the example given in figure 27 including the bypassed wavebands. This is to be used when we will study the internal flexibility in section III.5.1.

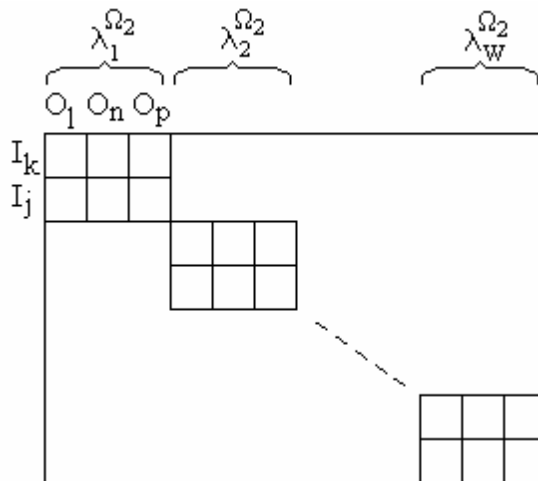


Figure 28: The  $\lambda$ XC model for a given waveband (e.g. O2).

Note how the bypassed waveband ( $I_i, O_m$ ) is spread on every wavelength sub-board but on the same local row  $I_i$  and column  $O_m$ .

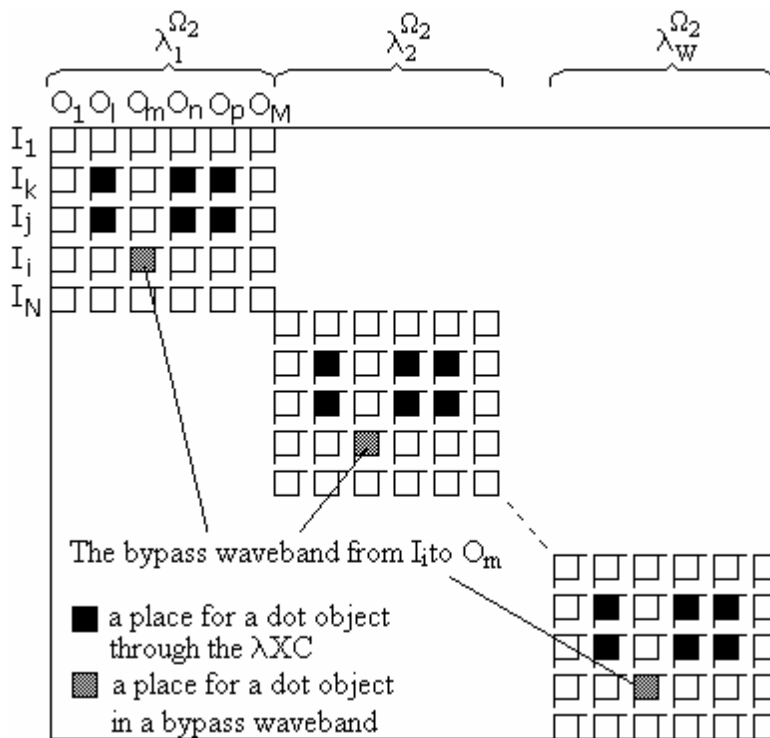


Figure 29: Another representation of the array of figure 27 for a given waveband (e.g. O2).

Having  $y$  connections, the number of possible connection patterns can be counted by distributing these connections on the  $B$  wavebands:  $j_1$  in the  $\Omega_1$  waveband,  $j_2$  in the  $\Omega_2$  waveband, ...,  $j_B$  in the  $\Omega_B$  waveband in order to have  $j_1 + j_2 + \dots + j_B = y$ . For each  $j$  in a given waveband  $\Omega_b$ , we count the number of possible connection patterns by considering the two disjoint cases:

- a. The case where (when it is possible) all the  $j_i$  connections are passing through the  $\lambda$ XC using at most  $\mathfrak{w}^{\text{in}}$  input cross-connecting wavebands and at most  $\mathfrak{w}^{\text{out}}$  output cross-connecting wavebands, where  $\mathfrak{w}^{\text{in}}$  and  $\mathfrak{w}^{\text{out}}$  fix the hardware design of the HXC. Let  $\mathbf{x}_{\mathbf{v}^{\text{in}}, \mathbf{v}^{\text{out}}}^{N, M, W}(j_i)$  be the number of ways for this case (to be evaluated later).
- b. The case where  $x$  of the  $j_i$  connections are served using a bypassed waveband and the other  $j_i - x$  connections are passing through the  $\lambda$ XC. To count the number of possible ways for this case, we consider also for each value of  $x$  all possible number of bypassed wavebands represented by the number of boxes in the array of figure 27. For a given  $x$  and a given number of boxes  $b$ , we must find:
  - The number of ways to place  $x$  objects (dots) in exactly  $b$  boxes and where each box can contain up to  $W$  objects since this is the number of places in the diagonal (no box could be empty). Let  $P_W^{b,b}(x)$  be this number where  $P_W^{b,u}(x)$  is the number of ways to place  $x$  objects in  $b$  boxes using exactly  $u$  of them (exactly  $b-u$  empty boxes) and where each box can contain up to  $W$  objects.  $P_W^{b,u}(x)$  is found by choosing the  $u$  boxes to be filled:  $\binom{b}{u}$  ways, then by distributing the  $x$  objects on the  $uW$  places excluding the case where the  $x$  objects are fitted in less than  $u$  of the  $u$  chosen boxes. We have then:

$$P_W^{b,u}(x) = \left[ \binom{u \cdot W}{x} - \sum_{i=\lfloor \frac{x}{W} \rfloor}^{u-1} P_W^{u,i}(x) \right] \cdot \binom{b}{u}$$



$$P_W^{b, \left\lfloor \frac{x}{W} \right\rfloor}(x) = \left( \left[ \begin{array}{c} x \\ \frac{x}{W} \\ x \end{array} \right] \cdot W \right) \cdot \left( \left[ \begin{array}{c} b \\ \frac{x}{W} \end{array} \right] \right)$$

- The number of ways to place the  $b$  boxes in the  $N$  by  $M$  sub-board of figure 27 is the non taking rooks problem:  $TT_b^{N,M}$  ways.
- The number of ways to serve the remaining  $j_i - x$  connections by passing through the  $\lambda$ XC using at most  $\overline{\omega}_i$  input cross-connecting wavebands and at most  $\overline{\omega}_o$  output cross-connecting wavebands connected to the remaining unused input and output wavebands. This is given by  $\mathbf{x}_{\mathbf{v}^{in}, \mathbf{v}^{out}}^{N-b, M-b, W}(j_i - x)$ .

$CP_{HXC}(y)$  is then given by:

$$CP_{HXC}(y) = \sum_{j_1 + \dots + j_B = y} \left\{ \prod_{i=1}^B \left[ \mathbf{x}_{\mathbf{v}^{in}, \mathbf{v}^{out}}^{N, M, W}(j_i) + \sum_{x=1}^{j_i} \sum_{b=\left\lfloor \frac{x}{W} \right\rfloor}^{\min(x, N, M)} P_W^{b, b}(x) \cdot TT_b^{N, M} \cdot \mathbf{x}_{\mathbf{v}^{in}, \mathbf{v}^{out}}^{N-b, M-b, W}(j_i - x) \right] \right\}$$

### III.5.1 Internal Flexibility and Evaluation of $\mathbf{x}_{\mathbf{v}^{in}, \mathbf{v}^{out}}^{N, M, W}(y)$

Having the array of figure 27, to evaluate  $\mathbf{x}_{\mathbf{v}^{in}, \mathbf{v}^{out}}^{N, M, W}(y)$  we consider all combinations of input and output crossing wavebands having a number less or equal than  $\overline{\omega}^{in}$  and  $\overline{\omega}^{out}$  respectively (at most  $\overline{\omega}^{in}$  horizontal strips and  $\overline{\omega}^{out}$  vertical strips). To avoid counting the same connection pattern several times, we must keep only combinations having all chosen wavebands with at least one used wavelength (strips containing at least one dot).

From another point of view, we must consider the HXC as a black box while studying its performance and count the number of connection patterns as seen from the input and output to the HXC without considering what we call in this chapter the internal flexibility. We mean by internal flexibility the capability of implementing the same connection pattern by different internal ways (i.e. passing through the  $\lambda$ XC or not when it is possible) as shown in figure 30.

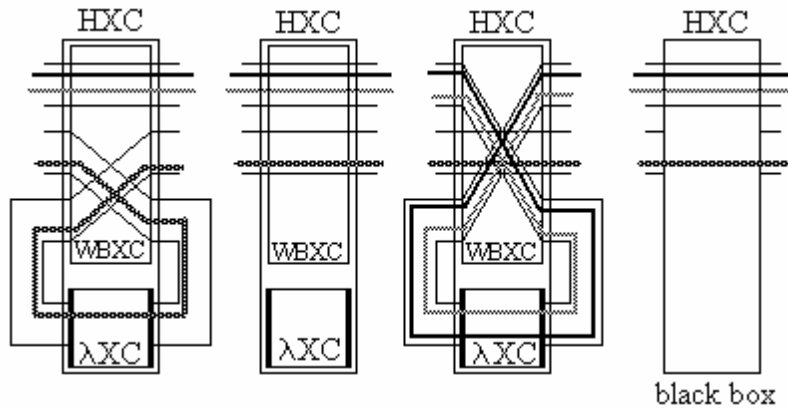


Figure 30: Internal flexibility: three ways to implement the same connection pattern.

To avoid this, we must exclude the cases where the bypassed waveband can be substituted to a crossed waveband. We show in figure 31 the case where a bypassed waveband cannot be substituted to a crossed waveband.

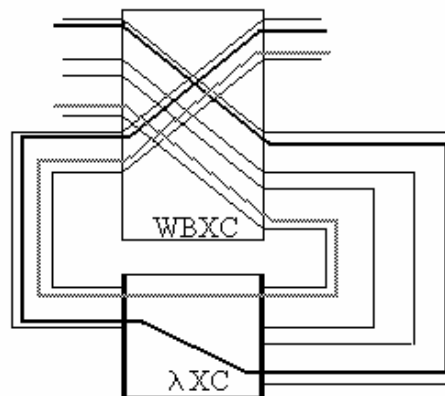


Figure 31: An example where a bypassed waveband cannot be substituted to a crossed waveband.

A bypassed waveband reserves, as shown in figure 29, in the array for a given waveband the same local row and local column in each sub-board to allow putting objects (dots) only at these row/column intersections. So while placing objects in the  $\lambda XC$  array model, we must exclude the cases where we can find the same local column and row for all sub-boards having objects (dots) only at the row/column intersections. So we must use  $\mathbf{r}_w^{n,m}(y)$  instead of  $r_w^{n,m}(y)$  where  $\mathbf{r}_w^{n,m}(y)$  is the number of ways to place  $y$  non taking rooks on  $W$  sub-boards of  $n$  rows and  $m$  columns each and where no cell in a sub-board shares the same row or column with any

other sub-board excluding the cases where for a given local row and column in each sub-board rooks are only found at the row/column intersections.

Since  $\mathbf{x}_{\mathbf{v}^{in}, \mathbf{v}^{out}}^{N, M, W}(y)$  is the number of possible connection patterns using at most  $\mathfrak{W}^{in}$  input crossed wavebands and  $\mathfrak{W}^{out}$  output crossed wavebands we can write:

$$\mathbf{x}_{\mathbf{v}^{in}, \mathbf{v}^{out}}^{N, M, W}(y) = \sum_{i=\lfloor \frac{y}{W} \rfloor}^{\mathbf{v}^{in}} \sum_{j=\lfloor \frac{y}{W} \rfloor}^{\mathbf{v}^{out}} \mathbf{h}_{i,j}^{N, M, W}(y)$$

where  $\eta_{i,j}^{N, M, W}(y)$  is the number of possible connection patterns using exactly  $i$  input crossed wavebands and  $j$  output crossed wavebands where we cannot substitute a bypassed waveband to a crossed waveband. It is given by:

$$\mathbf{h}_{i,j}^{n, m, W}(y) = \left[ \mathbf{r}_{\lfloor \frac{y}{W} \rfloor}^{i, j}(y) - \sum_{\substack{l=\lfloor \frac{y}{W} \rfloor, \dots, i \\ p=\lfloor \frac{y}{W} \rfloor, \dots, j \\ (l, p) \neq (i, j)}} \mathbf{h}_{l, p}^{n, m, W}(y) \right] \cdot \binom{n}{i} \cdot \binom{m}{j}$$

Since we have  $\binom{n}{i} \binom{m}{j}$  possible ways of choosing the  $i$  and  $j$  wavebands and then we must exclude from  $\mathbf{r}_{\lfloor \frac{y}{W} \rfloor}^{n, m}(y)$  the cases where the connection patterns could use a smaller number of crossed wavebands with:

$$\eta_{\lfloor \frac{y}{W} \rfloor, \lfloor \frac{y}{W} \rfloor}^{n, m, W}(y) = \mathbf{r}_{\lfloor \frac{y}{W} \rfloor}^{n, m}(y) \cdot \left( \binom{n}{\lfloor \frac{y}{W} \rfloor} \right) \cdot \left( \binom{m}{\lfloor \frac{y}{W} \rfloor} \right)$$

### III.5.2 Evaluation of $\mathbf{r}_{\lfloor \frac{y}{W} \rfloor}^{n, m}(y)$

The problem is to find the number of ways to place  $y$  non taking rooks in  $W$  sub-boards placed in staircase of  $n$  row and  $m$  column each, excluding the case where, for the same local row and local column of all sub-boards, rooks may only be placed on the row/column

intersection. To solve this problem, we propose to use the principle of inclusion and exclusion (Appendix C).

We enumerate the set of positions in a sub-board from 1 to  $n \cdot m$  and we consider that a rook pattern have the property  $i$  if at the corresponding row and column (of the  $i$  position), rooks may only be placed at this row/column intersections for all sub-boards.

The number of ways to place  $y$  rooks while having the  $i$  property is the same as placing  $y$  rooks on the set of the  $W$  sub-boards where we exclude all entries of the corresponding row and column except the intersection ones as in figure 32 and excluding the cases where none of these intersections is filled.

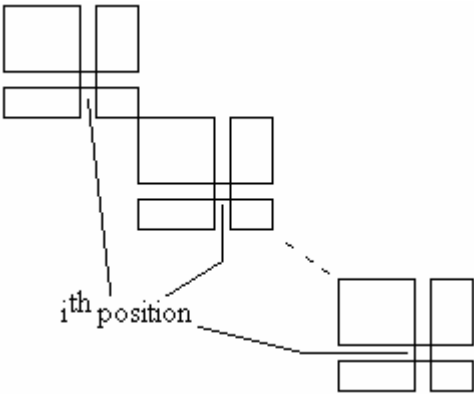


Figure 32: The set of  $W$  sub-boards for a given waveband where for the  $i$ th position we exclude all other entries in the same row and column.

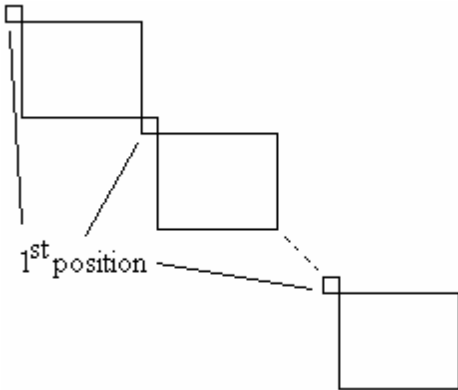


Figure 33: We have the same number of connection patterns for all positions so we consider the first one.

For all nm properties, we have the same number of ways to place the y rooks so we consider the shape of figure 33.

For that, we consider that x of the y rooks are placed in a sub-board at the position i where  $1 \leq x \leq \min(W, y)$  with  $\binom{W}{x}$  ways and the other y-x rooks are placed as non taking rooks in the W sub-boards of n-1 row and m-1 column each with  $r_W^{n-1, m-1}(y-x)$  ways. Since we have  $n \cdot m = \Gamma_1^{n, m}$  properties the total number of ways to have one of the i properties is  $\chi_1^{n, m, W}(y) \cdot \Gamma_1^{n, m}$ , where:

$$\chi_1^{n, m, W}(y) = \sum_{x=1}^{\min(W, y)} \binom{W}{x} \cdot r_W^{n-1, m-1}(y-x)$$

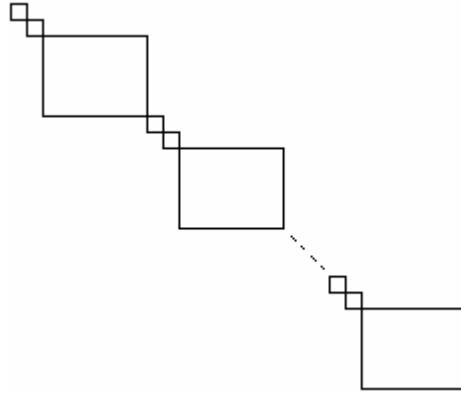


Figure 34: Considering that for a given waveband we have the property 1 and the property 2.

Now we consider the case where we have at the same time two properties i and j. We have  $\Gamma_2^{n, m}$  such cases. The number of ways for each case is given by considering the board shape of figure 34. That is:

$$\chi_2^{n, m, W}(y) = \sum_{x=1}^{\min(W, y)} \binom{W}{x} \cdot \chi_1^{n-1, m-1, W}(y-x)$$

Using the same logic when having i of the properties and applying the principle of inclusion and exclusion (Appendix C) we obtain:

$$r_W^{n,m}(y) = r_W^{n,m}(y) + \sum_{i=1}^{\min(n,m)} (-1)^i \cdot \chi_i^{n,m,W}(y) \cdot TT_i^{n,m}$$

where  $\chi_i^{n,m,W}(y)$  is the number of ways to place  $y$  rooks having  $i$  of the properties from 1 to  $n \cdot m$  and it is given by:

$$c_i^{n,m,W}(y) = \sum_{x=1}^{\min(W,y)} \binom{W}{x} \cdot c_{i-1}^{n-1,m-1,W}(y-x)$$

with  $\chi_0^{n,m,W}(y) = r_W^{n,m}(y)$ .

### III.6. Numerical Results

We consider first a 6-input 6-output ( $N=M=6$ ) optical cross-connect with  $\Lambda=32$  wavelengths. For each waveband granularity ( $W=32, 16$  and  $8$ ), we find  $OCIR(y)$  for different HXC design (number of interlayer multiplexer per waveband =  $\mathfrak{W}^{\text{in}}$  = number of interlayer multiplexer per waveband =  $\mathfrak{W}^{\text{out}} = 1, \dots, 4$ ) and hence different HCRR.

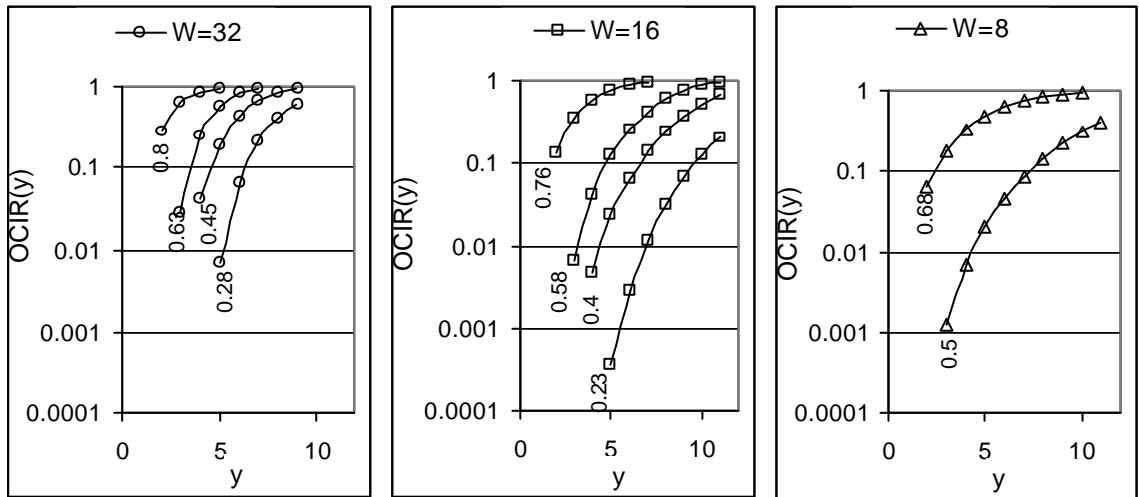


Figure 35:  $OCIR(y)$  for different waveband granularities and different HCRRs.

The results are shown in figure 35 where the hardware complexity reduction ratio is shown near the corresponding data series.

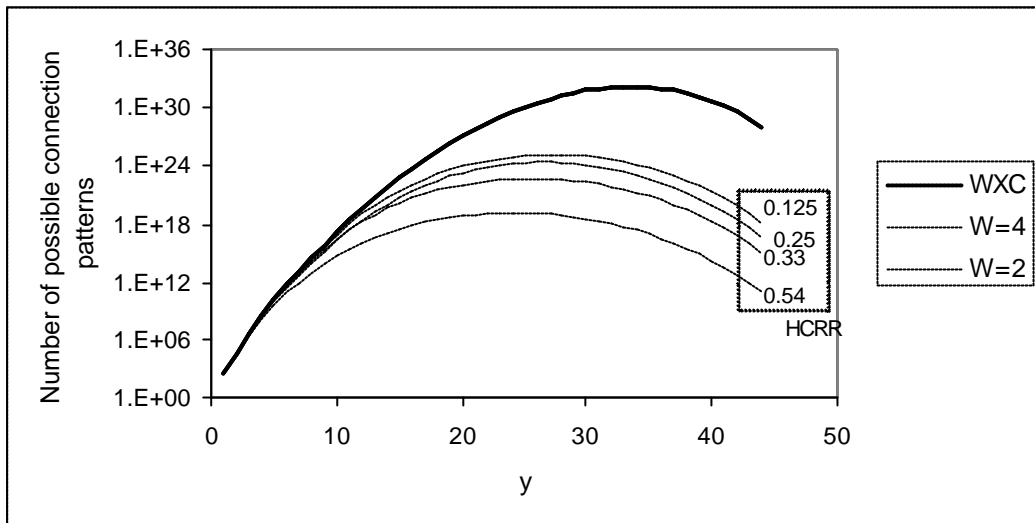


Figure 36: The number of possible connection patterns for  $N=M=6$  and  $\Lambda=8$ .

Note that a small difference in the hardware complexity reduction relaxes the operational complexity when the granularity is reduced (for instance when  $HCR=0.63$  for  $W=32$ ,  $HCR=0.58$  for  $W=16$  and  $HCR=0.5$  for  $W=8$ ) so we must fix a minimal hardware complexity reduction and then consider the minimum possible waveband granularity  $W$  to reach that  $HCR$ .

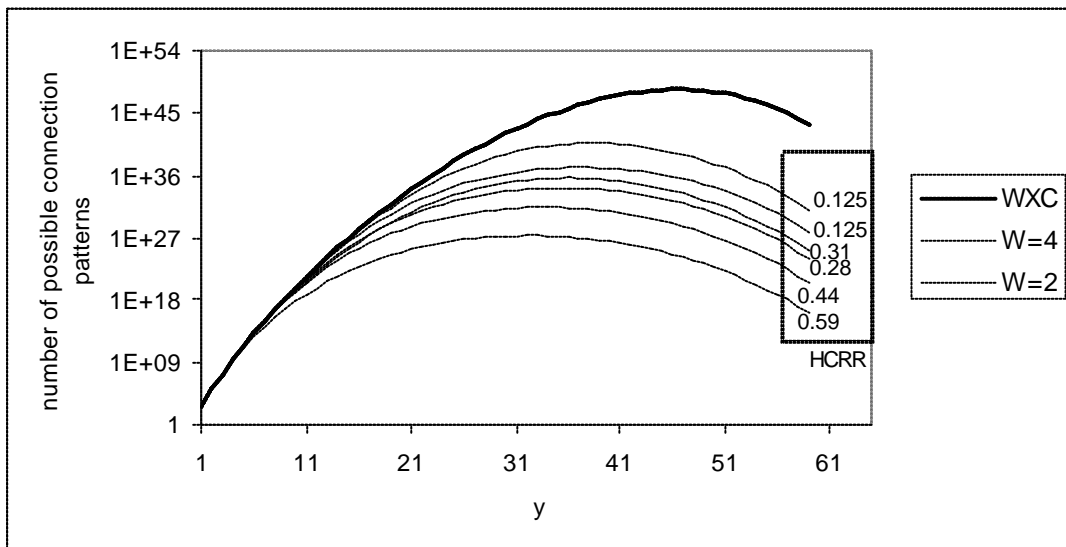


Figure 37:  $N=M=8$  and  $\Lambda=8$ .

OCIR tends rapidly towards 1. However this is not as disastrous as it seems. In fact, if we represent the number of possible connection patterns we can have a better idea on the operational complexity.

Figure 36 shows the number of possible connection patterns for  $N=M=6$  and  $\Lambda=8$  for different waveband granularities  $W$ .

Figure 37 shows the results for  $N=M=8$  and  $\Lambda=8$  for different values of  $W$ .

Note how for the same HCRR the lower waveband granularity gives better performances as deduced from figure 35.

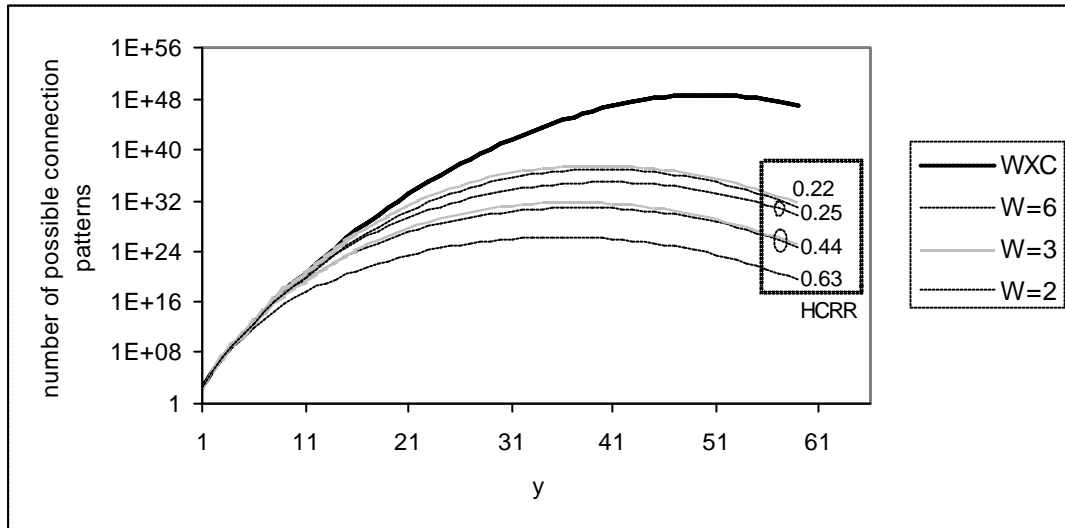


Figure 38:  $N=M=6$  and  $\Lambda=12$

Figure 38 shows also the result when  $N=M=6$  and  $\Lambda=12$ .

### III.7. Conclusion

In this chapter, the hierarchical optical cross-connect is modeled to evaluate the operational complexity increase when the hardware complexity is reduced. The operational complexity increase ratio is independent of the routing and wavelength assignment algorithm and hence does not exactly reflect the blocking probability but is useful to compare the difficulty of RWA for different hardware implementations.



## IV. STATIC TRAFFIC AND WAVELENGTH REARRANGEMENT

### IV.1. Introduction

We consider the problem of wavelength rearrangement to optimize the use of hierarchical cross-connects (HXC) in order to reduce the optical cross-connect (OXC) complexity with no wavelength conversion. These HXCs implement optical bypass at coarse granularity, using the wavelength banding technique with waveband cross-connects (WBXC), and at fine granularity using wavelength cross-connects (WXC).

After doing routing and wavelength assignment (RWA), we propose a wavelength rearrangement that consists of changing the order of wavelengths without changing the distribution plan resulting from RWA and so reducing the size of the design problem. The main idea is to prevent the use of wavelength converters, which are not cost-effective, while satisfying the contiguity of wavelengths making a useful waveband. At each node, maximizing the number of packed wavebands where all or no included wavelengths are dropped results in reducing the total number of switching units.

During online operation, reassignment is usually not allowed since it causes traffic interruption. However, in some cases (e.g., during failure recovery) we can tolerate short interruptions and hence apply the wavelength rearrangement in order to optimize the wavebanding and hence reduce the blocking probability of subsequent demands. The described rearrangement reduces the information to communicate to achieve the reassignment.

We present in this chapter an integer linear programming formulation for wavelength rearrangement and then we propose a heuristic method to find a solution for large-scale networks. Numerical results are given to show the complexity reduction.

#### IV.1.1 Wavelength Banding and Hierarchical Cross-Connect

As mentioned before, we can benefit from the wavelength banding by using a hierarchical OXC where we have an efficient two-stage multiplexing methodology. Note that in this

chapter, we do not allow wavelength conversion. WBXC is a waveband cross-connect which implements optical bypass at the waveband granularity.

At the end of a fiber-link entering a node, we distinguish three types of wavebands:

1. Empty or unused waveband: all wavelengths making this waveband carry no traffic flows. In this case, no port is dedicated for this waveband in the WBXC of the corresponding node.
2. Packed waveband: either all included and used wavelengths are dropped (waveband drop) or all included and used wavelengths bypass the node to catch the same waveband in the same destination fiber. In this case, no ports are dedicated in the WXC for this waveband.
3. Unpacked waveband: This is when the included wavelengths must be demultiplexed to enter the WXC.

Hardware complexity is characterized by the total number of ports at each node. This is the sum of the WBXC ports and the WXC ports of the corresponding node.

#### **IV.1.2 Related Works**

In [23], the problem is formulated on RWA while using wavelength converters to decrease the wavelength requirement and to satisfy the wavelength contiguity in a waveband. In this chapter, we consider that RWA are already done and that contiguity is assured by rearrangement with no wavelength converters.

### **IV.2. Wavelength Rearrangement**

#### **IV.2.1 The Purpose of Wavelength Rearrangement**

Having the traffic pattern for a given network, we apply the routing and wavelength assignment (RWA) algorithm. The result is a dedicated path (lightpath) and a dedicated wavelength for each connection in order to satisfy some criteria such as minimizing the number of supported wavelengths with no contention since only one connection can have a given wavelength in the same fiber-link. The wavelength assignment can be seen as the answer to the following question: “which lightpaths can have the same wavelength channel?”

independently of the wavelength channel to be assigned to these lightpaths. In other words, RWA assigns for each lightpath a wavelength  $\lambda_i$  from a set of wavelengths  $\{\lambda_1, \lambda_2, \dots, \lambda_n\}$  without being concerned if  $\lambda_i$  is, for instance, at 1300 nm, 1546 nm or any other wavelength channel. What does really matter is which spatially non-overlapped lightpaths must share the same wavelength channel; this is what we call here a distribution plan. We call logical wavelength, the wavelength (such as  $\lambda_i$ ) characterizing lightpaths that must have the same wavelength channel as specified by RWA. If we consider that each position in the set of logical lightpath represents a wavelength channel (the first position for the first wavelength channel, the second position for the second wavelength channel and so on), exchanging the position of logical wavelengths changes the channel contiguity without changing the distribution plan.

The wavelength rearrangement consists in changing the order of wavelengths e.g. the position of logical wavelengths representing their wavelength channel, while keeping the same distribution plan as specified by the wavelength assignment.

The goal of wavelength rearrangement is to maximize the number of packed wavebands by privileging the channel contiguity of logical wavelengths that can make a packed waveband. Since the distribution plan is fixed by the wavelength assignment, changing the wavelength order to form a packed waveband at the end of a fiber-link can destroy the right contiguity in other wavebands in other fiber-links. The global performance must therefore be improved.

#### **IV.2.2 The Number of Possible Solutions**

In this chapter, we consider a fixed granularity  $W$  for all wavebands. We suppose that the total number of supported wavelengths is a multiple of  $W$  (if not, up to  $W-1$  unused wavelengths could be added). Let  $N$  be the number of supported wavelengths,  $B=N/W$  is then the number of wavebands at the end of each fiber-link. If we consider the wavelength axis, the position of the logical wavelength on this axis determines its wavelength channel. At the end of each fiber-link, the first waveband is made by the first  $W$  positions, the second one by the following  $W$  positions and so on.

When we permute the wavelengths inside a waveband, no new packed wavebands are formed nor are existing packed wavebands destroyed.

Consequently, to construct the  $B = \lambda / W$  wavebands we have the following number of different ways:

$$\binom{\lambda}{W} \binom{\lambda - W}{W} \binom{\lambda - 2W}{W} \cdots \binom{W}{W} = \prod_{i=0}^{B-1} \binom{\lambda - iW}{W}$$

This can be simply reduced to:

$$\prod_{i=0}^{B-1} \binom{\lambda - iW}{W} = \frac{\lambda!}{(W!)^B}$$

We must also consider that permuting the position of wavebands does not lead to a different solution so the total number of different solutions is:

$$\frac{\lambda!}{(W!)^B B!}$$

For instance, for only 16 wavelengths ( $\lambda = 16$ ) and a waveband granularity of 4 wavelengths ( $W = 4$ ) we have 2627625 different solutions. This is to give an idea on the large size of the problem.

### IV.3. Problem Formulation

#### IV.3.1 Constants and Variables

We define the following constants depending on the network topology and resulting from routing and wavelength assignment:

$\lambda$  : the number of wavelengths per fiber.

$N$ : the number of nodes.

$T$ : the total number of fiber-links in the network.

$W$ : the waveband granularity.

$B$ : the number of wavebands per fiber ( $B = \lambda / W$ ).

$\sigma_{pq}$ : is 1 if fiber p enters a node while fiber q leaves the same node (p leads to q), 0 otherwise. An example is given in figure 39. Note that we do not consider that fiber p leads to fiber q if they share the same two end nodes.

$$\left( \mathbf{s}_{pq} \right)_{\substack{p=1,\dots,T \\ q=1,\dots,T}} = \begin{bmatrix} 0 & 0 & 0 & 0 & 0 & 0 & 0 & 0 & 0 & 1 \\ 0 & 0 & 1 & 0 & 0 & 0 & 0 & 0 & 0 & 0 \\ 0 & 0 & 0 & 0 & 1 & 1 & 0 & 0 & 0 & 0 \\ 1 & 0 & 0 & 0 & 0 & 0 & 0 & 0 & 0 & 0 \\ 0 & 0 & 0 & 0 & 0 & 0 & 0 & 0 & 1 & 0 \\ 0 & 0 & 0 & 0 & 0 & 0 & 0 & 0 & 1 & 0 \\ 0 & 0 & 0 & 1 & 1 & 1 & 0 & 0 & 0 & 0 \\ 0 & 0 & 0 & 0 & 0 & 0 & 0 & 0 & 0 & 0 \\ 0 & 0 & 0 & 0 & 0 & 0 & 1 & 0 & 0 & 0 \\ 0 & 0 & 0 & 0 & 0 & 0 & 0 & 0 & 1 & 0 \end{bmatrix}$$

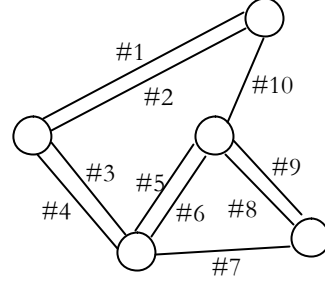


Figure 39: An example showing a network where  $T=10$  to clarify the definition of  $\sigma_{pq}$ .

$\delta_b$ : is 1 if the wavelength channel  $j$  is included in the waveband  $b$ , 0 otherwise. Since the first  $W$  wavelength channels form the first waveband, the second  $W$  wavelength channels form the second waveband and so on, we can write:

$$\mathbf{d}_{jb} = \begin{cases} 1 & \text{if } \left\lceil \frac{j}{W} \right\rceil \leq b < \left\lceil \frac{j}{W} \right\rceil + 1 \\ 0 & \text{otherwise} \end{cases}$$

$\eta_{ip}$ : is 1 if the logical wavelength  $\lambda_i$  is used (carries data flows) in fiber  $p$ , 0 otherwise.

$\psi_{ipq}$ : is 1 if the logical wavelength  $\lambda_i$  is bypassed from fiber  $p$  to fiber  $q$  at the corresponding node.

$\chi_{ipq}$ : is 1 if the logical wavelength  $\lambda_i$  is bypassed from fiber  $p$  to fiber  $q$  or if  $p$  leads to  $q$  while  $\lambda_i$  is not used by neither  $p$  nor  $q$ , 0 otherwise. This is to indicate if it is possible to include the logical wavelength  $\lambda_i$  in a bypassed waveband from  $p$  to  $q$ . It is given by:

$$\mathbf{c}_{ipq} = \mathbf{y}_{ipq} + (1 - \mathbf{h}_{ip})(1 - \mathbf{h}_{iq})\mathbf{s}_{pq} \quad \forall i = 1 \dots \Lambda, p = 1 \dots T, q = 1 \dots T$$

For instance, in figure 40 we have  $\eta_{1,1} = 1$ ,  $\eta_{1,3} = 0$ ,  $\psi_{1,1,2} = 1$ ,  $\psi_{1,1,3} = 0$ ,  $\chi_{1,1,2} = 1$ ,  $\chi_{1,3,4} = 1$  and  $\chi_{1,1,3} = 0$ .

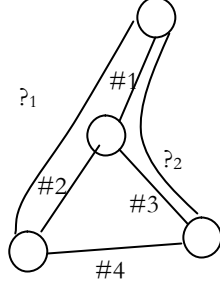


Figure 40: example to clarify the definition of  $\eta_{ip}$ ,  $\psi_{ipq}$  and  $\chi_{ipq}$

$I_n^{link}$ : is the set of input links to node n.

$O_n^{link}$ : is the set of output links from node n.

We also define the following variables:

$\lambda_{ij}$ : is 1 if the logical wavelength  $?_i$  must occupy the position j which means that the wavelength channel j must be assigned to the logical wavelength  $?_i$ , 0 otherwise.

$p_{b,pq}$ : is 1 if the waveband b can be a packed waveband bypassed from fiber p to fiber q, 0 otherwise.

$u_{b,p}$ : is 1 if the waveband b is used (at least one included wavelength is used) in the fiber p, 0 otherwise.

Note that the following expression is 1 if the logical wavelength  $?_i$  (the RWA one) will be included in waveband b after rearrangement:

$$\sum_{j=1}^{\Lambda} d_{jb} \mathbf{1}_{ij}$$

### IV.3.2 The Integer Linear Programming

The integer linear programming (ILP) for wavelength rearrangement can be formulated as follows:

$$\text{Minimize: } \sum_{n=1}^N \sum_{b=1}^B \left\{ \sum_{p \in I_n^{\text{link}}} \left[ u_{bp} + \left( u_{bp} - \sum_{q=1}^T \mathbf{p}_{bpq} \right) W \right] + \sum_{q \in O_n^{\text{link}}} \left( u_{bq} - \sum_{p=1}^T \mathbf{p}_{bpq} \right) \right\} \quad (1)$$

Subject to:

$$\mathbf{p}_{bpq} W \leq \mathbf{s}_{pq} \sum_{i=1}^{\Lambda} \mathbf{c}_{ipq} \sum_{j=1}^{\Lambda} \mathbf{d}_{jb} \mathbf{l}_{ij} \quad \forall b = 1 \dots B, p = 1 \dots T, q = 1 \dots T \quad (2)$$

$$\mathbf{p}_{bpq} \leq \mathbf{s}_{pq} \sum_{i=1}^{\Lambda} \mathbf{y}_{ipq} \sum_{j=1}^{\Lambda} \mathbf{d}_{jb} \mathbf{l}_{ij} \quad \forall b = 1 \dots B, p = 1 \dots T, q = 1 \dots T \quad (3)$$

$$u_{bp} \leq \sum_{i=1}^{\Lambda} \mathbf{h}_{ip} \sum_{j=1}^{\Lambda} \mathbf{d}_{jb} \mathbf{l}_{ij} \quad \forall b = 1 \dots B, p = 1 \dots T \quad (4)$$

$$u_{bp} \geq \mathbf{d}_{jb} \sum_{i=1}^{\Lambda} \mathbf{h}_{ip} \mathbf{l}_{ij} \quad \forall b = 1 \dots B, p = 1 \dots T, j = 1 \dots \Lambda \quad (5)$$

$$\sum_{j=1}^{\Lambda} \mathbf{l}_{ij} = 1 \quad \forall i = 1 \dots \Lambda \quad (6)$$

$$\sum_{i=1}^{\Lambda} \mathbf{l}_{ij} = 1 \quad \forall j = 1 \dots \Lambda \quad (7)$$

All variables are binary (8)

The objective (1) is to minimize the total number of inputs to the HXC in order to increase the HCRR (since  $HCRR_n = \frac{I_n^W - I_n^H}{I_n^W}$ ). The number of inputs to the HXC at a given node  $n$  ( $I_n^H$ ) is, as already mentioned, the sum of inputs to the WBXC and the internal WXC.

The number of inputs to the WBXC equals the number of used wavebands in the input fibers plus the number of wavebands going out of the internal WXC, which is the number of used wavebands in the output fibers excluding those making packed wavebands (since packed wavebands do not pass through the internal WXC): 
$$\sum_{b=1}^B \left\{ \sum_{p \in I_n^{link}} u_{bp} + \sum_{q \in O_n^{link}} \left( u_{bq} - \sum_{p=1}^T p_{bpq} \right) \right\}.$$

The number of inputs to the internal WXC equals the numbers of added wavelengths plus the number of wavelengths of used wavebands in the input fibers demultiplexed to pass through the WXC, which is  $W$  times the number of used wavebands in the input fibers excluding those making packed wavebands:  $A_n + \sum_{b=1}^B \sum_{p \in I_n^{link}} \left( u_{bp} - \sum_{q=1}^T p_{bpq} \right) W$ .  $A_n$ , the number of added wavelengths to the OXC  $n$ , is not considered in the objective since it is constant for a given traffic demand. Note that multiplying by  $W$  assumes that all wavelengths included in a waveband passing through the internal WXC are used and applied to this WXC. This is not always the case. However, this assumption is needed since multiplying by the exact number of used wavelengths leads to a non linear expression. This approximation is compromised by the fact that this ILP tends to fill up wavebands by minimizing the number of used wavebands. From another point of view and for technical reasons (not to tailor a WXC for each case), we might have to count  $W$  inputs for each deaggregated waveband.

In the constraint (2)  $p_{bpq}$  can be 1 if all  $W$  wavelengths included in the  $b^{\text{th}}$  waveband can form a bypassed waveband from fiber  $p$  to fiber  $q$ . Note that the objective helps in setting  $p_{bpq}$  to 1 when it is possible.

Constraint (3) forces  $p_{bpq}$  to be 0 if the corresponding waveband  $b$  is empty.

Constraint (4) sets  $u_{bp}$  to zero if no included wavelength is used (fiber  $p$ , waveband  $b$ ).



Constraint (5) sets  $u_{bp}$  to one if any included wavelength is used (fiber  $p$ , waveband  $b$ ).

Constraints (6) and (7) assure that a given wavelength channel is assigned to one and only one logical wavelength.

In this formulation, wavebands dropped in bulk are not taken into account. To consider the waveband drop, we must exclude also from the number of wavebands applied to the internal WXC those dropped in bulk. We can add the variable  $d_{bp}$  where  $d_{bp}$  is 1 if the waveband  $b$  of the fiber link  $p$  is dropped in bulk, 0 otherwise:

$$d_{bp} \leq u_{bp} \quad \forall b = 1 \dots B, p = 1 \dots T \quad (9)$$

$$d_{bp} \leq 1 - \mathbf{y}_{ipq} \sum_{j=1}^{\Lambda} \mathbf{d}_{jb} \mathbf{l}_{ij} \quad \forall b = 1 \dots B, i = 1 \dots \Lambda, p = 1 \dots T, q = 1 \dots T \quad (10)$$

We implemented this ILP in GLPK and tried it on a small test network as given in appendix D. For low loads, the proposed heuristic comes close to the true optimal solution. Unfortunately and as expected, for higher loads or larger networks where the problem is critical the solution is not achieved in a feasible execution time.

### IV.3.3 Bounds on the Complexity Reduction

We define the following ratio to characterize the hardware complexity reduction at each node:

$$HCRR = \frac{I^W - I^H}{I^W}$$

where  $I^W$  is the number of inputs to the OXC when it is only a WXC and  $I^H$  is the total number of inputs to the OXC when HXC is considered.  $I^H$  is the number of inputs, in terms of wavelengths, to the included WXC plus the number of inputs, in terms of wavebands, to the included WBXC.

To find the upper bound on HCRR, we must consider the case where  $I^H$  is a minimum. In fact,  $I^W$  is fixed by the routing algorithm and it is not concerned by the wavelength rearrangement:

$$I^W = N_a + N_d + N_p$$

where  $N_a$  is the number of added wavelengths, since we do not consider waveband adds,  $N_d$  is the number of dropped wavelengths, since to be dropped a wavelength must enter the OXC and  $N_p$  is the number of wavelengths passing through the node (figure 41).

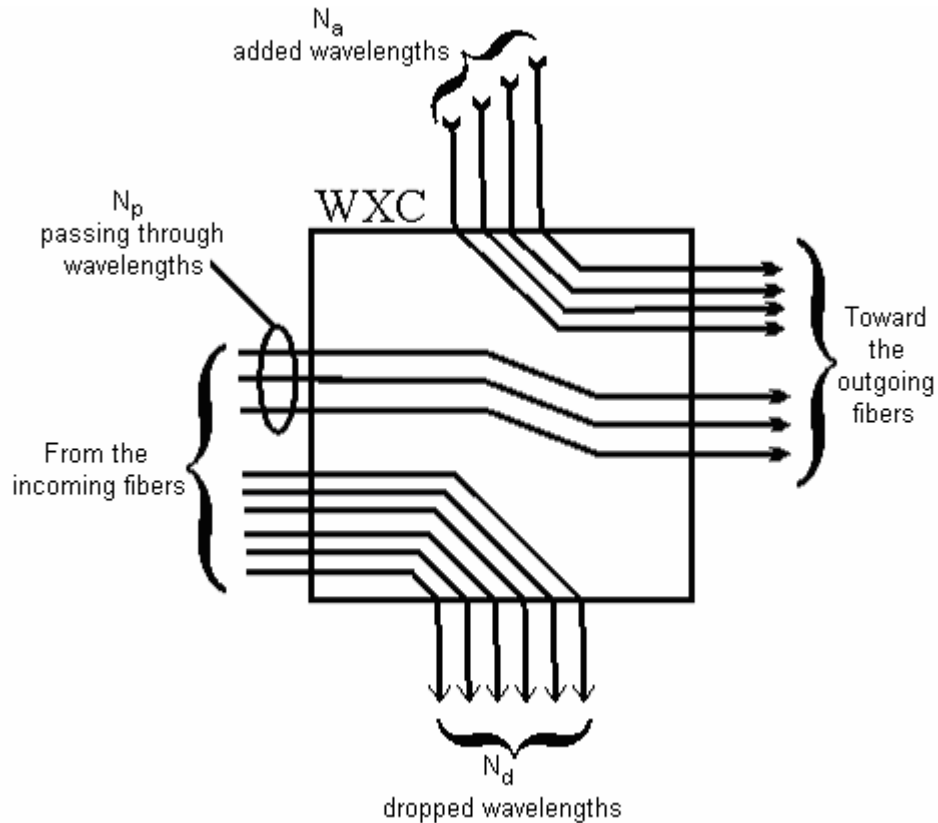


Figure 41: The number of input ports in a WXC

$N_a$  and  $N_d$  are fixed by the traffic demand matrix.  $N_p$  is fixed by the routing algorithm.

$$\text{Min}(I^H) = N_a + N_a/W + N_d/W + N_p/W$$

As shown in figure 42, all added wavelengths must enter the WXC ( $N_a$  inputs) and then to the WBXC.  $N_d/W$  inputs in the best case where we have  $W$  by  $W$  contiguous added wavelengths. Wavelengths to be dropped enter the OXC at the WBXC in the best case as  $W$ -by- $W$  contiguous wavelengths to form only dropped wavebands without entering the WXC.

Wavelengths passing through the node form in the best case  $N_p/W$  packed wavebands. In all cases, we must consider a fully filled packed waveband in order to minimize their number.

The upper bound on the saving ratio is then:

$$HCRR_{UB} = \frac{1}{1 + \frac{N_a}{N_d + N_p}} - \frac{1}{W}$$

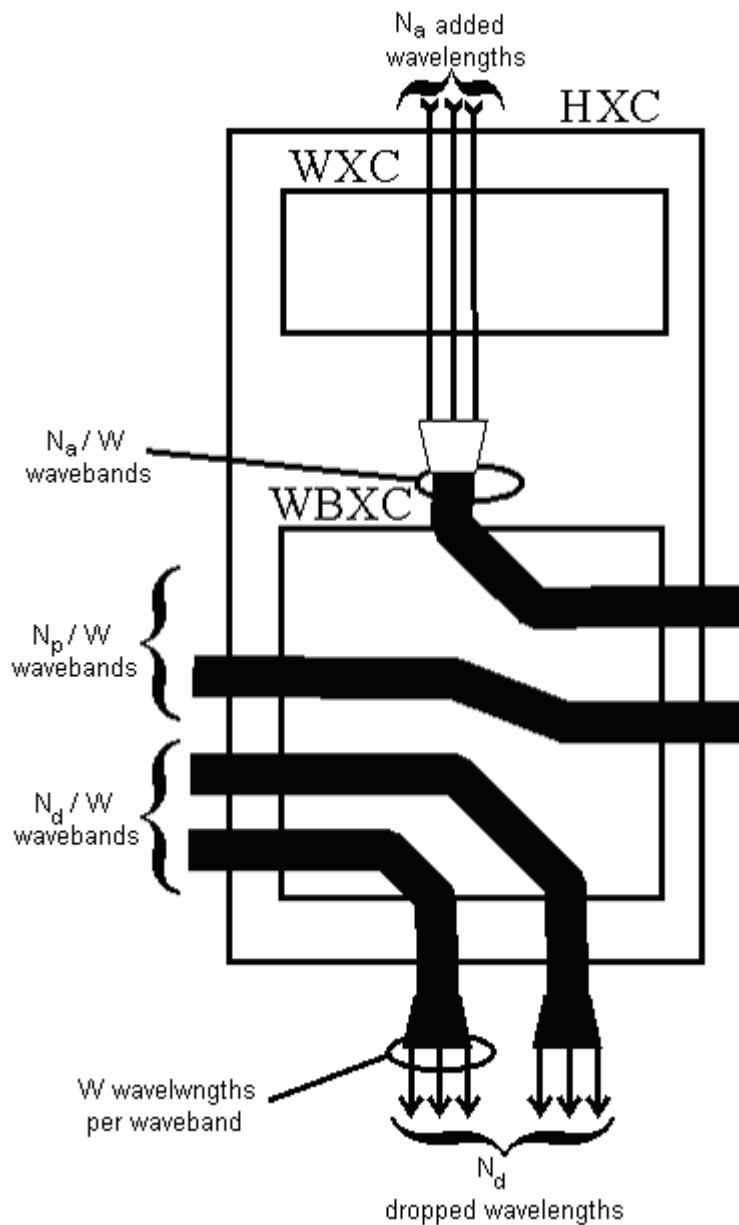


Figure 42: Best case for an HXC.

For instance, if we consider a uniform traffic having  $D$  traffic flow units between each two nodes we have:  $N_a = N_d = (N-1)D$ .  $N$  is the number of nodes. We can always write:  $N_p = \beta (N-1)D$ .  $\beta$  characterizes the passing through and is defined for each node by the topology of the network and as a result of routing.  $\beta$  can be a fraction and can go from 0 to  $N$  since the total number of traffic flows in this case is  $N(N-1)D$ . For uniform traffic, we can then write:

$$HCRR_{UB} = \frac{1+\beta}{2+\beta} - \frac{1}{W}$$

Figure 43 shows the upper bound on HCRR for different  $W$  and  $\beta$  when the uniform traffic is considered.

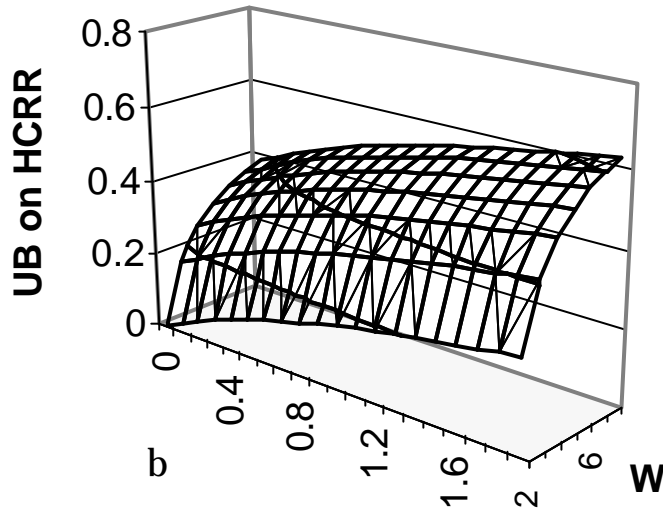


Figure 43: The upper bound on HCRR for uniform traffic

$\beta$  is defined by the routing algorithm but also by the network topology. For instance, for a unidirectional ring we have a large  $\beta$  ( $\beta = (N-2)/2$ ) and for a mesh network we have a notably lower  $\beta$  (for a full mesh network  $\beta = 0$ ).

In general, and since this upper bound does not only concern rearrangement, it is far from the rearrangement optimal value. However, it is reached for a uniform traffic when  $W = D$ .

In all cases, the upper bound is important as a measure of what do we expect from wavelength rearrangement at each node, especially when we consider the non-uniform traffic.

#### IV.3.4 The Proposed Heuristic Method

As already mentioned, the wavelength rearrangement consists in changing the order of wavelengths while keeping the same distribution plan resulting from wavelength assignment. The problem is then to find the new position of each wavelength. Positions  $1, 2, \dots, W$  form the first waveband and positions  $1+(b-1)W, 2+(b-1)W, \dots, W+(b-1)W$  form the  $b^{\text{th}}$  waveband.

To find a valid design solution for large-scale networks, we propose in list 1 the following heuristic method. Which fills the wavebands one after the other. For each unoccupied position in the waveband channel (i.e. wavelength channel), unplaced or candidate logical wavelengths (resulting from RWA) are estimated to fit in this position.

$\phi$  is the measure of how well a candidate contributes in forming a packed waveband. For each candidate, we find  $\phi$  by scanning all nodes. The one having the highest  $\phi$  is chosen to occupy the given position.

$\phi$  is found for each candidate starting from 0. While scanning each and every node the candidate fills the waveband channel according to the mapping of RWA.

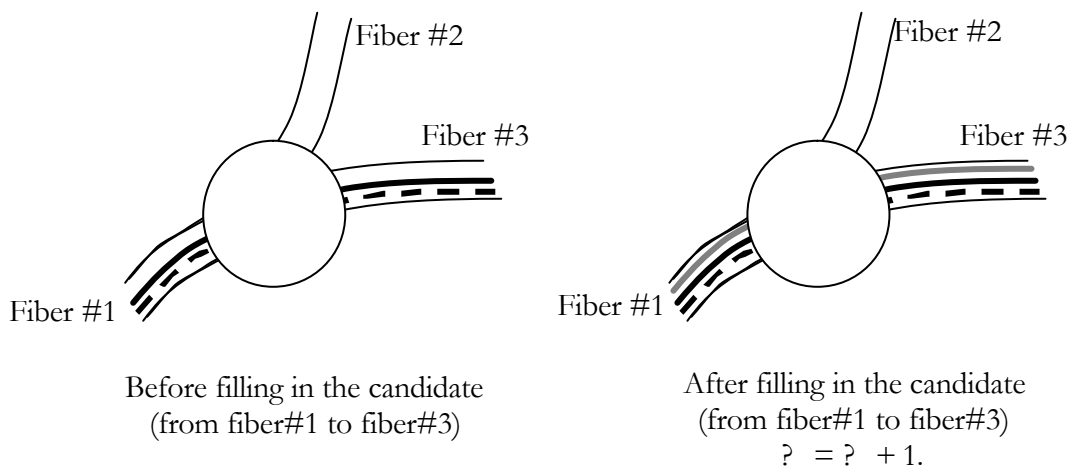


Figure 44: A candidate contributing in forming a packed waveband.

We have three possible cases:

4. The candidate contributes in forming a packed waveband as in figure 44,  $\varphi$  is then incremented by 1.
5. The candidate breaks the ability of preceding candidates to form a packed waveband as in figure 45.  $\varphi$  is then decreased by the number of already placed candidates.

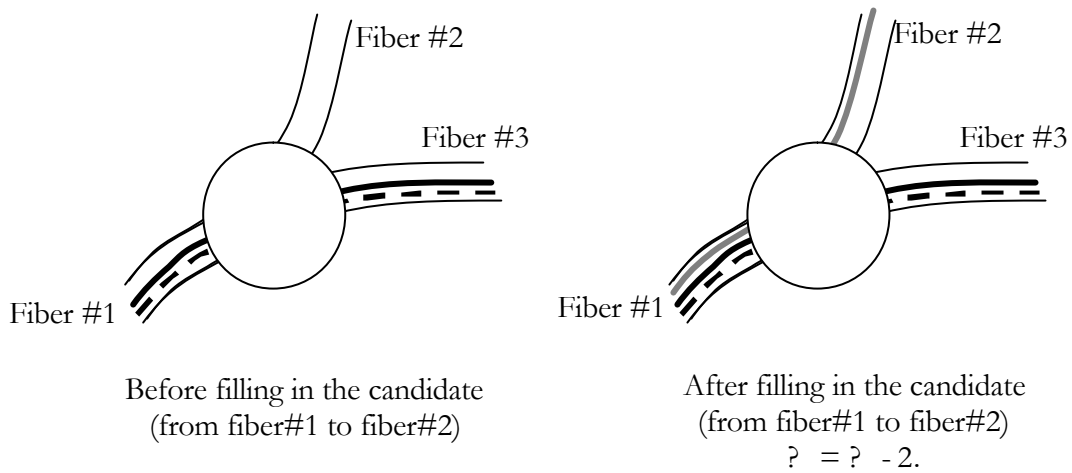


Figure 45: A candidate breaking a packed waveband.

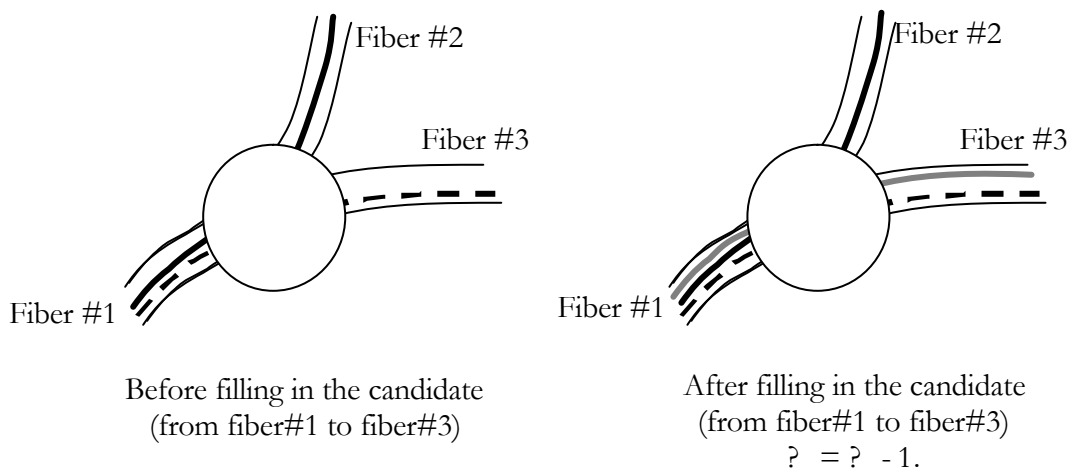


Figure 46: Already broken waveband.

6. The candidate is to be fitted in a waveband that cannot already be a packed one as in figure 46.  $\varphi$  is then decreased by 1.

Note that after finding the solution, each node is considered in its turn. If the total number of units in the HXC is less than the number of units when WXC is considered alone, the hierarchical cross-connect is chosen; otherwise the wavelength cross-connect is chosen.

**List 1: Heuristic Rearrangement ALGORITHM.**

```

For each waveband b
{Find the wavelength not already placed and having the greatest number of passing through.
  Assign this wavelength to the  $1+(b-1)W$  position (first position of b).
  For each position P going from  $2+(b-1)W$  up to  $W+(b-1)W$ 
  { For each wavelength  $\lambda$  not already placed (candidate)
    { Set the objective  $\varphi$  to 0
      For each node n
      { For each incoming link  $L_i$ 
        { If b can form a waveband drop from  $L_i$  (already placed wavelengths in b are either dropped from  $L_i$  or not used in  $L_i$ )
          { If  $\lambda$  is dropped from  $L_i$  then  $\varphi = \varphi + 1$ 
            Else in the case of a passing through  $\varphi = \varphi - \text{number of wavelengths already placed in b and dropped from } L_i.$ 
          }
        }
        Else if  $\lambda$  is dropped from  $L_i$  then  $\varphi = \varphi - 1$ 
        For each outgoing link  $L_o$ 
        { If  $\lambda$  is passing from  $L_i$  to  $L_o$ 
          { If b can form a bypassed waveband from  $L_i$  to  $L_o$  (already placed wavelengths in b are either passing from  $L_i$  to  $L_o$  or not used in both  $L_i$  and  $L_o$ ) then  $\varphi = \varphi + 1$ 
            Else if a wavelength already placed in b is dropped from  $L_i$  or added to  $L_o$  then  $\varphi = \varphi - 1$ 
          }
          Else if b can form a bypassed waveband from  $L_i$  to  $L_o$  and  $\lambda$  is dropped in  $L_i$  or added in  $L_o$  then  $\varphi = \varphi - \text{number of wavelengths already placed in b and passing from } L_i \text{ to } L_o.$ 
        }
      }
    }
    If  $\varphi$  is greater than the objectives of already scanned wavelengths make  $\lambda$  the best candidate for the P position.
  }
  Assign the best candidate to the position P.
}
}

```

#### IV.4. Numerical Results

We consider the 14-node, 21-link NSFNET physical topology. For RWA, the shortest path and the first fit algorithms are applied.

We consider the ratio HCRR already defined to reflect the complexity reduction.

##### IV.4.1 Uniform Traffic

For the given conditions,  $\beta$  goes from 0.3 up to 2.6 depending on the corresponding node. The results are given in figure 47 when we apply the heuristic algorithm for different traffic flows  $D=n$  where  $n$  is the number of traffic flows units between each two nodes.

To represent the HCRR, we consider the average result between all nodes.

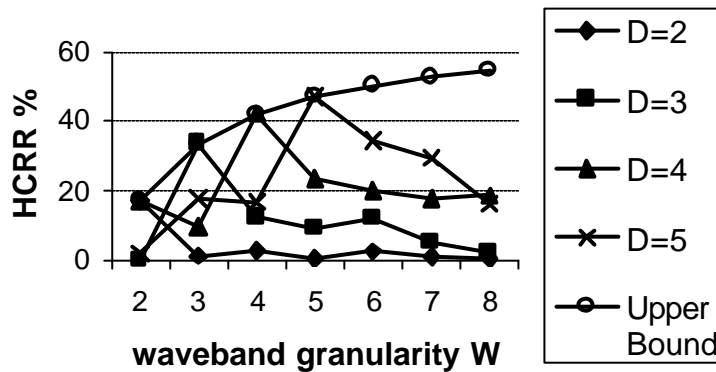


Figure 47: Complexity reduction for uniform traffic.

Note that for a uniform traffic, HCRR reaches its upper bound when  $D$  is a multiple of  $W$  since it is possible in this case to arrange wavelengths as represented in figure 42.

##### IV.4.2 Non Uniform Traffic

We must in this case consider each node alone since there is a big difference in the complexity reduction between nodes and mainly because we must chose, at each node, to consider a HXC or a WXC for the OXC.

Figure 48 shows the complexity reduction (heuristic and upper bound) for a non-uniform traffic pattern evenly distributed between 0 and  $2\mu$  ( $\mu=7$ ) and a waveband granularity  $W=4$ .



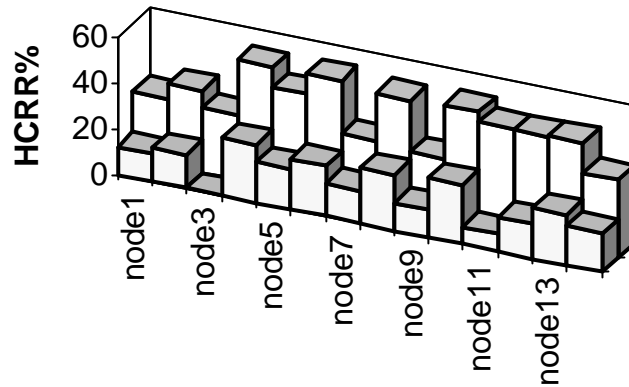


Figure 48: Complexity reduction for a non-uniform traffic pattern ( $\mu=7$ ) with a waveband granularity  $W=4$ . The results of the described heuristic algorithm and upper bounds are shown for each node.

Since the result is highly node-dependant and a mean value cannot reflect the real complexity reduction at particular nodes, we propose to represent the number of nodes in the network where the HXC is cost-effective for different traffic flows. We consider that a HXC is cost-effective if HCRR crosses a predefined threshold  $T_h$  depending on the cost estimation. Figure 49 shows the results for a non-uniform traffic pattern evenly distributed between 0 and  $2\mu$  for different values of  $T_h$ . For each  $\mu$ , we generated 20 traffic demand matrices and the average number of nodes where HXC is cost-effective is then reported for each  $T_h$ . For each traffic pattern, the waveband granularity  $W$  giving the best result is considered.

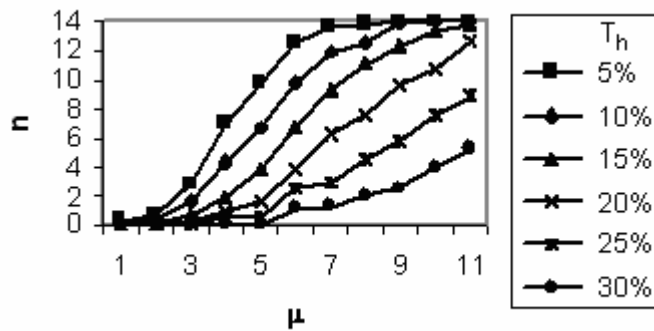


Figure 49: The number of nodes in the network where HXC is cost-effective

#### **IV.5. Conclusion**

The wavelength rearrangement reduces the complexity of a network without disturbing the normal network design procedures. Wavelength rearrangement is also useful when dealing with other network design problems where wavelength contiguity has a significant effect. For instance, it is useful where banding is used in some amplified systems to extend the optical spectrum of the amplified signal as mentioned in [29].

## V. DYNAMIC TRAFFIC AND TRAFFIC ENGINEERING

### V.1. Introduction

In the dynamic traffic context, the order in which demands arrive is important to the overall network performance especially when a bulk switching decision is to be taken such as a waveband switching. This bulk switching will cause an abrupt reduction in the number of possible connection patterns. These discontinuous changes in the logical topology are to be controlled in order to reduce the blocking probability for future demands. So we must also work out the cross-connect control in addition to routing and wavelength assignment (RWA).

#### V.1.1 Switching Granularity

Choosing the apparently best solution to set up a given connection is not limited to choosing the best candidate in terms of time slot, wavelength, waveband, fiber, etc...and the set of nodes to pass through but also to choose, when it is possible, the best switching granularity at each node. Note that the switching granularity does not necessarily affect the connection being established but has a great effect on future connection demands.

At a given node, using a multi-granularity scheme by means of hierarchical cross-connection or simply traffic grooming was not to be considered if working always at the finest granularity is cost effective since this assures the lowest blocking probability. To have a cost effective design, we must reduce “the number of inputs (or outputs)/granularity” ratio as we go down to finer granularities cross-connects. This will reduce the footprint and cost of the switch.

#### V.1.2 Cross-Connect Control

In the traffic engineering design, finer granularities must be considered as the expensive resources and choosing when to use finer granularities is the clue for a successful traffic engineering policy. If we travel through different granularities at a given node and arriving to a given granularity (e.g. waveband), we must compromise between, when we have the choice,

passing through a finer granularity (e.g. wavelength), and enhance the forwarding flexibility for co-located channels (e.g. other wavelengths in the waveband) and bypassing the finer granularity switching to save the use of these expensive resources. That is passing the flexibility to other traffic carriers that many need it more.

## V.2. Multi-Layer Switching

Let  $S$  be the sorted set of possible switching granularities or switching layers:  $S = \{g_s, g_{s-1}, \dots, g_2, g_1\}$  where  $s = |S|$ ,  $g_m/g_{m-1} = k_m$  is an integer and  $g_1 = 1$  that is the finest granularity at the base bandwidth rate or simply a traffic unit. The integer  $k_m$  represents the number of channels at the granularity  $g_{m-1}$  bundled in one channel having the granularity  $g_m$ .

For instance, if we have in a multi-layer switching (e.g. HXC) a waveband cross-connect with a waveband granularity of  $W=4$  wavelengths, a wavelength cross-connect where each wavelength multiplexes 3 time-slots and an electronic grooming supported to multiplex, demultiplex, add and drop slots then  $S = \{12, 3, 1\}$ . The traffic unit is then one time-slot.

We call  $i$ -layer cross-connect the one that switches at the granularity  $g_i$ , that is, switching  $g_i$  traffic units using one input/output port. This switching is called  $i$ -layer switching.

At a given  $i$ -layer cross-connect, input/output ports are connected to:

1.  $i$ -layer interlayer multiplexers: to come from the  $(i-1)$ -layer cross-connect.
2.  $i$ -layer interlayer demultiplexers: to pass to the  $(i-1)$ -layer cross-connect.
3.  $i$ -layer ADD: bulk  $g_i$  units add (waveband add for instance).
4.  $i$ -layer DROP: bulk  $g_i$  units drop (waveband drop for instance).

Note that at the highest layer, interlayer multiplexers/demultiplexers provide access to fiber links.

In a multi-layer hierarchical cross-connect and at given node, an  $i$ -layer switching is reached by:

1.  $i$ -layer ADD.
2. Switching at the  $(i+1)$ -layer to  $(i+1)$ -layer interlayer demultiplexers.
3. Switching at the  $(i-1)$ -layer to  $i$ -layer interlayer multiplexers.

Bypassing an  $i$ -layer switching (at a granularity  $g$ ) results in bypassing all finer switching. Passing through an  $i$ -layer switching results in passing through all coarser switching.

### **V.3. Multi-Layer Tunneling and the Layered Logical Topology**

This section gives a clear description of the problem and provides an important tool used in supplying the information base to apply traffic engineering solutions. We present an exhaustive example to illustrate how the layered logical topology is updated in different cases.

Multi-granular grooming and multi-layer switching result in a multi-layer tunneling scheme. It is crucial to map established tunnels at their proper layer in order to control the network cross-connects. Controlling a cross-connect means to decide at which granularity the switching must be done. That is answering the following question: how far must we proceed with demultiplexing/multiplexing channels for a given path at each node? The answer depends on the current traffic allocation, the logical topology and the objective to reach in network optimization.

The layered logical topology shows not only how resources are distributed in the network but also how they can be used. For a given path, two  $i$ -layer switching separated by coarser-layer switching make an  $(i+1)$ -layer tunnel. Included channels (although not yet used) cannot be demultiplexed inside this tunnel and are confined to a coarser granularity switching until a change is made in the cross-connect control (e.g. when related connections are torn down). This tunneling reduces the routing flexibility since an  $i$ -layer tunnel creates a virtual direct connection for  $g$  traffic units between its ends. Coarse-layer tunnels are more difficult to fill than finer-layer tunnels however they save the use of interlayer multiplexers/demultiplexers. All these details must be obviously marked on the logical topology in order to take the right decision to control cross-connects. The layered logical topology is essential to achieve traffic engineering strategies.

An  $(i+1)$ -layer tunnel is established starting at a node where one of the following occurs:

2. An  $i$ -layer ADD.
3. A channel is added at **a higher** granularity. In this case, we can only add to this tunnel at the given node since the channel does not pass through the  $i$ -layer cross-connect.
4. Passing from the  $i$ -layer to the  $(i+1)$ -layer cross-connect through an  $(i+1)$ -layer interlayer multiplexer.

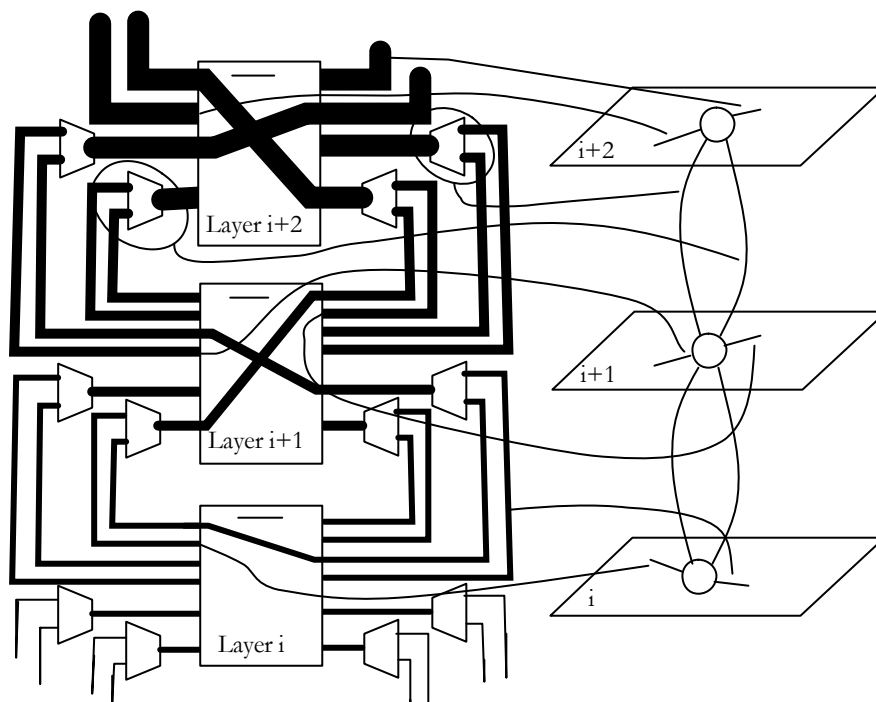


Figure 50: Mapping tunnels and interlayer multiplexers for a multi-layer MG-OXC.

An  $(i+1)$ -layer tunnel ends at a node where one of the following occurs:

1. An  $i$ -layer DROP.
2. The channel is dropped at **a higher** granularity. In this case, we can only drop from this tunnel at the given node since the channel does not pass through the  $i$ -layer cross-connect.

3. Passing to the  $i$ -layer from the  $(i+1)$ -layer cross-connect through an  $(i+1)$ -layer interlayer demultiplexer.

Figure 50 shows how tunnels and interlayer multiplexers are mapped in a layered logical topology.

Let us illustrate the layered logical topology structure and evolution by the example of the simple physical topology given in figure 51.

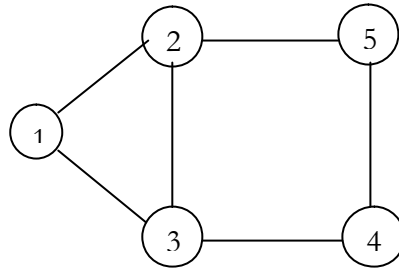


Figure 51: Example five-node network physical topology.

At each node, the multi-layer switching contains at the third layer a waveband cross-connect (WBXC) with a waveband granularity  $W=4$  wavelengths, at the second layer a wavelength cross-connect (WXC) where each wavelength multiplexes 3 time-slots and at first layer an electronic grooming (EG) supported to multiplex, demultiplex, add and drop slots.  $S=\{12,3,1\}$  and the traffic unit is then one time-slot.

Let  $MUX_i$  be the number of  $i$ -layer multiplexers,  $DEMUX_i$  the number of  $i$ -layer demultiplexers,  $ADD_i$  the number of  $i$ -layer ADD and  $DROP_i$  the number of  $i$ -layer DROP. In this example, we consider:  $MUX_3=DEMUX_3=2$ ,  $MUX_2=DEMUX_2=2$ ,  $ADD_3=DROP_3=1$ ,  $ADD_2=DROP_2=3$  and  $ADD_1=DROP_1=3$ . For instance,  $DEMUX_3=2$  means that two wavebands are going from the WBXC to the WXC.

Note that a wavelength add without passing through the digital switching box may not be a practical advantage but we include it to make the layered model more general.

Figure 52 shows the paths chosen for the three connections illustrated in this example. We assume that all these connections are served in the same waveband channel  $b_1$  and for each waveband we construct an independent logical topology. That is because no waveband

conversion is possible. Each connection is set up in one slot (one traffic unit). We assume also that the WXC has a waveband-range wavelength conversion.

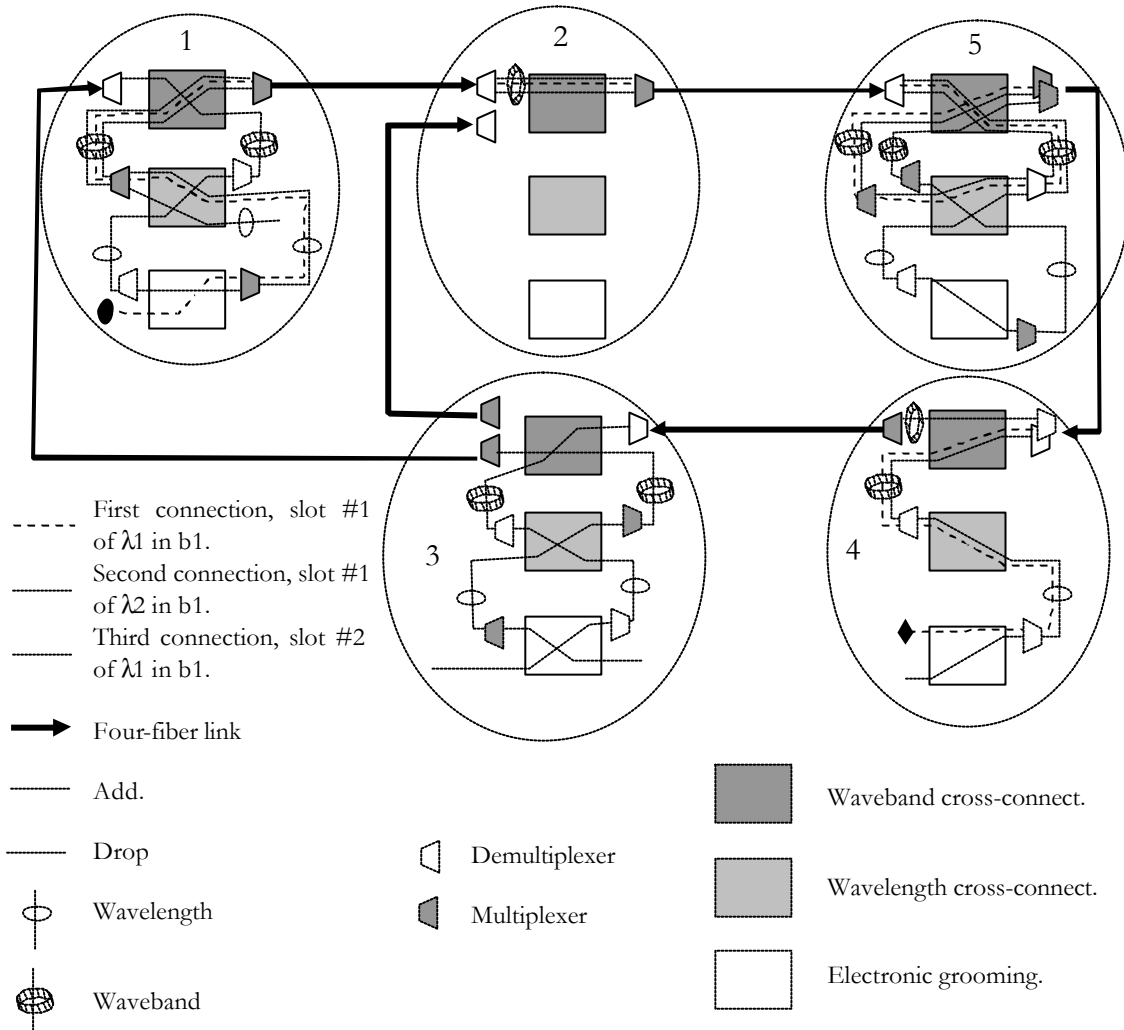


Figure 52: Example of establishing three connections through different grooming and granularity layers.

The first connection is from node 1 to node 4. At node 1, we have a slot add to the wavelength  $\lambda_1$ , a waveband bypass at node 2, a wavelength bypass at node 5 and finally a slot drop at node 4.

The second connection is from node 1 to node 3. At node 1, we have a wavelength add ( $\lambda_2$  as wavelength channel) however only one slot is used by this connection, this wavelength joins the waveband of the first connection until node 5. At node 5, it passes through the EG



and goes out of node 5 in a separate waveband (but always the same waveband channel b1). At node 4, we have a waveband bypass and finally a slot drop at node 3.

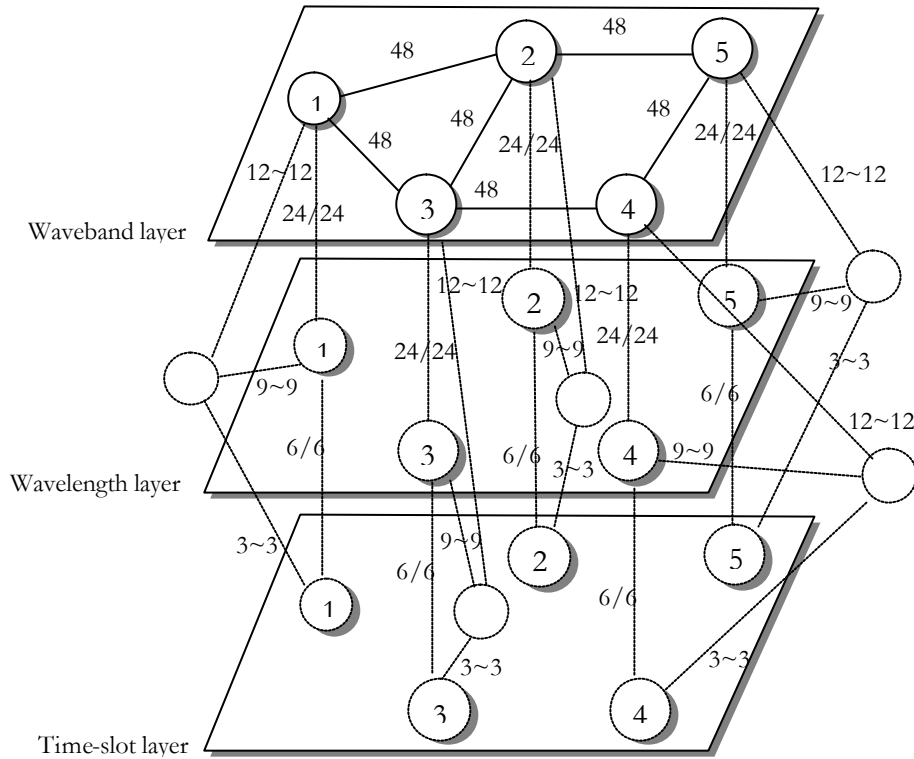


Figure 53: Initial layered logical topology.

The third connection is from node 3 to node 4. At node 3, we have a slot add to  $\lambda_1$ . At node 1, the connection passes through the EG to join the second slot of  $\lambda_1$  jointly with the first connection till node 4 where it is dropped (slot drop).

Let us sketch the building of the layered logical topology for the given example. First we start with the initial graph shown in figure 53.

An unlabeled vertex represents an add/drop end point for a given node. When the multi-hop grooming is not allowed, we must use two separate vertices, one for add and the other for drop. In a multi-hop grooming, we can drop and then add several times for a given connection. Note that this adds burden on electronic devices, which represent the dominant cost factor.

Each node is represented by 3 vertices each in a different switching layer.

All edges are labeled by the number of traffic units they still can carry (number of free slots).

An edge connecting two vertices of the same node, going from the vertex in layer  $i$  to the one in layer  $i+1$ , represents unused  $(i+1)$ -layer interlayer multiplexers. An edge connecting two vertices of the same node, going from the vertex in layer  $i$  to the one in layer  $i-1$ , represents unused  $i$ -layer interlayer demultiplexers. A bidirectional edge between layer  $i$  and layer  $i+1$  is used. This edge has a label in the form of  $x/y$ .  $x$  represents the number of free traffic units that can be multiplexed to pass from the layer  $i$  to the layer  $i+1$ , (i.e.  $x/g_{i+1}$  free multiplexers having  $k_{i+1}=g_{i+1}/g_i$  input ports each).  $y$  represents the number of free traffic units that can be demultiplexed to pass from the layer  $i+1$  to the layer  $i$ , (i.e.  $x/g_{i+1}$  free demultiplexers having  $k_{i+1}=g_{i+1}/g_i$  output ports each).

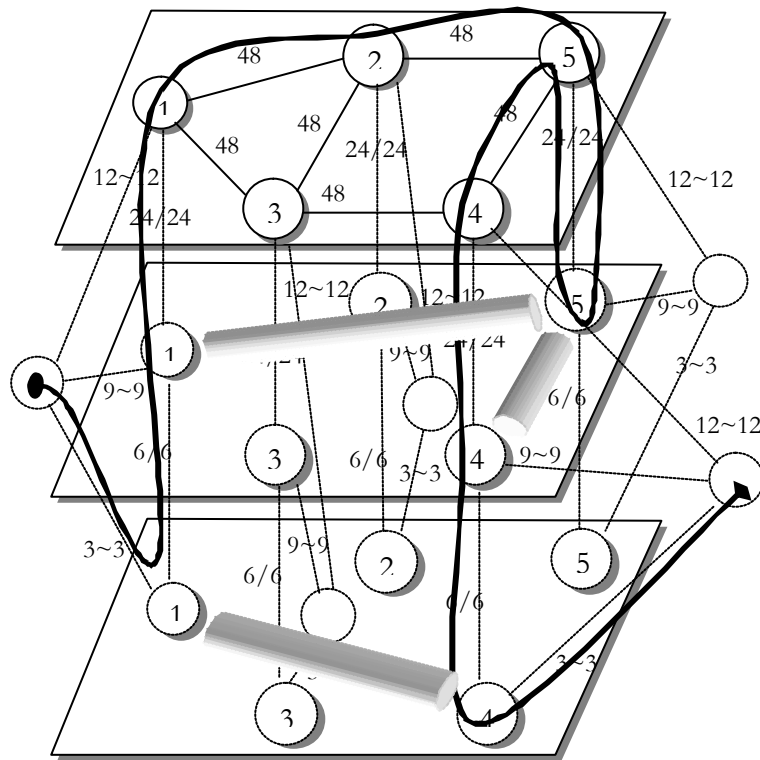


Figure 54: First connection path and multi-layer tunnels.

An edge connecting two vertices in the same **layer  $i$**  represents an  **$(i+1)$ -layer tunnel** or a physical connection (for the top layer) between the corresponding nodes. Such an edge in the

layer  $i$  is labeled by the number of free traffic units supported by the tunnel. This number is always a multiple of  $g_i$ .

Unlabeled vertices, representing the add/drop end points, are connected to their node's vertices in each layer by a bidirectional edge labeled by  $x \sim y$ .  $x$  represents the free traffic units that can be added at the layer's granularity. This is the number of free traffic units in the corresponding  $i$ -layer ADD.  $y$  represents the free traffic units that can be dropped at the layer's granularity. This is the number of free traffic units in the corresponding  $i$ -layer DROP.

Figure 54 shows the first connection path (from node 1 to node 4) and the new tunnels to be created after setting up this connection. Note how passing from layer to layer (i.e. the cross-connect control) is clearly illustrated on the layered logical topology.

In the first layer, the electronic grooming layer, we have a second-layer tunnel from node 1 to node 4. That is a wavelength tunnel. In the second layer, the wavelength layer, we have two third-layer tunnels. One waveband tunnel from node 1 to node 5 and the other waveband tunnel from node 5 to node 4.

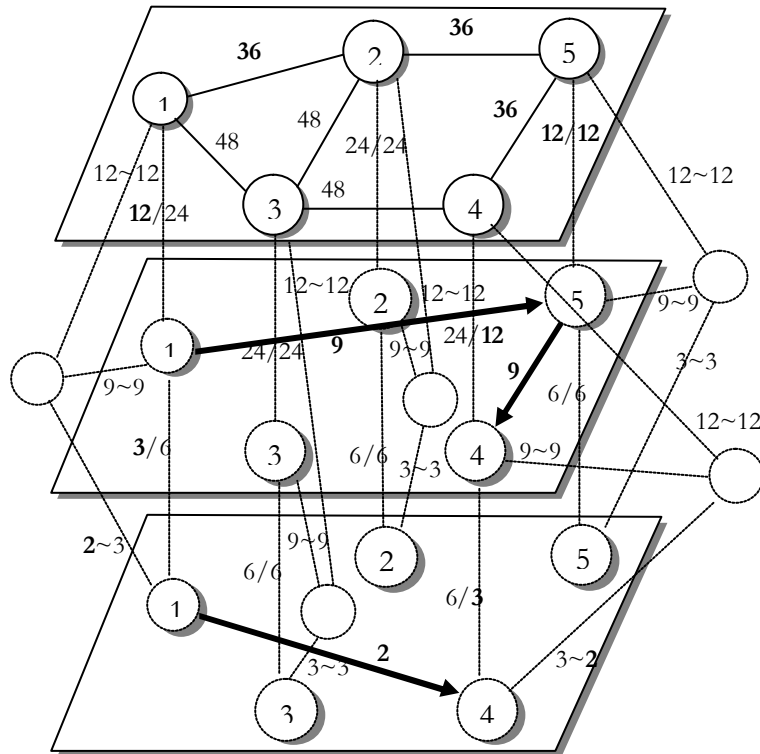


Figure 55: Logical topology after setting up the first connection.

Figure 55 shows the updated logical topology. Bold labels are those modified. In the first layer, we still have 2 free slots in the wavelength tunnel from node 1 to node 4 and 9 free slots, which is 3 free wavelengths, in the waveband tunnel of layer two.

Passing from layer  $i$  to layer  $i+1$  or vice versa is multiplexing  $k_{i+1}$   $i$ -layer channels or demultiplexing one  $(i+1)$ -layer channel. This is shown on the interlayer edge labeling.

Figure 56 shows the second connection path (from node 1 to node 3) and the new tunnels to be created after setting up this connection.

What is important to note here is the tunnel connecting the add vertex (unlabeled) of node 1 to the third layer vertex of node 5. The wavelength containing the slot supporting the connection is added at node 1 without passing through the digital switching box. Note again that a wavelength add without passing through the digital switching box may not be a practical advantage but we include it to make the layered model more general. Remaining free slots cannot be used in a switching operation for traffic passing through node 1; however they can support new traffic generated at node 1.

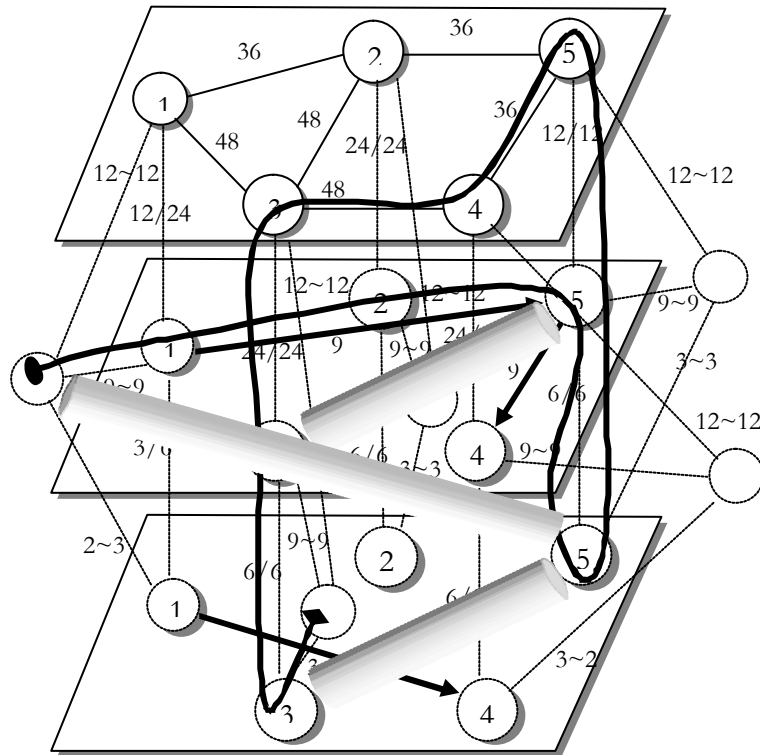


Figure 56: Second connection path and new multi-layer tunnels.

Note also the two tunnels from node 5 to node 3. One wavelength tunnel in the third layer and one waveband tunnel in the second layer. These tunnels are both created since the connection causes the demultiplexing/multiplexing of a waveband in node 5 and node 3 and also the demultiplexing/multiplexing of an included wavelength in the same nodes in order to use one slot of it.

Figure 57 shows the updated layered logical topology. Here also bold labels are those modified.

Figures 58 and 59 show how the third connection is set up. We can see the created tunnels and the updated layered logical topology.

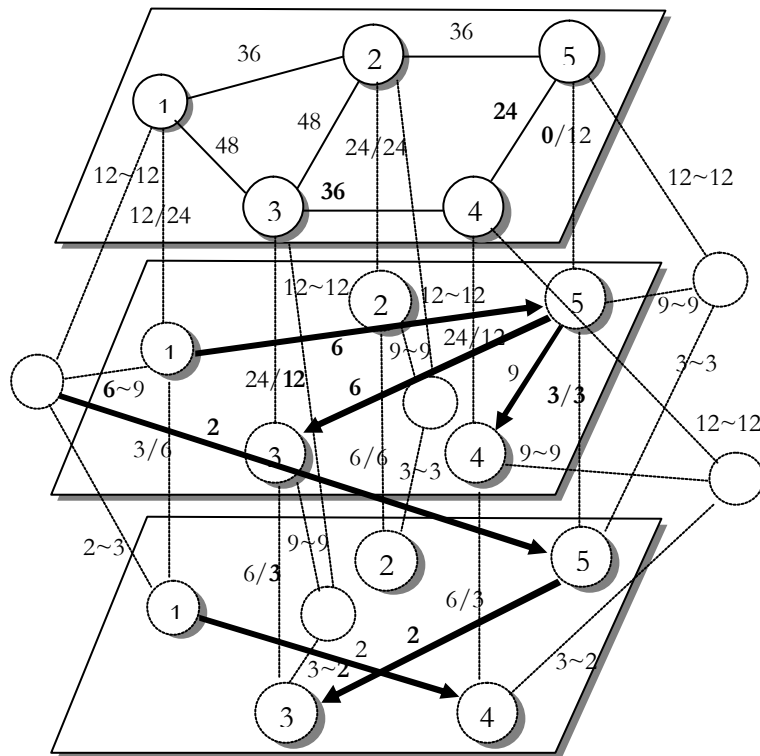


Figure 57: Logical topology after setting up the second connection.

#### V.4. Layered Logical Topology Construction Using MGGM

Next we have to see how to construct the layered logical topology and how to keep track of the inter and intra layer path in order to return backward after tearing down a connection.

The answer is the multi-granularity graph model (MGGM) where the MERGE and UNMERGE operations can trigger and maintain the multi-layer tunneling by analyzing the type of the merged groups. The type allows us to choose the layer.

To go into details, let us sketch how the connection is established in the MGGM. Note first that we have a cycle. The traffic engineering method, based on the layered logical topology, chooses the cost of different edges in the MGGM; then we apply the shortest path algorithm to find a multi-layer path since the MGGM contains all details on the network state by the groups' information; then the layered logical topology is updated after setting up the connection in the MGGM to apply the traffic engineering method again and so on. When tearing down a connection, the layered logical topology is also updated while freeing the connection in the MGGM.

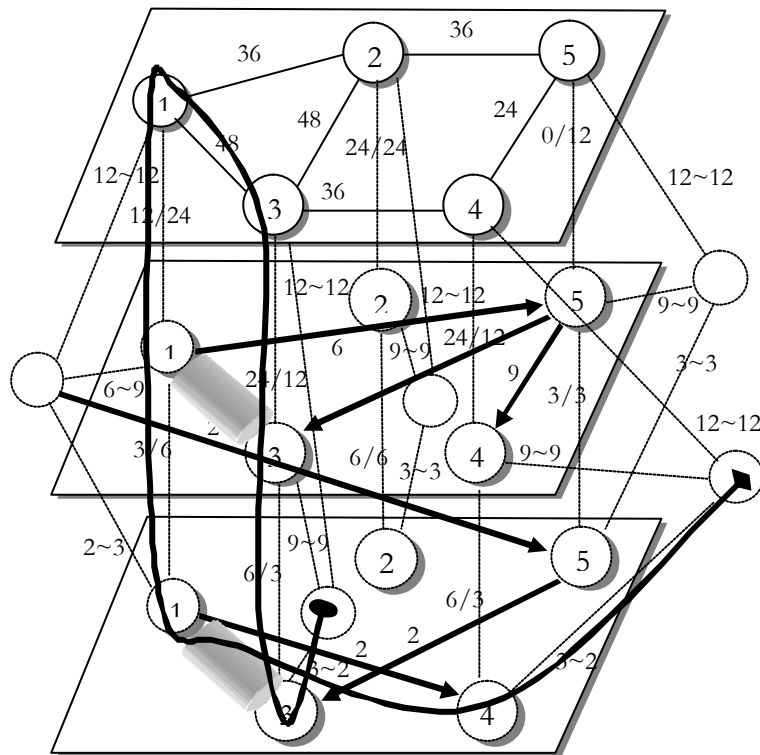


Figure 58: Third connection path and new multi-layer tunnels.

Setting up a connection in the MGGM, after finding the multi-layer path, starts by merging all unmerged consecutive groups along the path. Group to be merged must have the same type (merging condition). After this step, all edges along the path belong to merged

groups. Starting from the add vertex of the source node, the EXCLUDE operation is applied to these edges one by one while updating the layered topology in the following way.

When we pass in a node  $n$  from an edge belonging to an  $i$ -layer merged group to an edge belonging to an  $(i+1)$ -layer merged group, we save the ID of  $n$  to mark the input of an  $(i+1)$ -layer tunnel in the  $i$ -layer. We also update the involved interlayer edge.

When we pass in a node  $m$  from an edge belonging to an  $(i+1)$ -layer merged group to an edge belonging to an  $i$ -layer merged group we obtain the output of the  $(i+1)$ -layer tunnel in the  $i$ -layer having the node ID of its input already saved. Having the number of unused edges in the group information of the last edge (this number must be the same for all edges all along the tunnel which is already true) we can easily update the layered logical topology including the involved interlayer edge.

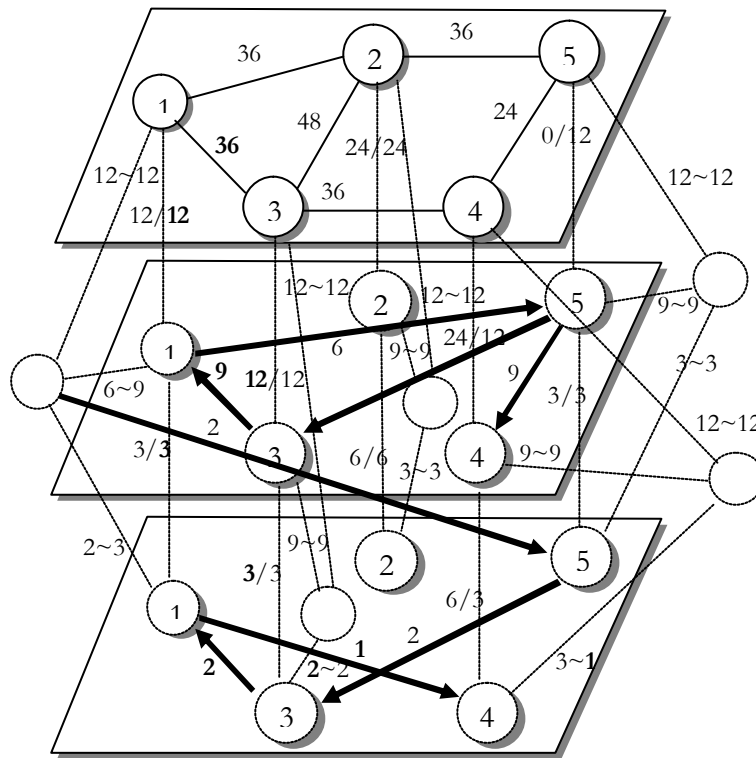


Figure 59: Logical topology after setting up the third connection.

While passing from an edge to another belonging to the same layer (usually in a different node) we shall update the tunnels' capacity of this layer.

Freeing a connection into the MGGM starts from the add vertex of the source node by applying the REINCLUDE operation to all edges used by the path. When the new number of unused edges in the merged group meets the total number of edges in the group, we apply the UNMERGE operation. At the same time, we update the layered topology using the same process as above.

## V.5. Traffic Engineering Solution

To establish a connection, we need to estimate possible paths in order to choose the best candidate. Using the MGGM, we must dynamically update edges' cost depending on the current network state and traffic distribution. We suppose that connection demands arrive at the finest granularity (one by one traffic unit arrival). This is the most critical problem for dynamic traffic. When the demand is at a higher granularity  $g$  we solve the problem as if we had  $g$  independent requests at the finest granularity between the same pair of nodes. As mentioned above it is not enough to value the path based on the physical channel (i.e. the set of fibers, nodes, waveband, wavelength ...) but we must also consider the cross-connect control and the switching granularity at each node.

### V.5.1 Problem Description

The main problem is how to share interlayer multiplexers/demultiplexers. For a given possible candidate path and at each node to cross, the question is: what is the best  $i$ -layer switching to pass through? In fact, we can choose one of the following switching states whenever this switching is possible:

1. Open a new  $i$ -layer tunnel: use a free  $i$ -layer demultiplexer to pass through an  $(i-1)$ -layer cross-connect and hence open a new  $i$ -layer tunnel in the layer  $i-1$ . Since rearrangement is not allowed in the dynamic traffic context, this  $i$ -layer tunnel must persist as long as it is used by any connection even though the pioneer connection is torn down. Then we can either bypass the layer  $i-1$  (and hence all  $j$ -layers where  $j < i-1$ ) or pass through the layer  $i-1$ :
  - i. Bypass the layer  $i-1$ : this forces  $g_i$  traffic units to go from the input link to the output link chosen for the candidate at this node. Most of these  $g$  traffic units are supposed to carry future demands. This bulk switching is



kept until no more included traffic unit is still in use. So that even if the opening connection is torn down, this switching decision continues to affect the network state as long as new connections use included traffic units. This will probably delay the adaptability to the future traffic map and increase the blocking probability if it is not well controlled by a good logical topology reconfiguration policy. The profit of a bulk switching is to save the utilization of interlayer multiplexers/demultiplexers and pass the flexibility to other, maybe more critical, input/output link pairs.

- ii. Pass through the layer  $i-1$ : this allows demultiplexing the  $i$ -layer channel and here also we have two different cases: opening a new  $(i-1)$ -layer tunnel or use an already opened  $(i-1)$ -layer tunnel. The same choices are then to be made as we go down from one layer to the other.
2. Use an already opened  $i$ -layer tunnel: for lower layers, the bypass or passing through decision is already taken by a previous connection (that may be already torn down). This new connection may increase the lifetime of this decision so we must study this consequence on the current logical topology and traffic map. Note here the difference between existing static heuristics that tend to fill already established tunnels as much as possible and what is expected from the traffic engineering in the dynamic traffic context to make a soft logical topology (without rearrangement) reconfiguration best adapted to the traffic demand evolution.

In the MGGM, the  $i$ -layer bypass or pass-through decision is realized by the cost difference between bypassing and passing-through. If we decide to bypass, then this difference must be positive otherwise it must be negative.

To take the maximum advantage of the  $i$ -layer interlayer multiplexers/demultiplexers (the expensive resources), we must apply to the  $(i-1)$ -layer cross-connect, input and output links that can highly interact to connect potential source/destination pairs. We mean by highly interact that most input/output pairs are able to support privileged paths to connect a potential source to a potential destination.

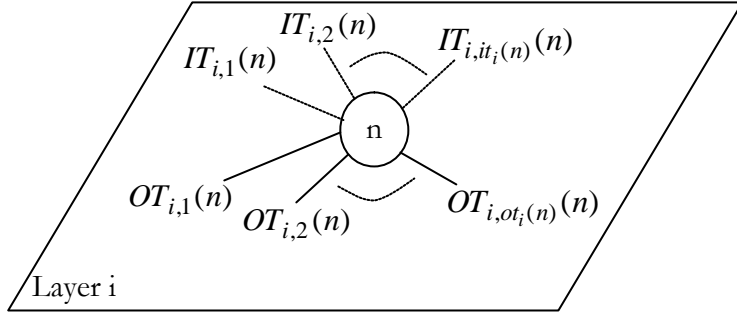


Figure 60: Tunnel indexing in layer  $i$ .

At a given node  $n$ , let  $d(n)$  be the number of unused  $i$ -layer interlayer demultiplexers,  $m_i(n)$  the number of unused  $i$ -layer interlayer multiplexers,  $it_i(n)$  the number of  $(i+1)$ -layer tunnels in the layer  $i$  arriving to  $n$  and  $ot_i(n)$  the number of  $(i+1)$ -layer tunnels in the layer  $i$  leaving  $n$ . Let  $IT_{i,p}(n)$  be the  $p^{\text{th}}$  arriving  $(i+1)$ -layer tunnel in the layer  $i$  to node  $n$  and  $OT_{i,q}(n)$  the  $q^{\text{th}}$  leaving  $(i+1)$ -layer tunnel in the layer  $i$  going out of node  $n$ . This is shown in figure 60.

The problem is then to find for each node  $n$  and each layer  $i$  the set of best  $x$  upper-layer tunnel candidates arriving to  $n$  and the set of best  $y$  upper-layer tunnel candidates leaving  $n$  to pass through an  $i$ -layer cross-connect. We mean by upper-layer tunnel each  $j$ -layer tunnel where  $j > i+1$ .

### V.5.2 Proposed Solution

To optimize the use of an interlayer multiplexer (or demultiplexer) by connecting it to an output (or input) link, we must find out how much this output (or input) link is solicited from different input (or output) links while expecting the best network use. Setting up a connection is based on the shortest path algorithm applied to the MGGM and the cost update of the MGGM edges is based on a flow approach. The flow approach is used to estimate the best potential utilization of the network resources. This is taken as a reference to provide an optimal feasible distribution of future connections. We try to reinforce this distribution by allocating interlayer multiplexers/demultiplexers to critical links.

First we apply the maximum flow (*maxflow*) algorithm for each potential source/destination pair on the layered logical topology. The Ford-Fulkerson maxflow algorithm (Appendix B) gives us not only the upper bound on total number of traffic units that

can be routed between a source/destination pair but also a possible occurrence of flow distribution to reach this upper bound. This will be used to promote the input/output links to be connected to the interlayer multiplexers/demultiplexers in order to reduce the blocking probability. As a result, we will have for each source destination pair (s,d) and each (i+1)-layer tunnel arriving to node n the flow  $f_{s,d}(IT_{i,p}^n)$  representing the number of traffic units to be used from this tunnel to reach the maxflow ( $p=1,2, \dots, it_i(n)$ ). We will have also for each source destination pair (s,d) and each (i+1)-layer tunnel leaving node n the flow  $f_{s,d}(OT_{i,q}^n)$  representing the number of traffic units to be used from this tunnel to reach the maxflow ( $q=1,2, \dots, ot_i(n)$ ). Note again that these flows are for one possible occurrence; however we will use this occurrence as a target and since it will be dynamically revised after each update of the layered logical topology this target will be the key to get to the network-to-traffic adaptability. We mean by target a possible traffic distribution that maximizes the use of available resources

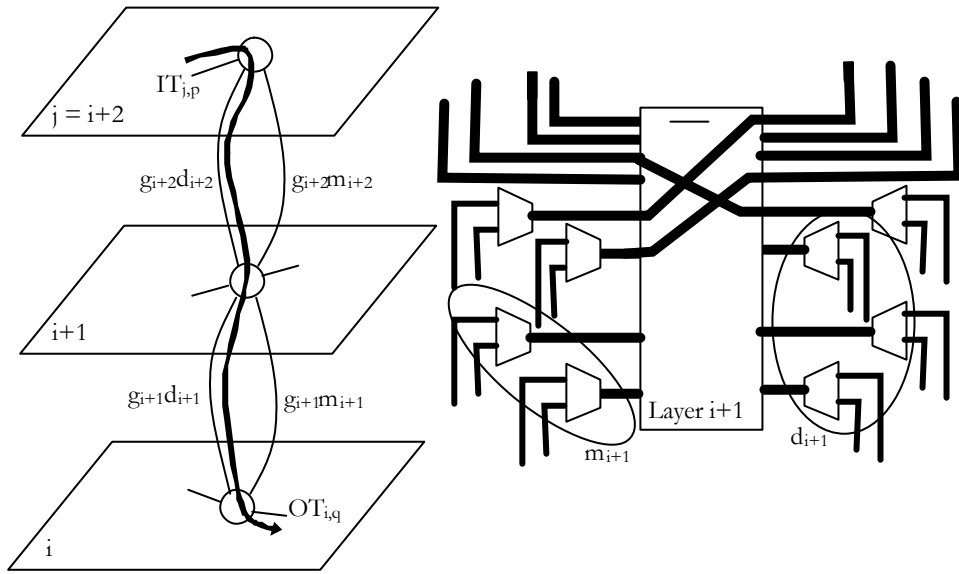


Figure 61: Passing from layer j to layer i and interlayer multiplexers/demultiplexers.

For each source/destination pair (s,d), we attribute a weight  $w_{s,d}$  reflecting its importance and priority. We define, at node n,  $md_{i,j}(n)$  to be the maximum number of traffic units that can pass from layer j to layer i ( $j \geq i$ ):

$$md_{i,j}(n) = \min_{i < k \leq j} g_k d_k(n) \quad j > i$$

$$md_{i,i}(n) = \infty$$

Figure 61 shows the passage from a layer to another one. We define also  $mm_{i,j}(n)$  to be the maximum number of traffic units that can pass from layer  $i$  to layer  $j$  ( $j \geq i$ ) at node  $n$ :

$$mm_{i,j}(n) = \min_{i < k \leq j} g_k m_k(n) \quad j > i$$

$$mm_{i,i}(n) = \infty$$

For a given source/destination pair  $(s,d)$  and for the defined occurrence of maxflow, the flow crossing node  $n$  from  $IT_{j,p1}(n)$  to  $OT_{k,p2}(n)$  is at most:

$$\min( f_{s,d}(IT_{j,p1}(n)), f_{s,d}(OT_{k,p2}(n)), dm_{k,j}(n) ) \quad j > k$$

$$\min( f_{s,d}(IT_{j,p1}(n)), f_{s,d}(OT_{k,p2}(n)), mm_{j,k}(n) ) \quad j \leq k$$

Projected on the layer  $i$ , this gives the maximum flow that can cross these tunnels by an  $i$ -layer switching as shown in figure 62:

$$\min( f_{s,d}(IT_{j,p1}(n)), f_{s,d}(OT_{k,p2}(n)), dm_{i,j}(n), mm_{i,k}(n) )$$

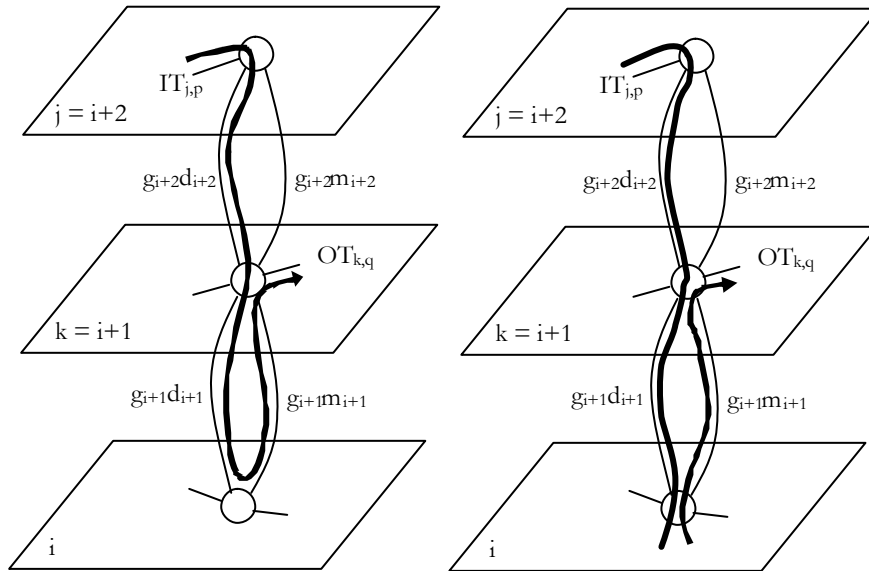


Figure 62: Passing from layer  $j$  to layer  $k$  through an  $i$ -layer switching.

The weight attributed to this pair of tunnels for an i-layer switching is:

$$\Omega_i^n(IT_{j,p1}(n), OT_{k,p2}(n)) = \sum_{(s,d)} w_{s,d} \min(f_{s,d}(IT_{j,p1}(n)), f_{s,d}(OT_{k,p2}(n)), dm_{i,j}(n), mm_{i,k}(n))$$

Let  $EI_i(n)$  be the set of tunnels arriving to node  $n$  in the layer  $i$  ( $(i+1)$ -layer tunnels) and  $EO_i(n)$  be the set of tunnels leaving node  $n$  in the layer  $i$ . Let  $SI_i(n)$  be the set of tunnels arriving to node  $n$  in layers  $j$  with  $j>i$  and  $SO_i(n)$  be the set of tunnels leaving node  $n$  in the layers  $j$  with  $j>i$  then:

$$SI_i(n) = \bigcup_{j>i} EI_j(n) \quad \text{with} \quad EI_j(n) = \{IT_{j,1}(n), IT_{j,2}(n), \dots, IT_{j,it_j(n)}(n)\}$$

$$SO_i(n) = \bigcup_{j>i} OI_j(n) \quad \text{with} \quad EO_j(n) = \{OT_{j,1}(n), OT_{j,2}(n), \dots, OT_{j,ot_j(n)}(n)\}$$

The set of tunnels arriving to  $n$  where we must promote an  $i$ -layer switching is  $X_{i,n} \subset SI_i(n)$  ( $|X_{i,n}| \leq d_{i+1}(n)$ ) and the set of tunnels leaving  $n$  where we must promote an  $i$ -level switching is  $Y_{i,n} \subset SO_i(n)$  ( $|Y_{i,n}| \leq m_{i+1}(n)$ ) giving the maximal value of:

$$\sum_{\substack{a \in (X_{i,n} \cup EI_i(n)) \\ b \in (Y_{i,n} \cup OI_i(n))}} \Omega_i^n(a, b)$$

Having  $X_{i,n}$  and  $Y_{i,n}$  for each  $i$  and each  $n$  we can assign the cost to the MGGM edges in order to promote the passing through of these and only these tunnels at the given node and given layer.

## V.6. Numerical Results

The test network used in our simulation experiments is shown in figure 63. We run the simulation on the MGGM of the given network. The proposed traffic engineering solution is applied by constructing the layered logical topology and updating it using the MGGM as described in this chapter.

In the test network, each edge node is a potential source/destination and each transit node is a two-layer MG-OXC with an internal WBXC and an internal WXC. The included WXC has no wavelength conversion capability.

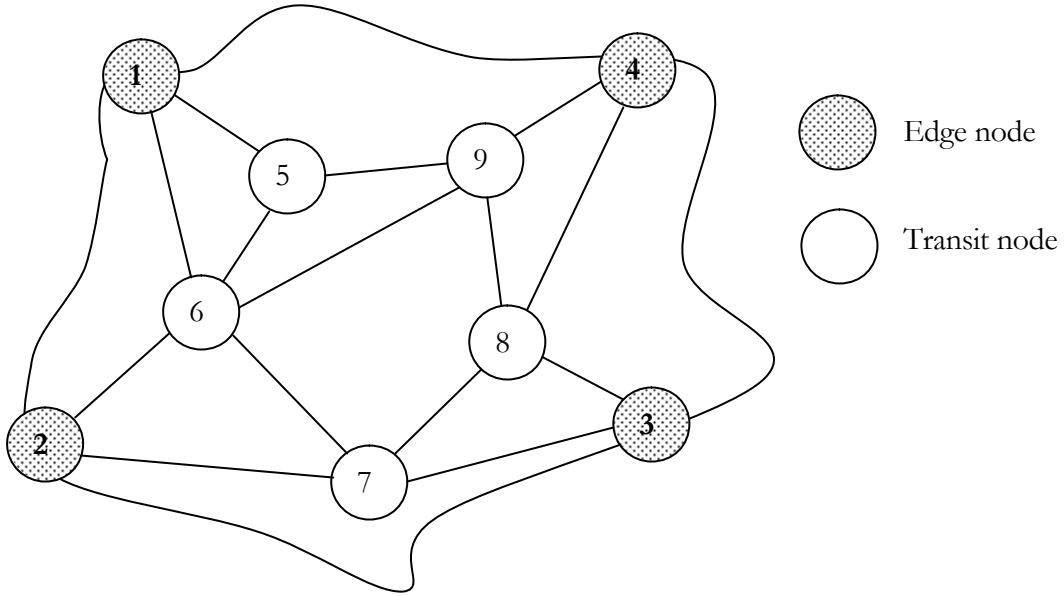


Figure 63: Test network for dynamic traffic.

Each link is bidirectional with three fibers in each direction. Each fiber has 24 wavelengths. We consider a waveband granularity equal to 4 ( $W=4$ ) so we have 6 wavebands per fiber ( $B=6$ ).

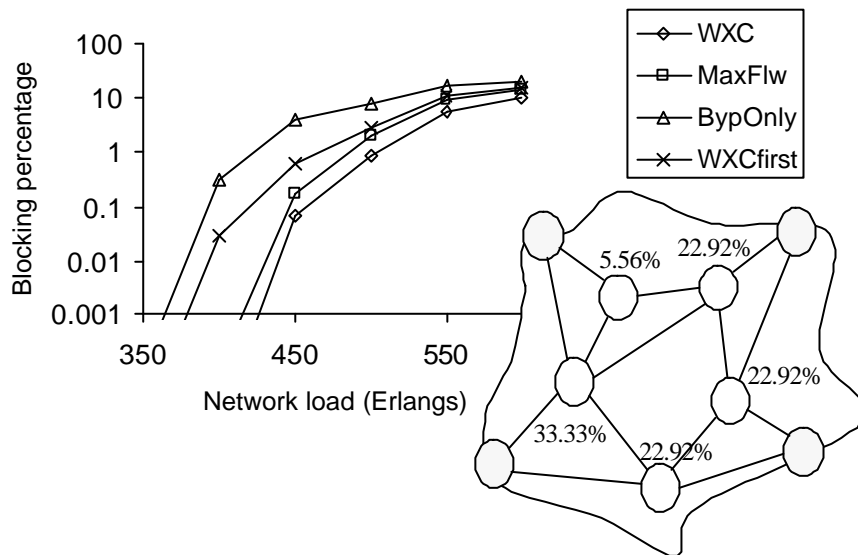


Figure 64: Results when we have **five** interlayer multiplexers/demultiplexers per waveband. HCR is shown for each node in the network.

All demands have a full wavelength capacity. The demands arrival is assumed to be a Poisson arrival with an exponential serving time and evenly distributed on source/destination pairs (pair of edge nodes). We vary the network load between 350 and 600 Erlangs.

In Figure 64, we show the blocking probability (percentage) when for each waveband channel the number of bands going from the WBXC to the WXC is five and vice versa, i.e., five interlayer multiplexers/demultiplexers per waveband channel.

We present in this figure four curves:

1. WXC: The blocking percentage when we consider, in every node, a non-hierarchical wavelength cross-connect with no wavelength conversion capability. This is considered as the **lower bound** since it is the most flexible where we can individually cross-connect each wavelength.
2. MaxFlw: The blocking percentage when we consider our proposal that consists in choosing the best waveband candidates to be multiplexed/demultiplexed by applying the maximum flow algorithm (maxflow) on the logical topology. This algorithm gives an occurrence of flow distribution that assures a maximum flow for each source/destination pair. This occurrence is used as a target to optimize the network performance. Having these flows, we consider the already demultiplexed/multiplexed wavebands and we choose a new set of wavebands to be demultiplexed/multiplexed. This choice is based on promoting a maximum of flow passing through the whole set of potentially and currently demultiplexed/multiplexed wavebands. This is done after updating the logical topology for each waveband channel.
3. BypOnly: The blocking percentage when all wavebands bypass the WXC, i.e., we consider only a WBXC. This is considered as the **upper bound** since this coarse granularity switching is the least flexible solution.
4. WXCfirst: The blocking percentage when we consider the fine granularity switching first, i.e., passing through the WXC whenever possible. Note that this

solution could be worst than the BypOnly solution if we promote already demultiplexed wavebands as in the case of the static traffic heuristic solutions.

Figure 65 shows the blocking probability (%) when we consider four wavelengths that can pass-through the wavelength cross-connect and back to the waveband cross-connect. By decreasing this number from five to four we increase the hardware complexity reduction ratio (HCRR). Note how in this case the difference between the Maximum flow solution and the WXC first solution is more convincing.

Figure 66 shows the blocking probability (%) for a hybrid network where the number of interlayer multiplexers/demultiplexers is chosen in order to have a HCRR=33.33% for all transit nodes. It is achieved if this number is 3 for nodes of degree 3, 4 for nodes of degree 4 and 5 for nodes of degree 5.

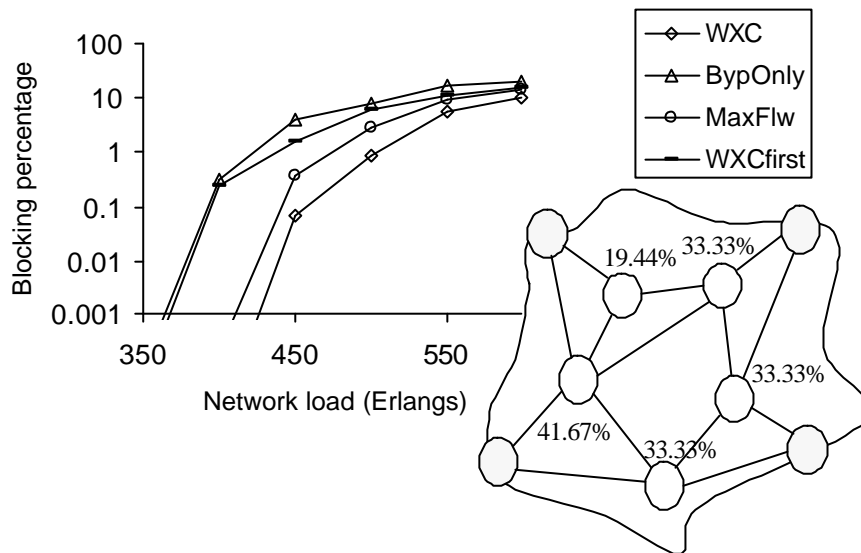


Figure 65: Results when we have **four** interlayer multiplexers/demultiplexers per waveband. HCRR is shown for each node in the network.



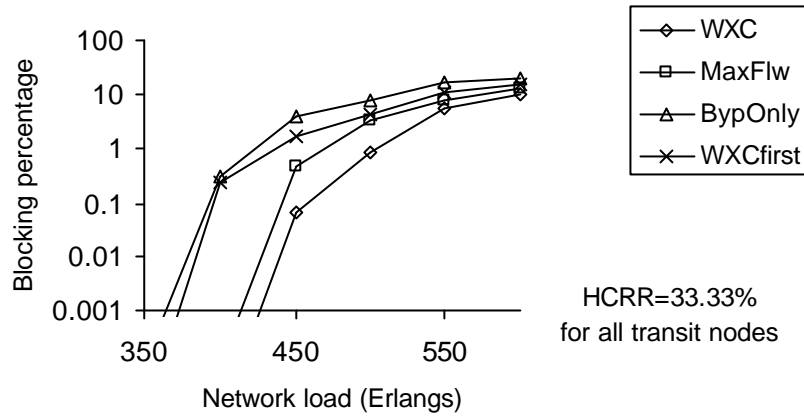


Figure 66: Blocking probability for hybrid network where the number of interlayer multiplexers/demultiplexers is chosen in order to have a HCRR=33.33% for all transit nodes.

## V.7. Conclusion

We considered in this chapter the dynamic traffic context in multi-granular optical networks. The MGGM is used to construct what we called the layered logical topology. In this logical topology, each layer represents a possible aggregation level or switching granularity. This forms an information base to the traffic engineering algorithm.

We proposed also a traffic engineering solution where we estimate how well a set of input/output pairs can support potential connections using the Ford-Fulkerson (maxflow) solution as a target. The best set is promoted to pass through the interlayer demultiplexers/multiplexers.

Simulation results for a given test network were shown to illustrate the blocking probability in the following cases:

- a. The upper bounds (bypassing all wavebands).
- b. The lower bounds (where we do not consider a reduction in the hardware complexity).
- c. Passing through the finest switching granularity when interlayer multiplexers/demultiplexers are available.

- d. Applying the proposed solution.

These simulation results showed the reduction of the blocking probability when setting up connections using our traffic engineering solution compared to the case where we choose to always bypass or always pass through finer granularities at intermediate nodes. This is to prove the correctness of our discussion on the crucial decision of how far to proceed with demultiplexing/multiplexing at intermediate nodes and the importance of including this decision in the graph optimization. This was not to be done without using the MGGM.

## VI. CONCLUSION OF THE THESIS

In this conclusion, we will review the contributions of our thesis to the design and optimization of multi-granular optical networks. We will propose at the end some topics to be further investigated.

Multi-granularity in optical networks is the solution toward a scalable and controllable optical network. This solution is cost-effective mainly in the backbone where the bypass traffic accounts for 60% to 80% of the total traffic [1].

Due to wavebanding, the hardware complexity of optical cross-connects can be reduced using hierarchical or multi-granular optical cross-connects where a choice can be made to bypass or to deaggregate a waveband. Due to time division multiplexing, electronic traffic grooming is widely used to exploit the huge bandwidth of a wavelength compared to the speed of electronic devices. Combining these two concepts of optical and electronic grooming and moreover defining different levels of aggregation is the main idea behind what we call multi-granular optical network.

Our work is mainly centered on the control of hierarchical optical cross-connects. This control is added to routing and wavelength assignment and consists in taking the following decisions:

- a. For static traffic, we must decide at each node, which traffic carriers are the best to be treated as a single entity and at which granularity.
- b. For dynamic traffic, to setup a connection, we must decide how far to proceed with demultiplexing/multiplexing, when to share used resources and when to inaugurate new ones.

In chapter 2, we proposed the Multi-Granularity Graph Model (MGGM). The importance of this model is to provide a complete base of information to be used by traffic engineering solutions. Compared to existing models, this one is characterized by:

- Supporting multi-levels of grooming.
- The ability of keeping track of the multi-granular network evolution.
- The fact that, when setting up a connection, the crucial decision of bypassing or passing through lower layers at intermediate nodes is part of the graph optimization in all cases.
- The possibility of modeling all components in the multi-granular context.

In chapter 3, we studied the hardware complexity reduction and the operational complexity increase when a wavelength cross-connect is replaced by a HXC or MG-OXC. We proposed an analytical model that allows us to describe how the connectivity is reduced when we consider the HXC instead of the WXC. This is important at the design and dimensioning phase of a multi-granular network where we must compare different implementations using the same resources with different granularities, different number of wavelengths in a fiber while adjusting the number of fibers in a multi-fiber network, ... etc. For instance, the same HCRR is obtained for different waveband granularities with different number of fibers per link but the blocking probability is not the same. The proposed analytical model tells us which implementation improves the network connectivity.

In chapter 4, we proposed the rearrangement of wavelengths as a solution to optimize the use of HXC within the static traffic context. This is done without changing the traffic mapping resulting from routing and wavelength assignment. Using a heuristic algorithm, we showed how in many cases the rearrangement results in a cost-effective solution. This does not concern only static traffic. In fact, the rearrangement proposed in this thesis opens new perspectives for enhancing the state of a multi-granular optical network by a minimum of changes to reduce the disrupted connections during rearrangement.

In chapter 5, we proposed to construct a layered logical topology using the MGGM in order to have an information base that can be used to apply traffic engineering solutions. We proposed also a traffic engineering solution based on the maxflow algorithm, particularly on the Ford-Fulkerson algorithm. This flow approach was used to estimate the best potential utilization of the network resources. This is taken as a target to provide an optimal feasible distribution of future connections. The solution consists in reinforcing this distribution by according interlayer multiplexers/demultiplexers (expensive resources) to critical links. The simulation results showed the reduction of the blocking probability when setting up connections using our traffic engineering solution compared to the case where we choose to always bypass or always pass through finer granularities at intermediate nodes. This is to prove the correctness of our discussion on the crucial decision of how far to proceed with demultiplexing/multiplexing at intermediate nodes and the importance of including this decision in the graph optimization. This could not be done without using the MGGM.

Some topics that can be further investigated:

- The protection and fault recovery in the multi-granular network context and how to benefit from rearrangement in this case.
- The control plane such as GMPLS implementation and the signaling needed to benefit from the proposed rearrangement to reduce the blocking probability while minimizing interrupted connections during rearrangement.
- Conceiving graph methods to be applied on the MGGM to reduce the number of edges and vertices in order to use it in the graph optimization algorithms for large networks. A starting point can be the passage proposed in this thesis from the MGGM to the layered logical topology.
- The adaptation of the proposed network engineering solutions and tools to be used in real-world networks.

## WAVELENGTH ASSIGNMENT AND TRAFFIC GROOMING IN RING NETWORK TOPOLOGIES

### **A.1 Introduction**

At the beginning of our research in the framework of this thesis, we were studying the cost reduction of ring based optical networks in the static traffic context. Due to the migration from ring to mesh topologies and from static to dynamic traffic in optical networks, we moved to work on multi-granular optical networks to follow their evolution and make a fruitful contribution. Grooming (electronic and optical) is a common theme around which our entire work is focused and wavelength assignment is an essential problem in wavelength division multiplexed (WDM) networks. For these reasons, we have found interesting to include this part of our work in this document.

Wavelength division multiplexing (WDM) is the most promising solution to exploit the huge bandwidth of a fiber in breaking the barrier between this tremendous bandwidth and the electronic speed.

Traffic grooming in a SONET/WDM rings reduces the number of SONET add-drop multiplexers (S-ADM or simply ADM) that represent the dominant cost factor. It appears to be a cost-effective solution since:

- The individual traffic streams have small bandwidth requirements compared to the bandwidth of a single wavelength even in a dense WDM (DWDM).
- The number of traffic streams is likely to be larger than the number of available wavelengths.

We assume that the WDM ring supports a four-fiber bidirectional SONET ring where one ADM can terminate all four fibers. Two fibers are reserved for protection and are, as the two other working fibers, each in a direction (clockwise and counterclockwise).

We present first in this appendix an introduction on wavelength assignment and traffic grooming where add-drop multiplexers (ADMs) are shared to reduce the cost of ring based optical networks. Then we show some existing solutions and we analyze some critical cases, which makes this work a commented summary on this subject. At the end, we propose a matrix based formulation of the problem and a simple integer linear programming (ILP) algorithm giving an optimal solution for a grooming factor  $g=2$  that we generalize to give a near optimal solution when  $g$  is a power of 2.

## A.2 Representing Lightpaths

Lightpaths in a WDM ring can be represented in different ways. For instance, as in [11], we can represent the ring by a set of  $N$  vertical lines numbered from 0 to  $N-1$  (for a ring of  $N$  nodes) where each line represents a node.

A lightpath connecting two nodes is then represented by a horizontal segment starting and ending by a symbol (small circle for example) representing a SONET add-drop multiplexer (or simply a drop). A drop indicates that the signal is electronically processed by the node. All lightpaths on the same horizontal line share the same wavelength. More than one horizontal line can have the same wavelength when traffic grooming is applied. Fig. 67 gives an example.

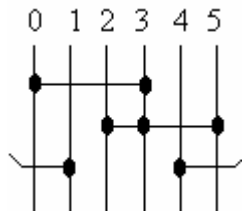


Figure 67: Representing lightpaths.

In this example, we represent 4 lightpaths :

$\{(0,3),(2,3),(3,5),(4,1)\}$  if we mean by  $(i,j)$  a connection (or a lightpath) from node  $i$  to node  $j$ .

or  $\{(0,3),(2,1),(3,2),(4,3)\}$  if we mean by  $(i,s)$  a connection from node  $i$  to node  $(i+s) \bmod N$ ,  $s$  is then the stride or number of hops. We will use this second notation in this appendix.

Here we consider bidirectional demands with shortest path routing. The stride  $s$  is at most  $(N-1)/2$  when  $N$  is odd and  $N/2$  when  $N$  is even. We represent connections in only one direction (for example clockwise), the connections in the other direction exist but are not represented. In the given example, connection  $(2,1)$  from node 2 to node 3 represents a clockwise connection on a working fiber. A connection from node 3 to node 2 is supported counterclockwise on the other working fiber but is not represented (note that the two other fibers of the 4-fiber ring are reserved for protection).

Another way to represent a ring is by using a set of circles each representing a wavelength or a fraction of a wavelength when grooming is applied. Nodes are distributed on these circles (each angle represents a node) and a segment joining two nodes represents a connection.

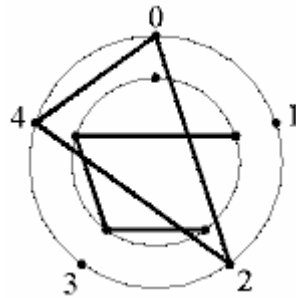


Figure 68: Example on circle representation.

Fig. 68 shows an example where we represent 2 circles for a ring of 5 nodes from 0 to 4. The inner circle represents the following set of connections  $\{(2,1),(3,1),(4,2)\}$  (remember that we are using the notation  $(i,s)$  which means a connection from  $i$  having  $s$  hops). The outer circle represents  $\{(0,2),(2,2),(4,1)\}$ . The outer circle is called a full circle because it fully uses the bandwidth of the wavelength, which maximizes the throughput on this wavelength.

### A.3 Problem Description

In the static traffic context, the demand between each pair of nodes is given prior to the ring design. For a given pair, an entry in the traffic demand matrix gives how many low speed tributaries (e.g. OC-3s) are to be carried between these two nodes.

The problem of traffic grooming and wavelength assignment is then to find which low speed tributaries are to be multiplexed in the same high-speed stream (e.g. OC-48) and to



which high-speed streams a given wavelength channel is to be assigned. Two goals are to be attained. The first is to minimize the number of ADMs. This is done by, on the one hand, combining added streams to dropped streams at the same node (RWA) and, on the other hand, grouping tributaries added or dropped at the same node (grooming). The second goal is to minimize the number of wavelengths by suitably filling each one. As shown in the next section, it is not always possible to achieve these goals simultaneously. We focus in this appendix on reducing the number of ADMs rather than the number of wavelengths.

Due to the difficulty of the problem, many attempts follow a two-step approach, as we shall see later in this appendix. This is discussed in [26] giving two methods found in literature:

- Grouping of tributaries into lightpaths and then routing and assigning wavelengths to these lightpath segments. In [10], it was shown that this two-step approach can lead to 20% more ADMs than considering these two steps jointly. Note that this conclusion is valid for a uniform all to all traffic.
- As in [34], packing non-overlapping low-speed tributaries of the traffic demand into circles and then grouping circles into wavelengths. The first step is done in order to suitably combine added to dropped tributaries at the same node. This is called circle construction or wavelength assignment since it is followed when wavelength assignment without grooming is considered. The second step is done in order to group into one stream and hence one wavelength, circles containing coherently added and dropped tributaries. This is called traffic grooming. This two-step method is claimed to be far better than the first one. It gives optimal results with uniform all to all traffic. However, we show in figure 69 an example where this two-step method can lead to 20% more ADMs than considering the two steps jointly. In fact, for the first step, the two circle constructions give the minimum number of ADMs (14 ADMs) for the same traffic demands. However, for a grooming factor of  $g=2$ , the right implementation gives better grooming results (8 ADMs instead of 10 ADMs for the left one).

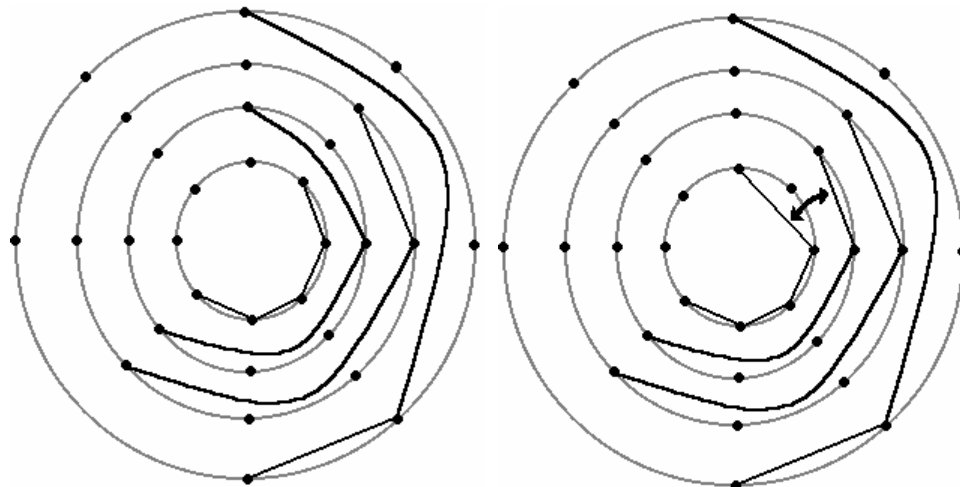


Figure 69: example showing that packing demands into circles and then grouping circles can lead to 20% more ADMs than considering the two steps jointly.

## A.4 Wavelength Assignment

### A.4.1 The Purpose of Wavelength Assignment

Wavelength assignment consists in distributing connections on different wavelengths (horizontal lines) without contention (without segment overlapping) in order to improve the network performance:

To reduce the electronic cost, we must reduce the number of S-ADMs by maximizing the case where two lightpaths share the same S-ADMs.

To raise the throughput of the network, we must maximize the filling of horizontal lines.

These two goals are not necessarily simultaneously achieved. For example, a given set of lightpaths can be connected as in figure 70 using 2 wavelengths and 8 S-ADMs.

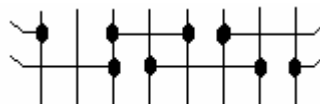


Figure 70: Wavelength assignment example minimizing the number of wavelengths.

The same set of lightpaths can be connected by using 3 wavelengths and 7 S-ADMs (fig. 71).

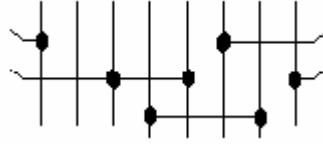


Figure 71: Wavelength assignment with more wavelengths but less ADMs.

#### A.4.2 Allocating Uniform Traffic

A circle construction method is described in [35] to support All-to-All Personalized connections (AAPC) in a ring with full mesh connectivity.

The goal is to connect each node to every other node by filling circles in order to minimize the number of circles (for instance wavelengths) and hence maximizing the network throughput. Constructing full circles does this.

Two algorithms are given in [35], CADS (complementary assembling with dual strides) for even number of nodes and CATS (complementary assembling with triadic strides) for odd number of nodes.

For CADS ( $N$  even), all the  $N(N-1)/2$  connections (in one direction and by the other working fiber in the other) can be set up by allocating the following sets of full circles (all additions are Modulo- $N$ ):

$\{(i,s),(i+s,N/2-s),(N/2+i,s), (N/2+i+s,N/2-s)\}$  for each  $i=0,1,2,\dots,N/2-1$  and for each  $s=1,2,\dots,N/4-1$ .

Two special cases are considered:

For  $s=N/2$  and  $i=0,1,\dots,N/4-1$ ,  $(N/2+i+s \text{ (Mod-}N))$  is the same as  $i$  and we have only two drops and two connections  $(i,N/2)$  and  $(i+N/2,i)$  these two connections fully occupy the working fiber in the same direction so the other working fiber is occupied using the same wavelength by the circle  $\{(i+3N/4,N/2),(i+N/4,N/2)\}$  in the other direction.

For  $s=N/4$  and  $i=0,1,2,\dots,N/4-1$  we have four connections of the same stride  $N/4$ .

For CATS ( $N$  odd), we need two types of circles:

- A four-connection circle

$$\{(i,(N-1)/2-s),(i+(N-1)/2-s,s+1),((N+1)/2+i,(N-1)/2-s),(i-s,s)\}$$

- A three-connection circle  $\{(i,(N-1)/2),(i+(N-1)/2,1),((N+1)/2+i,(N-1)/2)\}$

Fig. 72 shows an example for  $N=5$ .

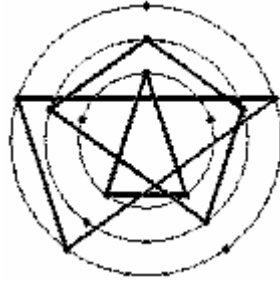


Figure 72: Four and three-connection circles.

With this construction, the lower bound on the number of circles is reached  $((N^2-1)/8$  circles when  $N$  is odd) so the job of minimizing wavelengths and ADMs is fully achieved in the case of uniform All-to-All traffic.

The same problem of allocating AAPC for a 4-fiber bidirectional ring was studied in [8] where a wavelength assignment algorithm using a matrix approach was presented. The problem is to fill a matrix of  $W$  lines (number of wavelengths) and  $N$  columns (number of nodes), where each value  $s$  in position  $(i,j)$  represents the stride (hops count) for a connection from node  $j$  to  $j+s \pmod{N}$  using the wavelength  $\lambda_i$ . A symbol  $X$  in position  $(i,j)$  states that  $\lambda_i$  is not dropped at node  $j$ . To minimize the number of ADMs, we must maximize the case where, for a given  $s$  in  $(i,j)$ , the entry in  $(i,j+s \pmod{N})$  is not an  $X$ .

As in circle construction, half of the connections in only one direction are represented for strides from 1 to  $\lfloor N/2 \rfloor$  while the other half is symmetrically supported by the other working fiber in the other direction.

The problem of allocating AAPC is reduced to filling in the first column and then by cyclically shifting the matrix entries by one for each column e.g.,

$$\begin{bmatrix} 1 & 2 & X & 2 & X \\ 2 & X & 1 & 1 & 1 \\ X & 1 & 2 & X & 2 \end{bmatrix}$$

#### A.4.3 Allocating Non-Uniform Traffic

Going back to the circle construction, each circle can be represented by a matrix as in [12] where the lines represent the nodes from 0 to N-1 and the columns the stride from 1 to  $\lfloor N/2 \rfloor$ .

Each entry in position (i,s) represents the number of connections from i to i+s (Mod-N). In a circle, as already defined, this entry is 1 if the connection (i,s) belongs to the circle or 0 otherwise. This matrix representation can be used to represent the traffic demand and hence the problem of wavelength assignment is reduced to the decomposition of the traffic demand matrix by a set of full and partial circle matrices.

A partial circle is a circle having non-overlapping connections but not filling the circle completely.

To reduce the number of wavelengths, we must decompose with the minimum number of matrices.

In a full circle, all ADMs are shared so we must maximize full circles to reduce the number of ADMs but in general, we must maximize the number of cases where for a non zero entry in position (i,s) we have a non zero entry in the line i+s mod-N (this ADM at node i+s is shared). Remember that minimizing the number of wavelengths will not necessarily reduce the number of ADMs.

To distribute non-uniform traffic, [12] proposes a two-stage circle construction. In the first stage, called FCCA(full circle construction algorithm), C1 full circles are constructed and the corresponding matrix is subtracted from the traffic demand matrix. In the second stage, called PCCA(partial circle construction algorithm), the remaining connections are distributed

into a minimum number of circles C2 if the goal is to minimize the number of wavelengths and in order to maximize shared ADMs when the goal is to minimize the cost.

Let  $G$  be the traffic demand matrix.

PCCA considers long connections first ( $s = \lfloor N/2 \rfloor$  down to 1).

For each connection  $G(i,s)$  that fits into a partial circle of the C2 circles created till now (which means that lines  $i$  up to  $i+s-1 \pmod{N}$  of a partial circle in C2 are all zero), update the matrix of the partial circle and set  $G(i,s) = G(i,s) - 1$ . Else increment C2 and create a new circle matrix to hold the current connection and set  $G(i,s) = G(i,s) - 1$ .

This algorithm intends to reduce the number of wavelengths.

The algorithm given in [34] is to reduce the number of SONET ADMs. First we must note that when we want to allocate a connection, if it adds a new gap this means that it adds an additional ADM (fig. 73).

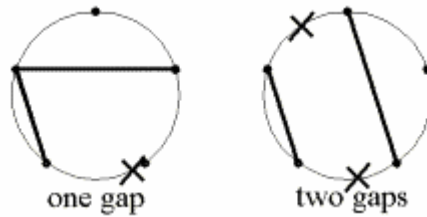


Figure 73: Gaps in a circle construction.

This algorithm is described as follows:

We construct and subtract the C1 full circles (as in FCCA).

For the remaining connections, we check one by one starting from the longer one to minimize blocking long connections. For all partial circles already created, choose one where the connection can fit without creating an additional gap to allocate it. If not found and if it can fit with an additional gap, put it in a pool (GapMaker list). If it doesn't fit at all (it overlaps with connections in all partial circles) then create a new partial circle.

After visiting all connections in the traffic demand matrix, try to allocate connections already put in the GapMaker to fit them without additional gap. Else, create a new partial circle for the connections that fits with additional gap or doesn't fit at all.

In [12], the authors consider the FCCA trivial by subtracting individually from the traffic matrix each full circle constructed by CADS or CATS until one or more corresponding element drop to zero in the traffic demand matrix. Since none of the circle matrices constructed by CADS or CATS contains overlapping elements, the sequence of matrix subtraction does not matter.

We mention here that full circle construction is not unique and if we consider the circles generated by CATS for example taking  $N=5$  three full circles are constructed as shown in fig.74(A). Even though it assures full connectivity, we can imagine many other full circles for example fig.74(B).

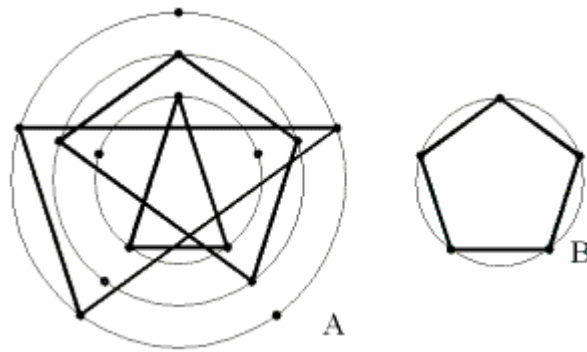


Figure 74: A. Full circles generated by CATS. B. Another type of full circles.

In particular, we can consider the circles deduced from those constructed by CADS or CATS by a simple rotation.

Let us consider what happens if we apply the described algorithms with a modified FCCA that considers circles constructed by CADS or CATS with all circles deduced by their rotation. Then the order of subtraction must be considered because not all these circles are non-overlapping.

This may improve the reduction of ADMs number. Example:

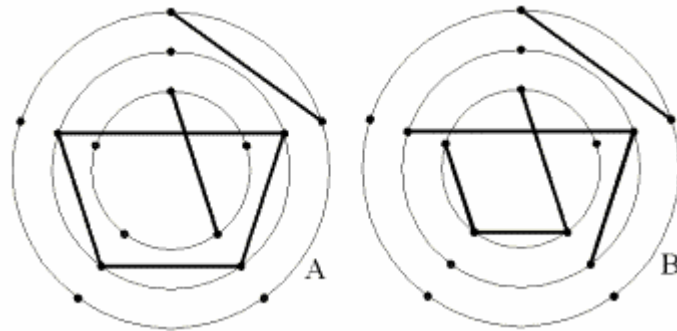


Figure 75: A. Trying CATS' full circles with all possible rotations. B. Trying CATS' full circles with no rotation.

Circles A of fig. 75 are constructed using full circles by CATS with their rotation and then the algorithm given in [34]. Circles B of fig.75 are constructed by applying FCCA as described in [12] and then the algorithm of [34]. We have 8 ADMs with rotation instead of 9.

The simulation results give almost the same global performance with a subtle difference if we take a look closely on 100 samples (fig. 76) where we show the number of ADMs saved with rotation versus non rotation. Negative points correspond to a traffic pattern where the algorithm with no rotation is better than the one with rotation and that is because of the order of the choice. This is not a great difference. The graph is for traffic demand matrices generated by random entries evenly distributed between 0 and  $2\mu$  where  $\mu=2.5$  which gives a mean number of ADMs for 15 nodes around 300. We conclude that deducting full circles generated by CADs or CATS is sufficient.

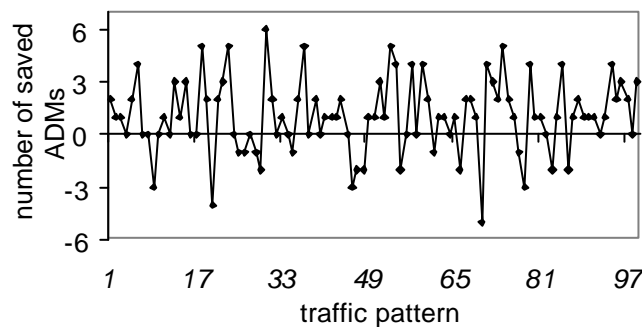


Figure 76: Saved ADMs when applying full circles rotation.

### A.5 Traffic Grooming

Having connections already allocated into circles, if a connection doesn't use all the bandwidth of a wavelength, we can groom  $g$  circles together in a single wavelength in order to



remove (and save the cost of) shared ADMs. This means that each circle is served in one of the  $g$  timeslots in the corresponding wavelength.

In this case, we consider that each connection uses  $1/g$  of the bandwidth of a wavelength.

For example, we can groom four OC-12 streams into one OC-48 stream. In this case,  $g=4$  and  $g$  is called the grooming factor or granularity.

In order to minimize the cost, we must maximize the number of shared ADMs. This is done by properly choosing circles to be groomed.

In [4], the general traffic grooming problem is proved to be NP-Complete by showing that Bin Packing problem can be transformed into the traffic grooming problem in polynomial time. This is why many papers on grooming rely on heuristics and simulation to evaluate the heuristics [26].

In [12] and [34], almost the same grooming algorithm is given to minimize the number of ADMs. First, connections are assigned to circles using a wavelength assignment algorithm minimizing the number of drops in a circle. Then the proposed grooming algorithm starts always with the circle having the greatest number of ADMs to fill in a given wavelength. Then  $g-1$  other circles are chosen one by one in order to have the greatest number of common ADMs with all already groomed circles in the current wavelength.

In this appendix, we call this algorithm Alg I. In analyzing a number of cases with different traffic demand matrices one by one, applying Alg I and drawing the corresponding circles for  $g=2$ , we have found that starting always with the greatest number of ADMs as first circle in the lightpath is not optimal. Fig.77 gives an example. Note that if rerouting is considered, the two inner circles can be merged together into one using the short path and the other using the long path. Here we suppose that rerouting is not considered..

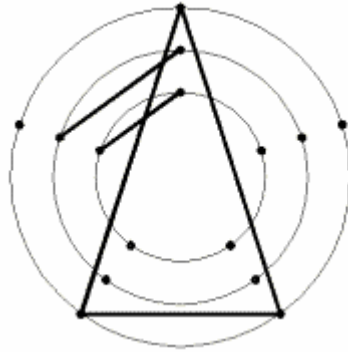


Figure 77: Example of traffic to groom.

In this example for  $g=2$  Alg1 grooms the circles (if we number the circles from 1 to 3 going from the inner to the outer circle) in the following two sets:

- a. Circle 3 (greatest number of ADMs) and circle 2 [ 4 ADMs].
- b. Circle 1 [2 ADMs]

The total number of ADMs is then 6 ADMs.

We could have groomed:

- a. Circle 1 and circle 2, having the greatest number of common ADMs with 2 ADMs.
- b. Circle 3 with 3 ADMs.

For a total of 5 ADMs instead of 6. That is what our algorithm does.

So we propose the following grooming algorithm denoted here Alg II:

1. After wavelength assignment, isolated connections (connections that occupy a circle by themselves) are tested to fit in an already allocated circle without overlapping (regardless of additional gap). Note that the effect of this step is minor comparing to step 2.

2. Instead of choosing the circle having the greatest number of ADMs as the first circle of the wavelength, we choose to groom first the two circles having the greatest number of common ADMs.

We apply the Wavelength Assignment algorithm and then the two grooming algorithms Alg I and Alg II on each traffic demand matrix generated randomly with entries evenly distributed between 0 and  $2\mu$  where  $\mu=2.5$ .

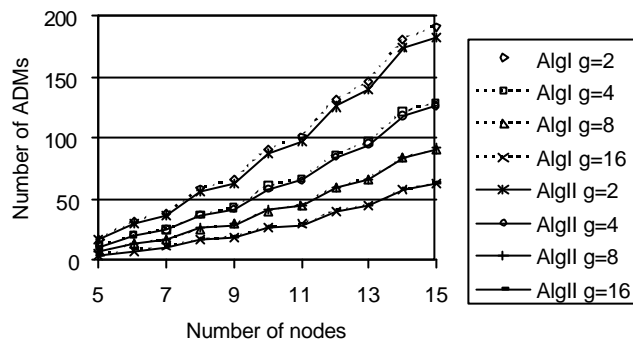


Figure 78: Comparing AlgI and AlgII ( $\mu=2$ ).

Fig. 78 shows the results where we can see that Alg II is better for small grooming factors ( $g=2$ ) in terms of number of ADMs. Fig. 79 shows the saving percentage (Alg II versus Alg I) as a function of  $g$  for  $N=5,9$  and  $15$ .

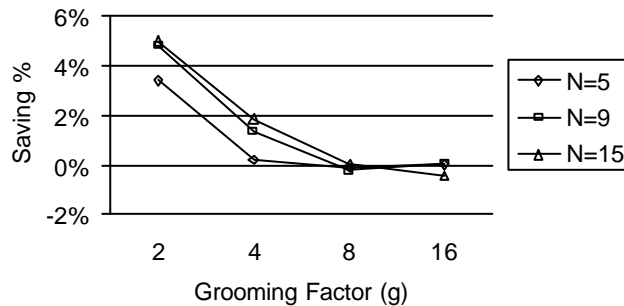


Figure 79: Saving in ADMs number using AlgII versus AlgI ( $\mu=2.5$ ).

What is important to notice here is that the results are not only improved in term of mean value. In fact, if we take a look to each occurrence of the traffic demand matrix generated randomly, we see that the enhancement is found for almost each sample. Fig. 80 shows the number of ADMs for 50 different traffic patterns generated randomly and groomed by AlgI and AlgII simultaneously.

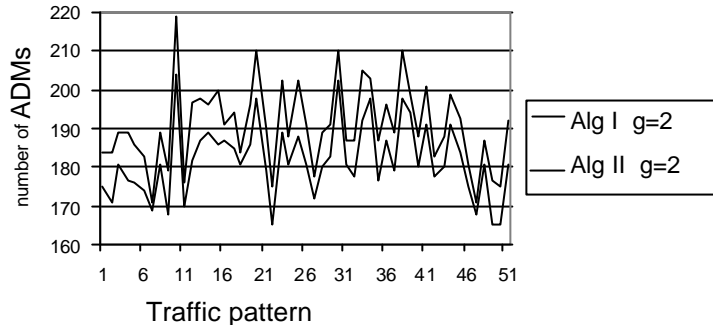


Figure 80: AlgI and AlgII applied on different randomly generated traffic demand matrix.

To improve results for  $g > 2$ , we propose the following algorithm (Alg III):

1. Apply the wavelength assignment, which produces the initial set of circles ( $g=1$ ).
2. Choose the 2 circles having the greatest number of common ADMs to form a circle of doubled grooming factor (i.e.:  $g=2$  if it was 1,  $g=4$  if it was 2, etc.) that will be added to the new set of circles. Exclude the chosen 2 circles from the initial set of circles.
3. Repeat step 2 until the initial set of circles becomes empty.
4. The new set of circles becomes the initial set and if the desired grooming factor ( $g=2^n$  where  $n$  is the number of times we repeat the algorithm) is not reached, go back to step 2.

Fig. 81 shows the resulting number of ADMs and fig. 82 shows the saving percentage.

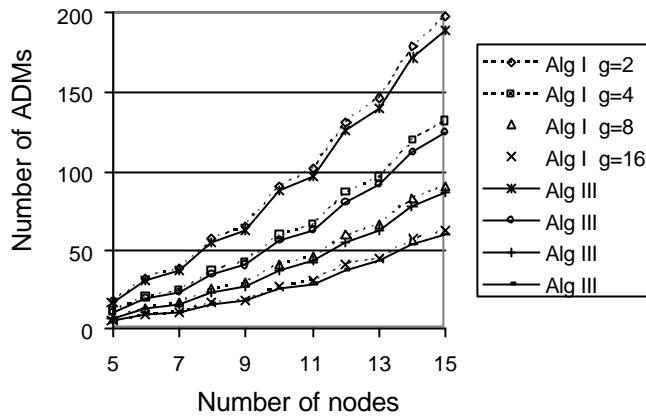


Figure 81: AlgI versus AlgII for  $\mu=2$ .

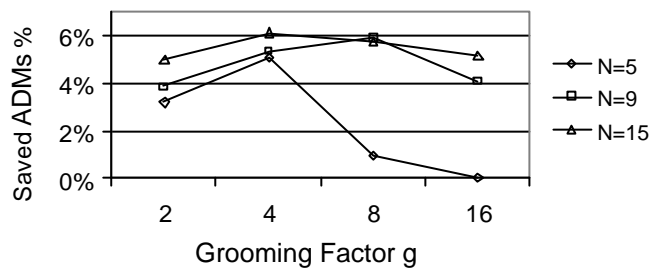


Figure 82: Saving ADMs (AlgII versus AlgI).

Note that algorithm III improves the method followed by Alg I but *this is not to say* that the idea of grooming circles having a grooming factor of  $g$  two by two to obtain a grooming factor equal to  $2g$  would be better than following the optimized method for grooming initial circles ( $g=1$ )  $2g$  by  $2g$  to obtain a grooming factor of  $2g$ . In fact, the opposite is true but the result is better since we are using heuristic algorithms.

We will use these results later in this appendix to propose an integer linear programming formulation adapted for  $g=2$ .

To complete our study, we must cover an interesting traffic grooming algorithm based on a stochastic approach given in [6]. It follows the Metropolis algorithm that can be described, for a grooming factor  $g$ , by the following:

Starting with an initial set of circles grouped by subsets of  $g$  circles each, e.g., we groom circles  $g$  by  $g$  in the same order they are constructed by wavelength assignment, we pick randomly two circles, each from a different subset, and we find  $dcost$  which is the number of ADMs added if we swap these two circles (or part of them). If  $dcost$  is negative (going in the optimal direction having lower number of ADMs) we keep the new configuration, otherwise we keep it with a probability equal to  $\text{Exp}(-dcost/control)$  where  $control$  (temperature) is a variable decremented while repeating the process until it becomes below some value where the probability becomes too low to keep a risky swap. At this point, we assume that the system has reached equilibrium.

We run this algorithm (Alg IV) in our simulation to find the results in fig. 83. Note that the results are based on random numbers so for different executions we could have different values. Usually, for a given traffic pattern we run different trials to keep the lowest number of ADMs obtained.

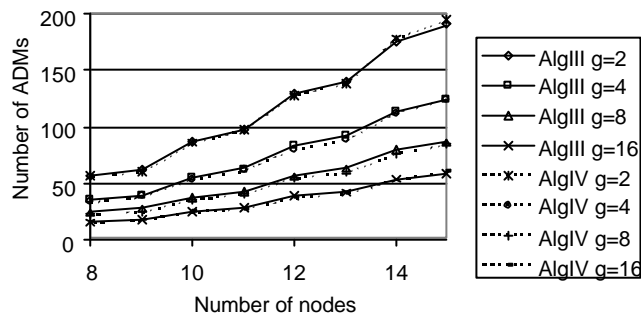


Figure 83: AlgIII versus AlgIV for  $\mu=2.5$ .

## A.6 Problem Formulation

### A.6.1 Matrix Representation

We redefine the traffic demand matrix  $G=\{G(i,s)\}$  where  $G(i,s)$  represents the number of connections from  $i$  to  $i+s \pmod{N}$ .  $N$  is the number of nodes,  $i=0,1,\dots,N-1$  and  $s=1,2,\dots, \lfloor N/2 \rfloor$ .

The wavelength assignment results in a sequence of circle matrices  $\{C^i\}$  decomposed from  $G$ . In a circle matrix, an entry  $C^i(i,s)$  is 1 if the connection  $(i,s)$  belongs to the circle or 0 otherwise where  $j=1,2,\dots,N_c$  and  $N_c$  is the number of circle matrices.

For example, the following traffic demand matrix (intentionally the same as the example given in [12]):

$$G = \begin{pmatrix} 2 & 2 \\ 0 & 3 \\ 1 & 0 \\ 1 & 2 \\ 1 & 2 \end{pmatrix}$$

results in the following circle matrices (this assignment is not unique, it depends on the wavelength assignment):

$$C^1 = \begin{pmatrix} 1 & 0 \\ 0 & 1 \\ 0 & 0 \\ 0 & 1 \\ 0 & 0 \end{pmatrix}, C^2 = \begin{pmatrix} 1 & 0 \\ 0 & 1 \\ 0 & 0 \\ 0 & 1 \\ 0 & 0 \end{pmatrix}, C^3 = \begin{pmatrix} 0 & 0 \\ 0 & 0 \\ 0 & 0 \\ 0 & 0 \\ 0 & 1 \end{pmatrix}$$

$$C^4 = \begin{pmatrix} 0 & 1 \\ 0 & 0 \\ 1 & 0 \\ 0 & 0 \\ 1 & 0 \end{pmatrix}, C^5 = \begin{pmatrix} 0 & 1 \\ 0 & 0 \\ 0 & 0 \\ 0 & 0 \\ 0 & 0 \end{pmatrix}, C^6 = \begin{pmatrix} 0 & 0 \\ 0 & 1 \\ 0 & 0 \\ 1 & 0 \\ 0 & 1 \end{pmatrix}$$

represented by fig. 84 (if circles are numbered 1,2,...,N<sub>c</sub> from the inner to the outer circle).

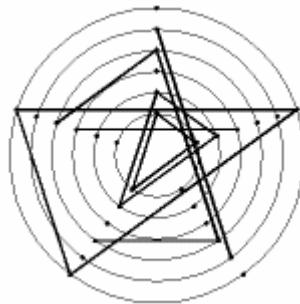


Figure 84: Example of circles to groom.

Now we define for each circle  $C^i$  an ADM column matrix  $A^i$  where  $A^i(i)=1$  if an ADM should be present at node  $i$  to serve connections belonging to  $C^i$ , otherwise  $A^i(i)=0$ .

To obtain the set of matrices  $\{A^i\}$ , we proceed as follows:

For each  $C^i$ , we construct the matrix  $D^i$  which corresponds to destination nodes of  $C^i$ , where  $D^i(i,s)=C^i(i-s,s)$ .  $D^i$  is constructed directly by cyclic rotations of  $s$  positions applied on each column  $s$  in  $C^i$ .

Since the same ADM can handle received and departing connections in the four-fiber ring  $A^i(i)=1$  if at least the line  $i$  of  $C^i$  or the line  $i$  of  $D^i$  has a non zero element. Otherwise  $A^i(i)=0$ .

We define:  $\bigcup_{s=1}^x C(s) = C(1) \wedge C(2) \wedge \dots \wedge C(x)$  where  $\wedge$  is the Boolean OR and  $C(s)$  can be either 0

or 1 and considered as Boolean variables. Now we can write:  $A^j(i) = \bigcup_{s=1}^{\lfloor N/2 \rfloor} C^j(i,s) \wedge \bigcup_{s=1}^{\lfloor N/2 \rfloor} D^j(i,s)$

For example, concerning  $C^4$  given in the preceding example, we have:

$$C^4 = \begin{pmatrix} 0 & 1 \\ 0 & 0 \\ 1 & 0 \\ 0 & 0 \\ 1 & 0 \end{pmatrix}, D^4 = \begin{pmatrix} 1 & 0 \\ 0 & 0 \\ 0 & 1 \\ 1 & 0 \\ 0 & 0 \end{pmatrix}, A^4 = \begin{pmatrix} 1 \\ 0 \\ 1 \\ 1 \\ 1 \end{pmatrix}$$

which can be seen directly on circle 4,  $A^4$  has a total number of 4 ADMs.

Now if we groom circles 4 and 5, we obtain a resulting ADM matrix  $A^{4,5}$ :

$$A^4 = \begin{pmatrix} 1 \\ 0 \\ 1 \\ 1 \\ 1 \end{pmatrix}, A^5 = \begin{pmatrix} 1 \\ 0 \\ 1 \\ 0 \\ 0 \end{pmatrix}, A^{4,5} = \begin{pmatrix} 1 \\ 0 \\ 1 \\ 1 \\ 1 \end{pmatrix}$$

$A^{4,5} = A^4 \text{ OR } A^5$ . Now we use four ADMs instead of  $4+2=6$ .

The problem of traffic grooming is now reduced to that of grouping ADM matrices  $g$  by  $g$  in order to minimize the number of ADMs.



### A.6.2 The ILP Formulation

Having the set of ADM matrices  $\{A^i\}$ ,  $j=1,2,\dots,Nc$  as a result of the wavelength assignment algorithm, we define the cost  $c_{ij}$  of combining  $A^i$  and  $A^j$  as the number of ADMs that are not shared between these two matrices ( $i \neq j$ ) or simply the Hamming distance between  $A^i$  and  $A^j$ , and the cost  $c_{ii}$  to have the circle  $C^i$  not groomed as the number of ADMs in  $A^i$  (in this case all ADMs are not shared).

Example: having a total of three ADM matrices for a ring of 5 nodes:

$$A^1 = \begin{pmatrix} 1 \\ 1 \\ 0 \\ 0 \\ 0 \end{pmatrix}, A^2 = \begin{pmatrix} 1 \\ 1 \\ 0 \\ 0 \\ 0 \end{pmatrix}, A^3 = \begin{pmatrix} 0 \\ 1 \\ 0 \\ 1 \\ 1 \end{pmatrix}$$

the cost matrix  $c = \{c_{ij}\}$  is then:

$$c = \begin{pmatrix} 2 & 0 & 3 \\ & 2 & 3 \\ & & 3 \end{pmatrix}$$

Note that for a given  $i$  and  $j$  ( $i \neq j$ ) if  $c_{ij}$  is defined  $c_{ji}$  must not be defined because grooming  $A^j$  and  $A^i$  is the same as grooming  $A^i$  and  $A^j$ .

The objective is to minimize the number of ADMs which is equivalent to minimizing the number of non-shared ADMs and for a grooming factor  $g=2$  the integer linear programming can be formulated as follows:

*Minimize:*

$$z = \sum_{i=1}^{Nc} \sum_{j=i}^{Nc} f_{ij} c_{ij} \quad (1)$$

*Subject to:*

$$\sum_{j=i}^{Nc} f_{ij} + \sum_{1 \leq j < i} f_{ji} = 1 \quad \forall i = 1, 2, \dots, Nc \quad (2)$$

$$f_{ij} \in \{0,1\} \quad \forall i = 1, 2, \dots, Nc \text{ and } \forall j = i, \dots, Nc \quad (3)$$

We have a set of  $\frac{Nc(Nc+1)}{2}$  variables  $\{f_{ij}\}$  where  $f_{ij}=1$  if circles  $i$  and  $j$  are groomed and  $f_{ij}=0$  otherwise. When circle  $i$  is not groomed, we have  $f_{ii}=1$  otherwise  $f_{ii}=0$ . So  $z$  is the total number of non-shared ADMs to minimize as defined in (1) and the set of constraint (2) is obtained if we consider the following:

Each ADM matrix  $A^i$  must be groomed to one and only one other ADM matrix  $A^j$  ( $f_{ij}=1$  or (exclusive)  $f_{ji}=1$ ) or (exclusive) it must stay not groomed ( $f_{ii}=1$ ).

Applying this ILP we have the optimized traffic grooming solution for  $g=2$ . Having this optimized solution, we construct the new set of ADM matrices. This is done by grooming matrices  $A^i$  and  $A^j$  having  $f_{ij}=1$ . Then we apply the same ILP on this new set to pass to  $g=4$  and then to  $g=8$ , etc. This construction is reinforced by the positive results of AlgIII simulation which gives good results even though it doesn't start from an optimal solution for  $g=2$  and doesn't find the optimal solution in each iteration as the described ILP. The same iterative approach has already been proposed in [32] where instead of the ILP a maximum-weighted perfect matching is proposed.

## A.7 Conclusion

We considered in this appendix the problem of minimizing the cost of SONET/WDM rings by appropriate wavelength assignment and traffic grooming. The whole problem of reducing the number of SONET add-drop multiplexers turns out to be an NP-complete integer linear programming. Heuristics are often used and the problem is usually separated into wavelength assignment and traffic grooming. These algorithms can be deterministic or stochastic. We have presented a comprehensive definition of the problem and proposed a size controllable formulation of the integer linear program ILP for a grooming factor  $g=2$  based on the separation between traffic grooming and wavelength assignment. Then, using simulation results, we extend the algorithm for  $g=4,8,16$ , etc. This algorithm gives optimal results for  $g=2$ . We have focused on non-uniform static traffic and bidirectional four-fiber self-healing rings.

A BRIEF ON THE FORD-FULKERSON MAXFLOW ALGORITHM

The Ford-Fulkerson maxflow algorithm introduced in the 1950s [9] finds an upper bound on the flow through a network from a given source  $s$  to a given destination  $d$ .

We represent a network by a weighted directed graph  $(V, E, C)$ .  $V$  is the set of vertices representing nodes,  $E$  is the set of edges representing links and  $C$  is a function from  $E$  to  $\mathbf{N}^+$  representing the capacity of a link in number of traffic units. The capacity of a link  $e \in E$  is represented by  $c(e)$ . A flow  $f$  for the network is an assignment of an integer value  $f(e)$  to every edge  $e \in E$ . For each  $e \in E$ :  $0 \leq f(e) \leq c(e)$ .

Starting with  $f(e)=0 \forall e \in E$  we repeatedly increase the flow by searching for an augmenting path. An augmenting path is a path from  $s$  to  $d$  in what is called residual network. The residual network  $(V, E', C')$  induced by the flow  $f$ , where  $E'$  covers the edges of  $E$  and those in their opposite direction, is characterized by  $C'$  where for each  $e' \in E'$  we have:

- The residual capacity  $c'(e')=c(e)-f(e)$  when  $e' \in E$  ( forward edge).
- The excess capacity  $c'(e')=f(e)$  where the edge  $e \in E$  is in the opposite direction of  $e'$ . This is to allow pushing the flow back towards the source.

The flow is incremented until no more augmenting path is found. As a result, we obtain a flow  $f$  that is a possible realization of the flow distribution to reach the upper bound on the flow from  $s$  to  $d$ .

THE PRINCIPLE OF INCLUSION AND EXCLUSION

The principle of inclusion and exclusion discovered 100 years ago by Sylvester and before, in another form, by De Moivre is a combinatorial principle used to count the number of arrangement of a set of objects under some conditions. This is a generalization of the familiar formula  $|A \cup B \cup C| = |A| + |B| + |C| - |A \cap B| - |B \cap C| - |A \cap C| + |A \cap B \cap C|$ .

Let us consider  $N$  objects where each may or may not have one or more given properties. Let  $m$  be the number of these possible properties;  $a_i$  is the  $i^{\text{th}}$  property ( $i = 1, 2, \dots, m$ ). Let  $N(a_i)$  be the number of objects that have the property  $a_i$ ,  $N(a'_i)$  be the number of objects that do not have the property  $a_i$ ,  $N(a_i, a'_j)$  be the number of objects that have the property  $a_i$  but do not have the property  $a_j$  and so on.

The principle of inclusion and exclusion states that the number of objects that have none of the properties is given by:

$$N(a'_1 a'_2 \dots a'_m) = N - \sum_i N(a_i) + \sum_{i \neq j} N(a_i a_j) - \sum_{\substack{i, j, k \\ \text{distinct}}} N(a_i a_j a_k) \\ + (-1)^k \sum_{\substack{i_1, i_2, \dots, i_k \\ \text{distinct}}} N(a_{i_1} a_{i_2} \dots a_{i_k}) + \dots + (-1)^m N(a_1 a_2 \dots a_m)$$

Proof: every object having none of the properties must be counted exactly once and every object having at least one property must be counted exactly zero times.

In the given expression:

1. An object having at least one property, for instance exactly  $p$  properties, is counted:  $(p - 0) = 1$  times in  $N$ ,  $(p - 1)$  times in  $\sum N(a_i)$ ,  $(p - 2)$  times in  $\sum N(a_i a_j)$ , ... that is (since  $p \leq m$ ):

$$\binom{p}{0} - \binom{p}{1} + \binom{p}{2} - \dots + (-1)^p \binom{p}{p} = [1 + (-1)]^p = 0 \text{ times}$$

2. An object having none of the properties is counted once in the term  $N$  and zero times in the other terms.

THE REARRANGEMENT ILP IN GLPK

The following model description of the proposed ILP for rearrangement is given in this appendix as an example and for documentation.

**D.1 Coding Model Rearr.mod**

```

param L integer;
param T integer;
param W integer;
param N integer;
set IIN {nd in 1..N};
set OON {nd in 1..N};
set Wavelength:=1..L;
param sigma{p in 1..T,q in 1..T} binary;
param delta{j in 1..L,b in 1..L/W} binary;
param etta{i in 1..L,p in 1..T} binary;
param psi{i in 1..L,p in 1..T,q in 1..T} binary;
param xsi{i in 1..L,p in 1..T,q in 1..T} binary;
var lambda{i in 1..L, j in 1..L},binary;
var pii{b in 1..L/W,p in 1..T, q in 1..T},binary;
var u{b in 1..L/W,q in 1..T},binary;
minimize c:sum {nd in 1..N}(sum {p in IIN[nd],b in 1..L/W} (u[b,p]+(u[b,p]-sum{q in 1..T}pii[b,p,q])*W)
+sum{q in OON[nd],b in 1..L/W}(u[b,q]-sum {p in 1..T}pii[b,p,q]));
s.t. cst2{b in 1..L/W,p in 1..T, q in 1..T}:pii[b,p,q]*W<=sigma[p,q]*sum{i in 1..L,j in 1..L}
xsi[i,p,q]*delta[j,b]*lambda[i,j];
s.t. cst3{b in 1..L/W,p in 1..T, q in 1..T}:pii[b,p,q]<=sigma[p,q]*sum{i in 1..L,j in 1..L}
psi[i,p,q]*delta[j,b]*lambda[i,j];
s.t. cst4{b in 1..L/W,p in 1..T}:u[b,p]<=sum{i in 1..L,j in 1..L} etta[i,p]*delta[j,b]*lambda[i,j];
s.t. cst5{b in 1..L/W,p in 1..T,j in 1..L}:u[b,p]>=delta[j,b]*sum{i in 1..L} etta[i,p]*lambda[i,j];
s.t. cst6{i in 1..L}: sum{j in 1..L} lambda[i,j]=1;
s.t. cst7{j in 1..L}: sum{i in 1..L} lambda[i,j]=1;
solve;
printf {i in 1..L, j in 1..L} "%d\n",lambda[i,j];
end;

```

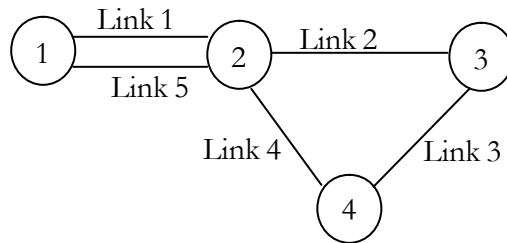


Figure 85: Test network used to generate the data model.

## D.2 Data Model Rearr.dat

The following data model is for the test network given in figure 85 and where the traffic is uniform with  $D=2$  traffic units between each pair of nodes and a waveband granularity  $W=3$ .

```

data;          12 0 0 0 0 0          4 0 0 0 1 0          9 0 0 0 0 0
param L:= 12;  [*,* ,2]: 1 2 3 4 5      5 0 0 0 1 0          10 0 0 0 0 0
param T:= 5;   :=                      6 0 0 0 1 0          11 0 1 0 0 0
param W:= 3;   1 0 0 0 0 0          7 0 0 0 0 0          12 0 1 0 0 0
param N:= 4;   2 0 0 0 0 0          8 0 0 0 0 0          [*,* ,4]: 1 2 3 4 5
set IIN[ 1]:= 5; 3 1 0 0 0 0          9 0 0 0 0 0          :=
set OON[ 1]:= 1; 4 1 0 0 0 0          10 0 0 0 0 0         1 0 0 1 0 0
set IIN[ 2]:= 1 4; 5 1 0 0 0 0          11 0 0 0 0 0         2 0 0 1 0 0
set OON[ 2]:= 2 5; 6 1 0 0 0 0          12 0 0 0 0 0;        3 0 0 1 0 0
set IIN[ 3]:= 2; 7 0 0 0 0 0          param xsi:=          4 0 0 1 0 0
set OON[ 3]:= 3; 8 0 0 0 0 0          [*,* ,1]: 1 2 3 4 5  5 0 0 0 0 0
set IIN[ 4]:= 3; 9 0 0 0 1 0          :=                  6 0 0 0 0 0
set OON[ 4]:= 4; 10 0 0 0 1 0         1 0 0 0 0 0         7 0 0 0 0 0
param etta: 1 2 3 4  11 0 0 0 0 0         2 0 0 0 0 0         8 0 0 0 0 0
5 :=              12 0 0 0 0 0         3 0 0 0 0 0         9 0 0 0 0 0
1 1 1 1 1 1      [*,* ,3]: 1 2 3 4 5      4 0 0 0 0 0         10 0 0 0 0 0
2 1 1 1 1 1      :=                    5 0 0 0 0 0         11 0 0 1 0 0
3 1 1 1 1 1      1 0 0 0 0 0         6 0 0 0 0 0         12 0 0 1 0 0
4 1 1 1 1 1      2 0 0 0 0 0         7 0 0 0 0 0          [*,* ,5]: 1 2 3 4 5
5 1 1 1 1 1      3 0 0 0 0 0         8 0 0 0 0 0          :=
6 1 1 1 1 1      4 0 0 0 0 0         9 0 0 0 0 0         1 0 0 0 0 0
7 0 1 1 1 0      5 0 1 0 0 0         10 0 0 0 0 0        2 0 0 0 0 0
8 0 1 1 1 0      6 0 1 0 0 0         11 0 0 0 0 0        3 0 0 0 1 0
9 0 1 1 1 0      7 0 1 0 0 0         12 0 0 0 0 0        4 0 0 0 1 0
10 0 1 1 1 0     8 0 1 0 0 0          [*,* ,2]: 1 2 3 4 5  5 0 0 0 1 0
11 0 0 0 0 0     9 0 0 0 0 0          :=                  6 0 0 0 1 0
12 0 0 0 0 0;    10 0 0 0 0 0         1 0 0 0 0 0         7 0 0 0 0 0
param sigma: 1 2 3  11 0 0 0 0 0         2 0 0 0 0 0         8 0 0 0 0 0
4 5 :=           12 0 0 0 0 0         3 1 0 0 0 0         9 0 0 0 0 0
1 0 1 0 0 0      [*,* ,4]: 1 2 3 4 5      4 1 0 0 0 0         10 0 0 0 0 0
2 0 0 1 0 0      :=                    5 1 0 0 0 0         11 0 0 0 1 0
3 0 0 0 1 0      1 0 0 1 0 0         6 1 0 0 0 0         12 0 0 0 1 0;
4 0 1 0 0 1      2 0 0 1 0 0         7 0 0 0 0 0          param delta: 1 2 3 4
5 0 0 0 0 0;    3 0 0 1 0 0         8 0 0 0 0 0          :=
param psi:=      4 0 0 1 0 0         9 0 0 0 1 0         1 1 0 0 0
[*,* ,1]: 1 2 3 4 5  5 0 0 0 0 0         10 0 0 0 1 0        2 1 0 0 0
:=              6 0 0 0 0 0         11 1 0 0 1 0        3 1 0 0 0
1 0 0 0 0 0      7 0 0 0 0 0         12 1 0 0 1 0        4 0 1 0 0
2 0 0 0 0 0      8 0 0 0 0 0          [*,* ,3]: 1 2 3 4 5  5 0 1 0 0
3 0 0 0 0 0      9 0 0 0 0 0          :=                  6 0 1 0 0
4 0 0 0 0 0      10 0 0 0 0 0         1 0 0 0 0 0         7 0 0 1 0
5 0 0 0 0 0      11 0 0 0 0 0         2 0 0 0 0 0         8 0 0 1 0
6 0 0 0 0 0      12 0 0 0 0 0         3 0 0 0 0 0         9 0 0 1 0
7 0 0 0 0 0      [*,* ,5]: 1 2 3 4 5      4 0 0 0 0 0         10 0 0 0 1
8 0 0 0 0 0      :=                    5 0 1 0 0 0         11 0 0 0 1
9 0 0 0 0 0      1 0 0 0 0 0         6 0 1 0 0 0         12 0 0 0 1;
10 0 0 0 0 0     2 0 0 0 0 0         7 0 1 0 0 0
11 0 0 0 0 0     3 0 0 0 1 0         8 0 1 0 0 0

```

## LIST OF PUBLICATIONS

- Paul Ghobril and Samir Tohmé: *Multi-Granularity Graph Model (MGGM)*, Proceedings of the ONDM2005 the 9th IFIP/IEEE Conference on Optical Network Design & Modelling Milano-Italy, Feb. 2005, pp. 383-392.
- Paul Ghobril and Samir Tohmé: *Analytical Model for Hierarchical Optical Cross-Connects*, Proceedings of the ONDM2004 the 8th IFIP Working Conference on Optical Network Design & Modelling Gent-Belgium, Feb. 2004, pp. 619–633.
- Paul Ghobril and Samir Tohmé: *Wavelength Rearrangement – To benefit from Hierarchical Cross-Connect without Wavelength Conversion*, Proceedings of the ONDM2003 the 7th IFIP Working Conference on Optical Network Design & Modelling Budapest-Hungary, Feb. 2003, pp. 939–952.
- Paul Ghobril and Samir Tohmé, *Towards a Dynamic Hierarchical Cross-Connecting Without Wavelength Conversion in Multi-Fiber WDM Networks*, Proceedings of the ICTON 2003 the 5th International Conference on Transparent Optical Networks, Warsaw-Poland, June 29-July 3 2003, pp. 51-54.
- Paul Ghobril and Samir Tohmé, *Dynamic Multi-Stage Traffic Grooming in Optical Networks*, Proceedings of the SSGRR2003s International Conference on Advances in Infrastructure for e-Business, e-Education, e-Science, e-Medicine and Mobile Technologies on the Internet, L’Aquila-Italy, July 28-August 3, 2003.
- Paul Ghobril: *Practical Traffic Grooming Formulation for SONET/WDM Rings*, Proceedings of the SSGRR2002s International Conference on Advances in Infrastructure for e-Business, e-Education, e-Science and e-Medicine on the Internet, L’Aquila-Italy, July 29-August 4 2002.



## MAIN REFERENCES

- [1] Xiaojun Cao, Vishal Anand and Chunming Qiao: *Multi-Layer Versus Single-Layer Optical Cross-connect Architectures for Waveband Switching*, IEEE INFOCOM 2004.
- [2] Xiaojun Cao, Vishal Anand, Yizhi Xiong and Chunming Qiao: *Performance Evaluation of Wavelength Band Switching in Multi-Fiber All-Optical Networks*, IEEE INFOCOM 2003
- [3] Teck Yoong Chai, Tee Hiang Cheng, Sanjay K. Bose, Chao Lu and Gangxiang Shen: *Analytical Model for a WDM Optical Cross-Connect with Limited Conversion Capability*, IEEE Communications Letters, Vol. 4, No. 11, November 2000, pp. 369-371.
- [4] Angela L. Chiu and Eytan H. Modiano: *Traffic Grooming Algorithms For Reducing Electronic Multiplexing Costs in WDM Ring Networks*, Journal Of Lightwave Technology, Vol.18, No.1, January 2000, pp.2-12.
- [5] Imrich Chlamtac, Andreas Farago and Tao Zhang: *Lightpath (Wavelength) Routing in Large WDM Networks*, IEEE Journal on Selected Areas in Communications, Vol. 14, No. 5, June 1996, pp. 909-913.
- [6] Wonhong Cho, Jian Wang and Biswanath Mukherjee: *Improved Approaches for Cost-Effective Traffic Grooming in WDM Ring Networks: Uniform-Traffic Case*, Photonic Network Communications, 3:3, pp. 245-254, 2001.
- [7] Ernesto Ciaramella: *Introducing Wavelength Granularity to Reduce the Complexity of Optical Cross Connects*, IEEE Photonic Technology Letters, Vol. 12, No. 6, June 2000, pp. 699-701.
- [8] Georgios Ellinas, Krishna Bala and Gee-Kung Chang: *A Novel Wavelength Assignment Algorithm for 4-fiber WDM Self-Healing Rings*, ICC'98.
- [9] L.R. Ford, Jr. and D.R. Fulkerson: *A Simple Algorithm for Finding Maximal Network Flows and an Application on the Hitchcock Problem*, Canadian Journal of Mathematics, 1957, Vol. 9, pp. 210-218.
- [10] Ori Gerstel, Philip Lin and Galen Sasaki: *Combined WDM and SONET Network Design*, Proc. INFOCOM, New York, NY, Mar. 1999, pp.734-743.
- [11] Ori Gerstel, Philip Lin and Galen Sasaki: *Wavelength Assignment in a WDM Ring to Minimize Cost of Embedded SONET Rings*, Proc. INFOCOM, San Francisco, CA, Apr. 1998, pp.94-101.
- [12] H. Ghafoury-Shiraz, Guangyu Zhu and Yuan Fei: *Effective Wavelength Assignment Algorithms for Optimizing Design Costs in SONET/WDM Rings*, Journal Of Lightwave Technology, Vol.19, No. 10, October 2001, pp.1427-1439.
- [13] Hiroaki Harai, Yuji Takimoto and Takeshi Ozeki: *Lightpath Routing for Equipment Cost Minimization in Hierarchical Optical Networks*, PS2002 Technical Digest (2002 International Topical Meeting on Photonic in Switching, Chejir Island (Korea), pp. 223-225, July 2002.
- [14] Pin-Han Ho and Hussein T. Mouftah: *Routing and Wavelength Assignment with Multi-Granularity Traffic in Optical Networks*, Journal of Lightwave Technology, Vol. 20, pp. 1292-1303, August 2002.
- [15] Pin-Han Ho, Hussein T. Mouftah and Jing Wu: *A Scalable Design of Multigranularity Optical Cross-Connects for the Next-Generation Optical Internet*, IEEE Journal on Selected Areas in Communications, Vol. 21, No. 7, September 2003, pp. 1133-1142.

- [16] Rauf Izmailov, Samrat Ganguly, Ting Wang, Yoshihiko Suemura, Yoshiharu Maeno and Soichiro Araki: *Hybrid Hierarchical Optical Networks*, IEEE Communication Magazine, November 2002, pp. 88-94.
- [17] Rauf Izmailov, Samrat Ganguly, Viktor Kleptsyn & Aikaterini C. Varsou: *Non-Uniform Waveband Hierarchy in Hybrid Optical Networks*, IEEE INFOCOM 2003, Vol. II.
- [18] Xiaohong Jiang, Hong Shen, Khandker Md.M-ur-R. and Horiguchi S.: *Blocking Behavior of Crosstalk-Free Optical Banyan Networks on Vertical Stacking*, IEEE/ACM Transaction on Networking, Vol. 11, No. 6, Dec. 2003, pp.982-993.
- [19] M. Kodialam and T.V. Lakshman: *Integrated Dynamic IP and Wavelength Routing in IP over WDM Networks*, INFOCOM2001, vol. 1, Anchorage-Alaska, 2001, pp. 358-366.
- [20] Aleksandar Kolarov and Bhaskar Sengupta: *An Algorithm for Waveband Routing and Wavelength Assignment in Hierarchical WDM Mesh Networks*, Workshop on High Performance Switching and Routing 2003, pp. 29-36.
- [21] Josue Kuri, *Optimization Problems in WDM Optical Transport Networks with Scheduled Lightpath Demands*, Ph.D. Thesis, ENST, 2003.
- [22] Josue Kuri, Nicolas Puech, Maurice Gagnaire and Emmanuel Dotaro, *Routing and Wavelength Assignment of Scheduled Lightpath Demands in a WDM Optical Transport Network*, ICOCN 2002, Singapore, IEEE Communications Society, November 2002, pp. 270-273.
- [23] Myungmoon Lee, Jintae Yu, Yongbum Kim, Chul-Hee Kang and Jinwoo Park: *Design of Hierarchical Crossconnect WDM Networks Employing a Two-Stage Multiplexing Scheme of Waveband and Wavelength*, IEEE Journal on Selected Areas in Communications, Vol. 20, No. 1, Jan 2002, pp.166-171.
- [24] Yiu-Wing Leung, Gaxi Xia and Kwok -Wah Hung: *Design of Node Configuration for All-Optical Multi-Fiber Networks*, IEEE Transaction on Communications, Vol. 50, No. 1, January 2002, pp. 135-145.
- [25] Weifa Liang and Xiaojun Shen: *Improved Lightpath (Wavelength) Routing in Large WDM Networks*, IEEE Transactions on Communications, Vol. 48, No. 8, September 2000.
- [26] Eytan Modiano and Philip J. Lin: *Traffic Grooming in WDM Networks*, IEEE Communications Magazine, July 2001, pp.124-129.
- [27] Ludovic Noirie, Martin Vigoureux and Emmanuel Dotaro : *Impact of Intermediate Traffic Grouping on the Dimensioning of Multi-Granularity Optical Networks*, Optical Fiber Communication Conference and Exhibit, 2001, OFC2001, Vol. 2, pp. TuG3-1 – TuG3-3.
- [28] Rajendran Parthiban, Rodney S. Tucker and Chris Leckie: *Waveband Grooming and IP Aggregation in Optical Networks*, Journal of Lightwave Technology, Vol. 21, No. 11, November 2003, pp.2476-2488.
- [29] Adel A. M. Saleh and Jane M. Simmons: *Architectural Principles of Optical Regional and Metropolitan Access Networks*, Journal of Lightwave Technology, Vol. 17, No. 12, December 1999, pp. 2431-2448.
- [30] Gangxiang Shen, Sanjay K. Bose, Tee Hiang Cheng, Chao Lu, Teck Yoong Chai: *The Impact of the Number of Add/Drop Ports in Wavelength Routing All-Optical Networks*, Optical Networks Magazine, Sept./Oct. 2003, pp. 112-122.
- [31] Jane M. Simmons, Evan L. Goldstein and Adel A. M. Saleh: *Quantifying the Benefit of Wavelength Add-Drop in WDM Rings with Distance-Independent and Dependent Traffic*, Journal of Lightwave Technology, Vol. 17, No. 1, January 1999, pp.48-57.

- [32] Peng-Jun Wan, Gruia Calinescu, Liwu Liu and Ophir Frieder: *Grooming of Arbitrary Traffic in SONET/WDM*, IEEE Journal on Selected Areas in Communications, Vol. 18, No. 10, Oct. 2000, pp.1995-2003.
- [33] Shun Yao, Canhui (Sam) Ou and Biswanath Mukherjee: *Design of Hybrid Optical Networks with Waveband and Electrical TDM Switching*, Available from URL: [http://networks.cs.ucdavis.edu/~ouc/publications/yao\\_gcom03.pdf](http://networks.cs.ucdavis.edu/~ouc/publications/yao_gcom03.pdf).
- [34] Xijun Zhang and Chunming Qiao: *An Effective and Comprehensive Approach for Traffic Grooming and Wavelength Assignment in SONET/WDM Rings*, IEEE/ACM Transaction On Networking, Vol.8, No.5, October 2000, pp.608-617.
- [35] Xijun Zhang and Chunming Qiao: *On Scheduling All-to-All Personalized Connections and Cost-Effective Designs in WDM Rings*, IEEE/ACM Transactions On Networking, Vol.7, No.3, June 1999, pp.435-445.
- [36] Hongyue Zhu, Hui Zang, Keyao Zhu and Biswanath Mukherjee: *A Novel Generic Graph Model for Traffic Grooming in Heterogeneous WDM Mesh Networks*, IEEE/ACM Transactions on Networking, April 2003, Vol 11, No.1, pp. 285-299.
- [37] Hongyue Zhu, Hui Zhang, Keyao Zhu and Biswanath Mukherjee: *Dynamic Traffic Grooming in WDM Mesh Networks Using a Novel Graph Model*, SPIE Optical Networks Magazine, May/June 2003, Vol. 4, No. 3, pp. 65-75.
- [38] Keyao Zhu, Hui Zang and Biswanath Mukherjee: *A Comprehensive Study on Next-Generation Optical Grooming Switches*, IEEE Journal on Selected Areas in Communications, September 2003, Vol. 21, No. 7, pp. 1173-1186.
- [39] Keyao Zhu, Hongyue Zhu and Biswanath Mukerjee: *Traffic Engineering in Multi-Granularity, Heterogeneous, WDM Optical Mesh Networks through Dynamic Traffic Grooming*, IEEE Network Magazine, Special issue on "Traffic Engineering in Optical Networks", March 2003.
- [40] Yong Zhu, Admela Jukan, Mostafa Ammar and Wesam Alanqar: *End-to-End Service Provisioning in Multi-granularity Multi-Domain Optical Networks*, Available from URL: [www.cc.gatech.edu/~yongzhu/publications/icc04\\_cameraready.pdf](http://www.cc.gatech.edu/~yongzhu/publications/icc04_cameraready.pdf).

## INDEX

- ?**
- $\lambda$ XC, 28, 48, *See* WXC
- 3**
- 3R, 3
- A**
- AAPC, 110  
add vertex, 32  
ADM, 106, 123  
analytical model, 10  
ASON, 1
- B**
- Basic Network Element, 10, 19, 20, 38  
Bin Packing, 116  
BNE, ii, 10, 19, 20, 21, 22, 28, 37  
*box* object, 48
- C**
- CADS, 110  
CATS, 110  
circle matrix, 122  
complexity of OXC, 39  
Control plane, 6
- D**
- Dead edges, 26  
differentiated cost, 33  
*dot* object, 48  
drop vertex, 32  
dynamic traffic, i, ii, iii, 11, 12, 14, 15,  
23, 33, 40, 46, 78, 91, 92, 97, 100, 104,  
105
- E**
- EXCLUDE operation, 23, 90
- F**
- FCCA, 112  
Ford-Fulkerson, iii, 14, 93, 100, 104, 126  
full circles, 110  
FXC, 4
- G**
- gap, 113  
GapMaker, 113  
GMPLS, 6  
granularity, i, ii, iii, 2, 3, 4, 5, 7, 9, 10, 11,  
13, 14, 15, 19, 20, 21, 22, 28, 32, 35,  
36, 39, 40, 42, 48, 57, 58, 59, 60, 61,  
62, 63, 75, 76, 78, 79, 80, 81, 82, 83,  
86, 89, 91, 97, 98, 100, 101, 102, 132,  
133, 134  
graph model, 9, 16  
grooming factor, 116  
Group Concept, 21  
Group vertices, 22
- H**
- Hamming distance, 124  
hardware complexity reduction, 40  
HCRR, 42, 46, 57, 58, 59, 68, 71, 75, 76,  
97, 99, 100  
HXC, 28, 33, 39, 48, 60
- I**
- i-layer cross-connect, 79  
i-layer switching, 79  
i-layer tunnel, 80  
ILP, 66  
ILP formulation, 124  
interlayer multiplexer, 80, 85  
internal flexibility, 52
- L**
- layered logical topology, 80

lightpath, 106  
logical topology, 80

## M

Main vertices, 22  
maxflow, iii, 14, 93, 95, 98, 100, 104, 126  
MERGE operation, 23, 89  
Metropolis, 120  
MGGM, ii, iii, 10, 14, 15, 16, 30, 31, 32, 34, 35, 88, 89, 91, 92, 96, 100, 104  
MG-OXC, 4, 10, 39  
multi-granular optical network, ii, iii, 1, 2, 12, 15, 100, 105  
Multi-granular OXC taxonomy, 6  
Multi-granularity, 3  
multi-layer, 3  
multi-layer MG-OXC, 4

## N

non taking rooks, 47, 54  
non-uniform traffic, 112  
non-uniform wavebands, 5

## O

O/E/O, i, 3, 12, 13  
OCIR, 45  
operational complexity increase, 45  
optical grooming, 2  
OXC, 1, 39, 60

## P

partial circle, 112  
PCCA, 113  
principle of inclusion and exclusion, 15, 55, 56, 127

## R

REINCLUDE operation, 24, 91  
RWA, ii, 3, 11, 15, 40, 46, 59, 60, 61, 65, 72, 75, 78

## S

S-ADM, 105  
Shared vertices, 22  
single-layer MG-OXC, 4  
SLD, 11  
static traffic, ii, 5, 11, 12, 99, 103, 105, 125  
stride, 106  
*strip* object, 48  
switching granularity, 3, 20, 78, 91

## T

TDM, 1  
traffic demand, 112  
traffic engineering, ii, iii, 10, 12, 14, 15, 22, 30, 33, 34, 78, 80, 89, 92, 100, 104  
traffic grooming, 3, 9, 11, 12, 15, 39, 78, 102, 106, 116, 120, 123, 125  
tuned receiver, 36  
tuned transmitter, 37  
tunnel, 85

## U

uniform traffic, 110  
UNMERGE operation, 24, 89, 91

## W

waveband, 22, 39  
wavebanding, 1, 2, 60  
wavelength assignment, ii, 3, 9, 11, 14, 15, 39, 40, 43, 46, 59, 60, 61, 62, 63, 72, 78, 105, 106, 109, 111, 112, 116, 117, 119, 121, 122, 124, 125  
Wavelength Assignment, 109  
wavelength converter, 37  
wavelength rearrangement, ii, 10, 14, 60, 61, 62, 66, 68, 72, 77  
WBXC, 4, 39, 48, 60  
WDM, i, 9, 105, 106, 125, 131, 132, 133, 134  
WXC, 4, 25, 39, 46, 60

